# Influence of the Maillard reaction on the allergenicity of food allergens

Zur Erlangung des akademischen Grades eines Doktor-Ingenieurs (Dr.-Ing.) genehmigte Dissertation von Dipl.-Ing. Monika Hofmann

TECHNISCHE UNIVERSITÄT DARMSTADT

# Influence of the Maillard reaction on the allergenicity of food allergens

Vom Fachbereich Chemie
der Technischen Universität Darmstadt

zur Erlangung des akademischen Grades eines

Doktor-Ingenieurs (Dr.-Ing.)

genehmigte

Dissertation

vorgelegt von

Dipl.-Ing. Monika Hofmann
aus Bad Soden Ts.

Referent: Prof. Dr. Harald Kolmar
Korreferent: Prof. Dr. Stefan Vieths

Tag der Einreichung: 01. September 2014
Tag der mündlichen Prüfung: 13. Oktober 2014

Darmstadt 2014

**D17**

# Acknowledgements

Special thanks to Dr. Masako Toda for her excellent supervision and for giving me the opportunity to work on this interesting and challenging project. I would also like to thank her for the many helpful discussions during the whole time of my PhD-studies.

Many thanks to Prof. Dr. Stefan Vieths for his supervision, the helpful discussions and comments, and his support during my PhD-studies.

Many thanks to Prof. Dr. Harald Kolmar for his supervision, helpful comments, his interest in the progress of the project and the frequent visits.

Very much thanks to Prof. Dr. Thomas Henle and Dr. Anne Wellner for preparation and analysis of the modified proteins, which were used in this study. This thesis would not have been possible without these proteins. I would also like to thank them for many helpful comments and support.

I would also like to thank Dr. Max Bastian for helpful discussions and being my mentor.

I would also like to say “thank you very much” to all members of former NG 1, Maren, Susi and Manja. I had a very nice time with you and I really enjoyed the nice atmosphere in and outside of the lab. Thank you, Maren, for your help and technical assistance.

Next, I would like to thank Dr. Stephan Scheurer and all members of former section 5/4, Dr. Stefan Schülke, Dr. Kay Fötisch, Andrea Wangorsch, Sonja Wolfheimer, Annette Jamin and Kirsten Kuttich, as well as Stefanie Randow for their help and support and for the nice atmosphere in the lab.

I would also like to thank Dorothea Kreuz for breeding and providing me frequently with the gene-modified mice.

I also want to thank PD Dr. Zoé Waibler and Stefanie Bauer for their expertise in and introducing the field of culture of primary human cells to me.

Ein ganz großer Dank gilt Heiko für seine Unterstützung in dieser Zeit. Du warst, bist und wirst immer für mich da sein!!!

Und zuletzt bedanke ich mich bei meinen Eltern, die mich schon während meines Studiums immer unterstützt und gefördert haben.

# Table of Content

# List of Figures

# List of Tables

# List of Abbreviations

**Used abbreviations:**

| | |
|---|---|
| 3-DG | 3-desoxyglucosulose |
| 3DG-H | 3-desoxyglucosulose-derived hydroimidazolones |
| aa | amino acid(s) |
| acLDL | acetylated low density lipoprotein |
| AGE | Advanced Glycation Endproducts |
| AGE-BSA | crude glycated bovine serum albumin |
| AGE-OVA | crude glycated ovalbumin |
| ALUM | aluminium hydroxide |
| APC | allophycocyanin |
| APCs | antigen-presenting cells |
| APS | ammonium persulphate |
| Arg | arginine |
| BCA | bicinchoninic acid |
| BD | Becton Dickinson |
| BMDCs | bone marrow-derived dendritic cells |
| BSA | bovine serum albumin |
| CCL | CC chemokine ligand |
| CD | cluster of differentiation |
| CD-spectroscopy | circular dichroism spectroscopy |
| CE | $N^{\varepsilon}$-carboxyethyl- |
| CEL | $N^{\varepsilon}$-(carboxyethyl-)lysine |
| CFSE | carboxyfluorescein succinimidyl ester |
| CM | $N^{\varepsilon}$-carboxymethyl- |
| CML | $N^{\varepsilon}$-(carboxymethyl-)lysine |
| CTL | C-type lectin receptor |
| DAPI | 4’,6-diamidino-2-phenylindole |
| DC | dendritic cell |
| DMSO | dimethyl sulphoxide |
| e.g. | exempli gratia; for example |
| EDTA | ethylenediaminetetraacetic acid |
| EEA-1 | early endosomal antigen-1 |
| ELISA | enzyme-linked immunosorbent assay |
| et al. | et alia; and others |

| | |
|---|---|
| EW | egg white |
| $F_{ab}$ | fragment, antigen-binding |
| FACS | fluorescence activated cell sorting |
| $F_c$ | fragment, crystallisable |
| FCS | foetal calf serum |
| FITC | fluorescein isothiocyanate |
| GA | glycolaldehyde |
| GC-MS | gas chromatography-mass spectrometry |
| GlcNAc | *N*-acetylglucosamine |
| GM-CSF | granulocyte macrophage colony-stimulating factor |
| HEPES | 2-[4-(2-hydroxyethyl)-piperazin-1-yl]ethane sulphonic acid |
| HLA | human leukocyte antigen |
| HRP | horseradish peroxidase |
| i.e. | id est; that is |
| i.p. | intraperitoneal |
| ICC | immunocytochemistry |
| iDCs | immature human dendritic cells |
| IFN | interferon |
| IgE | immunoglobulin E |
| IgG | immunoglobulin G |
| IL | interleukin |
| inc. | incubated |
| LN | lymph node |
| LPS | lipopolysaccharide |
| LSM | laser scanning microscope |
| Lys | lysine |
| mAb | monoclonal antibody |
| MACS | magnetic cell separation |
| Man | mannose |
| M-CSF | macrophage colony-stimulating factor |
| mDCs | mature human dendritic cells |
| MG-H1 | methylglyoxal-induced hydroimidazolones |
| MGO | methylglyoxal |
| MHC | major histocompatibility complex |
| MLN | mesenteric lymph nodes |
| MR | mannose receptor |

| | |
|---|---|
| OVA | ovalbumin; chicken egg albumin |
| oxLDL | oxidized low density lipoprotein |
| pAb | polyclonal antibody |
| PBMC | peripheral blood mononuclear cell |
| PBS | phosphate buffered saline |
| PdS | phosphatidylserine |
| PE | phycoerythrin |
| PFA | paraformaldehyde |
| $PGE_2$ | prostaglandin $E_2$ |
| PRRs | pattern-recognition receptors |
| RAGE | receptor for Advanced Glycation Endproducts |
| RP-HPLC/DAD | reversed phase high performance liquid chromatography with diode array detector |
| RPMI | Roswell Park Memorial Institute |
| SDS | sodium dodecyl sulphate |
| SDS-PAGE | sodium dodecyl sulphate-polyacrylamide gel electrophoresis |
| SIT | allergen-specific immunotherapy |
| SR-A | macrophage scavenger receptor class A |
| SR-AI/II | macrophage scavenger receptor class A type I and type II |
| SR-BI | macrophage scavenger receptor class B type I |
| TCR | T-cell receptor |
| TEMED | *N,N,N',N'*-tetramethylethylenediamine |
| TGF-β | transforming growth factor-β |
| $T_H$ | T helper |
| TLRs | toll-like receptors |
| TMB | 3,3',5,5'-tetramethylbenzidine |
| TNF | tumour necrosis factor |
| $T_{Reg}$ | regulatory T-cell |
| TRIS | tris(hydroxymethyl)aminomethane |
| TU | Technische Universität |
| w/o | without |
| wt | wild type |
| $\beta_2$GPI | $\beta_2$-glycoprotein I |

**Used symbols and units:**

| | |
|---|---|
| °C | degrees Celsius |
| Ci | Curie |
| d | day(s) |
| Da | Dalton; molecular weight |
| g | gram |
| h | hour(s) |
| l | litre |
| m | meter |
| min | minute(s) |
| mol | amount of substance |
| n.d. | not detectable |
| ND | not determined |
| o/n | overnight |
| OD | optical density |
| rpm | rounds per minutes |
| RT | room temperature |
| U | units |
| V | Volt |
| v | volume |
| w | weight |
| xg | multiples of g |
| λ | wavelength |

# 1 Introduction

## 1.1 Food allergy

The prevalence of food allergies has increased over the last decades.(*1*) Food allergies are adverse immune reactions to otherwise innocuous food proteins.(*1*) Epidemiologic studies involving controlled food challenges for the diagnosis of food allergies indicated that 1 % to 10.8 % of the population have immune-mediated non-toxic food hypersensitivity.(*1*) Food allergies in small children are caused by various types of food including cow's milk, hen's egg, peanuts, tree nuts and shellfish.(*1, 2*) The major foods causing allergies in adults except pollen-related food allergy to fruits and vegetables are shellfish, tree nuts, cereals and peanuts.(*3-5*) In adulthood, allergy to cow's milk or hen's egg is of low prevalence.(*3, 4*) Food allergic patients suffer from symptoms affecting cutaneous, respiratory and gastrointestinal tissues and in the worst case systemic anaphylactic shocks occur, which can be life-threatening.(*6*) Unfortunately, many types of food allergy are persistent for life and thus, the quality of life of the allergic patients is dramatically reduced.(*2, 6*)

Until today, the only proven management for food allergies is the elimination of the allergenic foods from the diet.(*2, 6*) However, this is difficult in the case of ubiquitous foods such as milk and egg, which are ingredients of many compound foods and processed foods, e.g. bakery products.(*2, 6*) Non-precise labelling of compound foods or cross-contamination of foods in the production process by usage of the same equipment for allergen-free and allergen-containing foods are the main causes of inadvertent food intake.(*2, 6*) For an inadvertent intake of the allergenic foods a symptomatic treatment, antihistamines or other medications, is available.(*2, 6*) As a potential curative treatment, allergen-specific immunotherapy (SIT) has gathered great interest.(*6, 7*) SIT aims to induce desensitization or clinical tolerance, i.e. immunologically non-response condition, by continuous administration of allergen(s).(*6, 7*) However, recent clinical studies have shown limited efficacy and safety of SIT for persistent food allergies.(*8, 9*) To establish a safe and effective treatment, it is crucially important to elucidate the pathomechanisms of food allergies.

### 1.1.1 Basic pathomechanism of allergy

Most types of allergy including food allergy belong to the class of type I hypersensitivity reactions, whose mechanism is schematically depicted in figure 1.(*7, 10*) Clinical symptoms in type I hypersensitivity reactions are mediated by allergen-specific immunoglobulin E (IgE).(*7, 10*)

Contact of the immune system with an allergen may break innate tolerance and initiate the sensitization phase.(*2, 10*) The respective allergen is taken up by an antigen-presenting cell (APC), like

a dendritic cell (DC) or a macrophage.(*10*) Inside the cell, the allergen is processed into small antigenic peptides, which are then loaded onto major histocompatibility complex (MHC) class II molecules and are presented on the cell surface.(*10*) Binding of a specific T-cell receptor (TCR) on a naive $CD4^+$ T-cell to the MHC class II peptide complex leads to T-cell activation and differentiation.(*11*) T-cell differentiation depends on the cytokine milieu (see chapter 1.6).(*11*)

Allergy is mediated by T helper 2 ($T_H2$) cells, a subset of $CD4^+$ effector T-cells.(*7, 10*) $T_H2$ cells produce the cytokines interleukin-4 (IL-4), IL-5, and IL-13. IL-4 and IL-5 induce maturation of mast cells and eosinophils, respectively.(*10, 11*) Moreover, IL-4 and IL-13 induce class switching and the production of allergen-specific IgE antibodies by B-cells.(*7*) The secreted IgE antibodies are captured by the high affinity IgE receptor, $F_c\varepsilon RI$, on the cell surface of mast cells or basophils.(*7*) The allergic response is suppressed by IL-10 or transforming growth factor-β (TGF-β) produced by $T_H1$ cells or regulatory T-cells ($T_{Reg}s$), other $CD4^+$ effector T-cell subsets.(*7, 10*)

Subsequent exposure to the allergen after sensitization provokes the elicitation phase.(*10*) The allergen cross-links the captured IgE antibodies on the cell surface, which subsequently induces mast cell and basophil degranulation.(*7, 10*) This step to induce degranulation is called the early-phase reaction.(*7, 10*) Mast cells and basophils then release the anaphylactic mediator histamine and other physiologically active substances inducing the immediate allergic symptoms.(*7, 10*)

The late phase allergic reaction is characterized by a more sustained mainly cell-mediated inflammation, in contrast to the above mentioned IgE-mediated acute symptoms.(*10*) Activated mast cells release prostaglandins, cytokines (e.g. IL-5 and IL-13) and chemokines (e.g. CC chemokine ligand 3 (CCL3), CCL5 and CCL11) which recruit other leukocytes, like $T_H2$-cells and eosinophils, to local tissues.(*10*) Finally, cytokines and tissue-damaging proteases secreted by these cells are responsible for chronic allergic inflammation.(*10*)

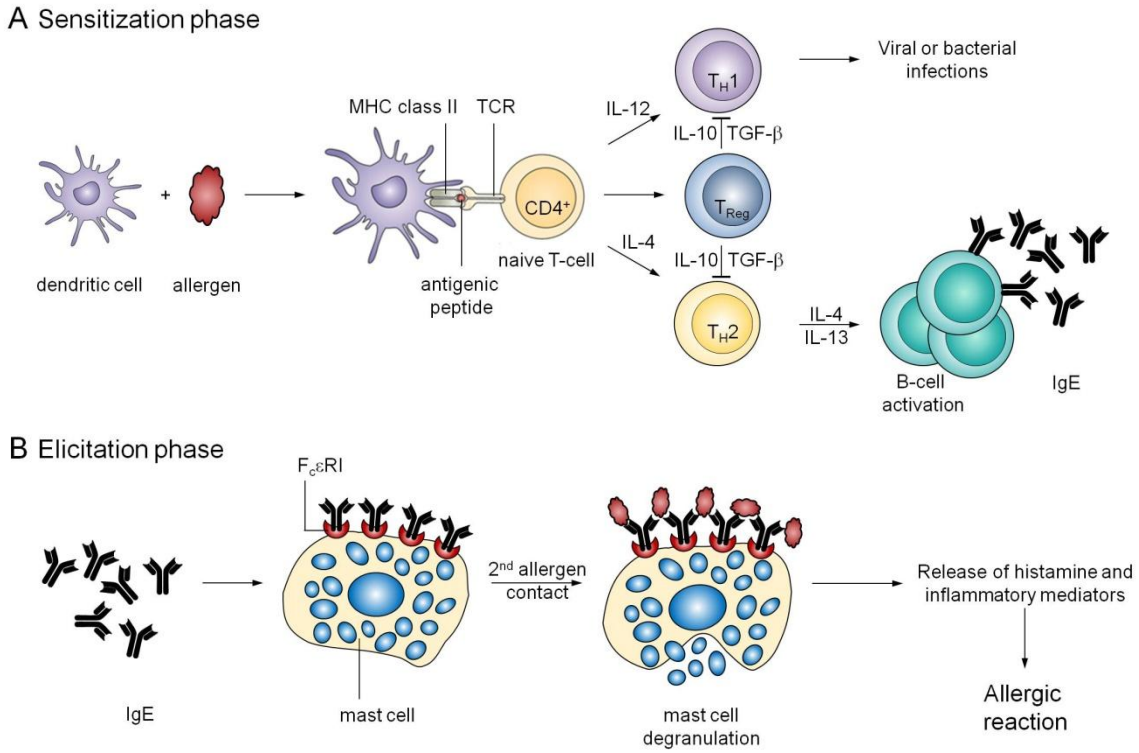


**Figure 1: Overview over the basic pathomechanism of allergy.** Allergen contact may trigger (A) the sensitization phase and immediate allergic symptoms are induced by (B) the elicitation phase upon repeated allergen exposure.

### 1.1.2 Egg allergy and its model allergen ovalbumin

Egg allergy is one of the most prevalent food hypersensitivities in infants and small children.(*12-14*) It was thought that the majority of children with an egg allergy become tolerant to hen's egg by school age.(*2*) However, a recent study suggested that egg allergy persists into adolescence.(*15*) The most clinically relevant major egg white allergen is ovomucoid, whereas ovalbumin (OVA) is the most abundant one with about 54 % of the whole egg white protein.(*16*) Although its allergenicity is weaker than that of ovomucoid, OVA is used as a reference protein in biochemistry and as a model allergen in immunology and allergology due to its high amount in egg white and its availability as single purified protein in high amounts.(*16, 17*) The allergen used in this thesis is this major chicken egg white allergen OVA.

OVA is built up of 386 amino acids (aa) resulting in a molecular weight of about 45 kDa. The protein fold is made up of nine α-helices and three β-sheets containing one disulphide bond, two phosphorylated serine residues and a mannose-rich glycosylation on Asn293.(*16, 18, 19*) This structural motif belongs to the serine protease inhibitor superfamily.(*17*) The single glycosylation on Asn293 consists of branched chains of neutral glycans linked to OVA by *N*-acetylglucosamine (GlcNAc).(*19, 20*) These glycans are mainly of the high-mannose (consisting of five to six mannose

(Man) and two GlcNAc residues) type or the hybrid type (varying composition also with high abundance of Man in relation to GlcNAc and galactose).(*19, 20*)

The biochemical, the immunological and the allergenic properties of OVA have been extensively studied. The T-cell epitopes of OVA in human and several mice strains share a common immunodominant epitope in the region of aa 323 – 339, suggesting that mice reacting to this $OVA_{323-329}$ peptide could be used as a model of egg allergy.(*16*) Other immunodominant peptides recognized by human TCRs are aa 1 – 33, aa 105 – 122, aa 198 – 213 and aa 261 – 277.(*16*) Additionally, the immunodominant sequences bound by IgE from allergic patients are located in the segments of aa 39 – 49, aa 95 -102, aa 191 – 200, aa 243 – 248 and of aa 251 - 260 and are only marginally overlapping with the peptides recognized by TCRs.(*21*) There seems to be no similarity in the peptides bound by human and murine IgE antibodies, but the sequences in both groups consist mainly of hydrophobic and charged amino acids.(*21, 22*) In BALB/c mice the immunodominant peptides recognized by IgE from sensitized mice are aa 53 – 60, aa 77 - 84, aa 103 – 108, aa 127 - 136, aa 275 – 280, aa 301 – 306, aa 323 – 329 and aa 375 – 384.(*22*) Another key feature of OVA is its relative stability against intestinal digestion and thermal processing.(*16, 23*) For example, Astwood et al. showed that OVA stayed intact after 60 min digestion in simulated gastric fluid.(*24*) All these facts together with the many established murine models of allergic diseases using OVA made this allergen an excellent candidate for this study.

## 1.2 Impact of thermal processing on the allergenicity of foods

The majority of foods is processed before being consumed and this can influence the immunogenic and allergenic properties of food allergens.(*23, 25*) The most common food processing techniques cooking, roasting, boiling and frying may cause protein unfolding, aggregation and/or chemical modification of the respective proteins.(*25, 26*) There are many factors influencing the extent of protein changes, like the temperature, the processing method, the food matrix and the duration of the treatment, thus, making a prediction of the outcome regarding the protein structure and its allergenicity difficult.(*25, 26*)

A reduction in allergenicity after cooking has been observed for many types of fruits or vegetables, e.g. Bet v 1 homologue allergens, the major cherry allergen Pru av 1, the major carrot allergen Dau c 1 and the allergen Api g 1 from celery.(*23, 27-29*). Thermal processing of the egg white allergen OVA has also been studied and a reduction in immunogenicity and allergenicity was observed.(*30-32*) In all studies heat-induced structural changes of OVA contributed to a higher susceptibility to gastric digestion and reduced IgE-binding of sera from allergic patients.(*30-32*) The opposite effect, i.e.

tolerance of the raw food and induction of allergic symptoms by consumption of the respective food in its cooked state has been observed for shrimp, shellfish and pecan nuts.(*33-35*) For the highly allergenic peanuts a comparison of the allergenicity of raw and roasted peanuts is difficult, because they are primarily consumed after roasting.(*36, 37*) Nevertheless, there is evidence that roasting may increase the allergenic properties of peanut allergens by reducing the susceptibility of the proteins towards degradation and gastric digestion.(*36, 37*) The enhanced allergenicity of all mentioned allergenic foods including peanuts was not only caused by structural changes of the proteins, like denaturation of conformational epitopes and exposure of usually buried linear ones, but also by chemical modification of the allergens.(*25, 26*)

During thermal processing of foods, proteins chemically react with many components such as carbohydrates, lipids and the food matrix.(*25, 26*) The main chemical reaction between proteins and carbohydrates is the Maillard reaction.(*25, 26*)

## 1.3 The Maillard reaction

The Maillard reaction was identified by Louis Camille Maillard in 1912.(*38*) It is a non-enzymatic glycation reaction between the carbonyl group of a reducing sugar and compounds with free amino groups, like amino acids or proteins, occurring during thermal processing or long-term storage of foods as well as *in vivo* during the process of aging.(*38, 39*) The condensation of sugar and protein in the early phase Maillard reaction results in the formation of so-called Amadori products, e.g. $N^{\varepsilon}$-fructosyllysine, $N^{\varepsilon}$-lactulosyllysine or protein-bound polysaccharides.(*39*) In the advanced phase Maillard reaction these Amadori products become degraded to highly reactive 1,2-dicarbonyl substances, which subsequently react in a complex cascade finally forming stable Maillard reaction products.(*39*) The stable products at the final stage of the Maillard reaction are collectively called Advanced Glycation Endproducts (AGEs).(*39*) A scheme of the overall Maillard reaction with representative AGE-structures as final products is shown in figure 2. The shown reaction products are only a selection of a pool of several hundreds of different compounds, which are known to be formed by the complex cascade of the Maillard reaction.(*39, 40*)

Until today a vast variety of different AGE-structures linked to either lysine or arginine residues in proteins have been identified.(*41*) The first AGEs identified in foods were the melanoidins, a collective term for all brown-coloured AGEs, since the Maillard reaction is also called a non-enzymatic browning reaction.(*39, 41*) Besides of the brown colour, the melanoidins and many other AGEs also contribute to the flavour and the aroma of processed foods.(*42, 43*) Some representative AGEs found in foods are $N^{\varepsilon}$-carboxymethyllysine (CML), pentosidine, pyrraline as well as hydroimidazolones.(*39,*

*43*) Some of the presented AGE-structures, like CML, are also formed by the *in vivo* Maillard reaction during aging.(*44*) It has been suggested that products of the *in vivo* Maillard reaction trigger inflammation and thus, contribute to the pathology of human diseases, e.g. diabetes, rheumatoid arthritis or Alzheimer's disease.(*44*)

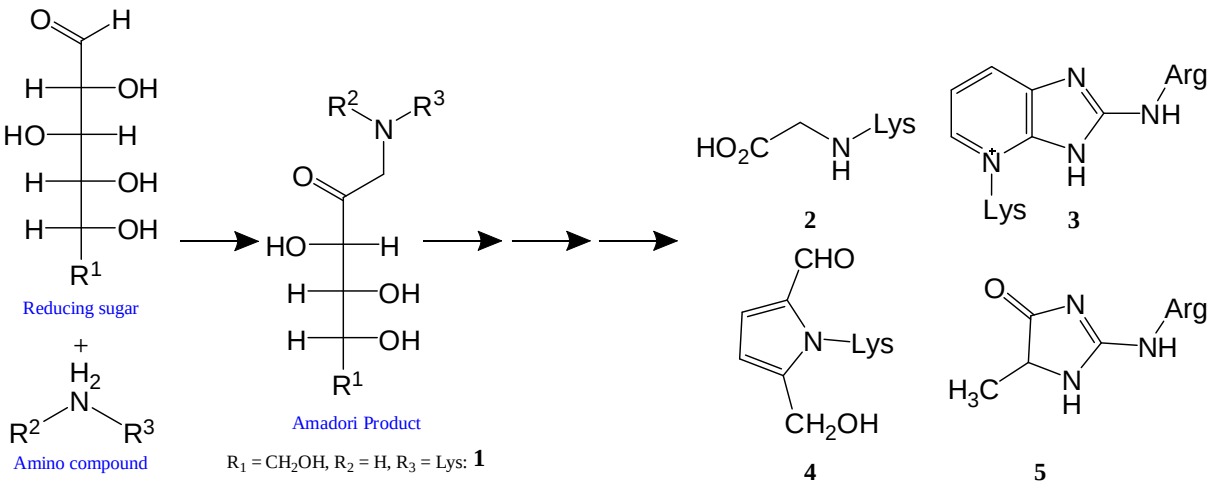


**Figure 2: Simplified mechanism of the Maillard reaction resulting in the formation of AGE-structures.** Representative AGEs found in processed foods are $N^{\varepsilon}$-fructoselysine (1), CML (2), pentosidine (3), pyrraline (4) and methylglyoxal-induced hydroimidazolones (5).

### 1.3.1 AGE-binding receptors

The contribution of AGEs in the pathology of many diseases has led to the identification of several receptors binding to AGEs. Important receptors binding to AGEs are schematically shown in figure 3. First, the receptor for AGEs (RAGE) was identified in 1992 by Schmidt et al.(*45*) together with Neeper et al.(*46*) as the one mediating the binding of AGEs to endothelial cells in the pathogenesis of diabetic angiopathy.(*45, 46*) Several studies have shown a possible involvement of RAGE in Alzheimer's disease and diabetic complications by inducing an inflammatory signal.(*44*)

Using the macrophage-like cell line RAW264.7, Vlassara et al.(*47*) reported the binding of AGE-modified proteins to galectin-3, which usually binds to galactose-containing carbohydrates.(*47*)

Several members of the macrophage scavenger receptor family, another group of carbohydrate binding receptors, were also identified to bind to AGEs.(*48, 49*) Araki et al. showed that the endocytosis of AGE-modified BSA is mediated by macrophage scavenger receptors class A type I and type II (SR-AI/II).(*50*) Ohgami et al. found that the class B scavenger receptors SR-BI and CD36 are AGE-binding receptors.(*51, 52*)

Importantly, RAGE, galectin-3, SR-AI/II, SR-BI and CD36 are expressed on the surface of APCs and thus, binding of food allergens linked to AGE-structures to these receptors could have an influence on cell function.

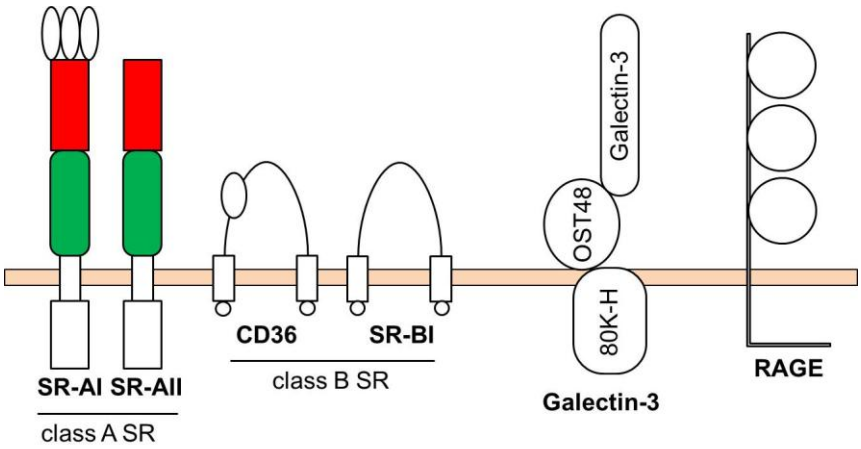


**Figure 3: AGE-binding receptors (inspired by Horiuchi et al.(*49*)).**

### 1.3.1.1 Scavenger receptors

The members of the scavenger receptor family are endocytic and phagocytic receptors expressed on the surface of DCs and macrophages.(*53, 54*) Many scavenger receptor ligands are polyanionic molecules.(*53, 54*) Identified ligands of scavenger receptors are AGEs, oxidized and acetylated low density lipoproteins (oxLDL respectively acLDL), lipopolysaccharide (LPS) as well as gram-positive bacteria.(*48, 53, 54*) The scavenger receptors are divided into eight classes (class A to H) based on their structure and only class A and class B scavenger receptors, which are schematically depicted in figure 4, have been reported to bind to AGEs.(*48, 54*)

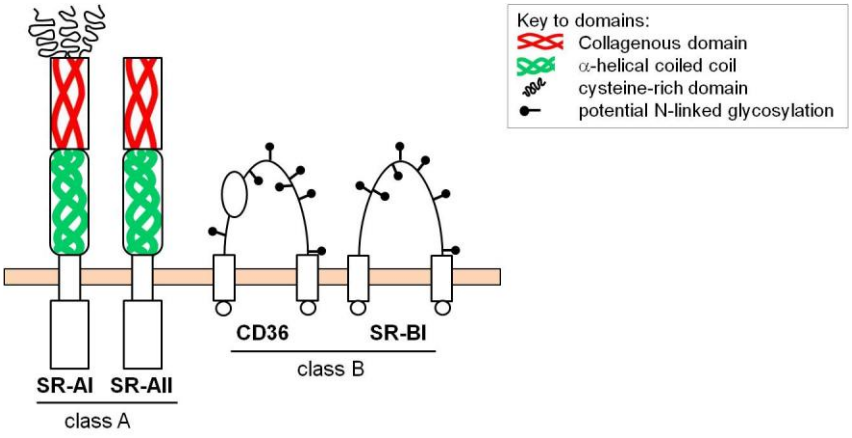


**Figure 4: Domain structure of class A and class B scavenger receptors (inspired by Plüddemann et al.(*48*)).**

Class A scavenger receptors (SR-A) are transmembrane glycoproteins and are composed of a cytoplasmic tail, a transmembrane region, an extracellular spacer, an α-helical coiled-coil domain, a collagenous domain and a C-terminal scavenger receptor cysteine-rich domain.(*48*) Antigen recognition by and binding to the collagenous domain of the functional equivalent isoforms SR-A type I and type II (summarized as SR-AI/II) induces endocytosis, which is mediated by the cytoplasmic tail of the receptor.(*48, 55*) Antigen endocytosis leads to antigen-presentation for the induction of an adaptive $T_H$ response as well as cytokine secretion by the APC, originally determined for the clearance of bacterial infections.(*48, 53*)

The class B scavenger receptors CD36 and SR-BI are also transmembrane glycoproteins and consist of two short intracellular tails and a highly glycosylated extracellular loop.(*48*) The first binding of AGEs to CD36 and SR-BI *in vitro* was shown by Ohgami et al.(*51, 52*) Furthermore, the natural ligand oxLDL and AGEs are recognized by the same region in the extracellular domain.(*52*) Antigen internalization for antigen-presentation is then mediated by the C-terminal intracellular domain.(*48*) The natural function of SR-BI is in the metabolism of high density lipoprotein and control of cholesterol efflux.(*49*) AGEs served *in vitro* as inhibitor of SR-BI mediated cholesterol efflux, hence, a contribution of AGEs *in vivo* on SR-BI function can not be excluded although it was not yet demonstrated.(*49*)

#### 1.3.1.2 Galectin-3

The natural ligands of the galectin receptor family including galectin-3 are β-galactoside carbohydrates and their interaction is important in many different regulatory processes as well as in allergy by activation of mast cells.(*56, 57*)

Galectin-3 is built up of the ligand-binding C-terminal carbohydrate-recognition domain and a highly conserved N-terminal domain with tandem repeats and has a molecular weight of about 35 kDa. The expression of the receptor is not limited to a specific cell type or tissue as galectin-3 is expressed by macrophages, DCs, monocytes, neutrophils as well as epithelial cells of nearly all organs.(*56*) Another unique feature of galectin-3 is that the receptor can be found in the cytoplasm, in the cell nucleus, on the cell surface or extracellularly as a soluble form.(*47*)

As a cell surface receptor galectin-3 is involved in cell adhesion, cell signalling as well as immune reactions by binding bacterial glycans and induction of its pro-inflammatory activity.(*56*) It has been suggested that the interaction of galectin-3 with AGEs is involved in the pathogenesis of atherosclerosis.(*58*)

#### 1.3.1.3 The mannose receptor

Another receptor family recognizing carbohydrate structures are C-type lectin receptors (CTLs).(*59, 60*) CTLs have an important role in innate immunity in the endocytosis of pathogens by APCs.(*59, 60*) Many glycosylated allergens are recognized by CTLs, e.g. the egg white allergen OVA, the peanut allergen Ara h 1 as well as the house dust mite allergens Der p 1 and Der p 2.(*59, 61*)

The CTL mainly mediating the uptake of allergens is the macrophage mannose receptor (MR; CD206).(*60, 61*) The MR is primarily expressed on the surface of DCs and macrophages.(*60, 61*) The MR structurally is composed of an N-terminal cysteine-rich domain, a domain containing fibronectin type II repeats, eight C-type lectin-like domains, a transmembrane domain and a short cytoplasmic tail.(*54, 62*) Pathogens are bound by the C-type lectin-like domains, a unique feature of CTLs, and the domains of the MR have a strong affinity for glycans containing high levels of mannose and to a lesser extent glucose or fucose.(*60, 61*) The bound antigens are then transported by the cytoplasmic tail into the cytoplasm, where they are processed followed by presentation by MHC molecules on the cell surface.(*54, 62*) The detailed mechanisms of antigen routing after MR uptake are yet not fully understood. It has been suggested that the nature of the pathogen determines the type of immune reaction, either $T_H1$-type response, $T_H2$-type response or cross-presentation to $CD8^+$ T-cells.(*63*) Cross-presentation means that antigens, which are usually presented to $CD4^+$ T-cells by MHC class II molecules, like exogenous antigens, are transported to the MHC class I loading pathway and thus, are presented to $CD8^+$ T-cells.(*64*)

### 1.3.2 AGEs and food allergy

In the literature, there is a controversial discussion about the impact of the Maillard reaction on the allergenic properties of food allergens.(*41*)

Several studies have investigated the influence of the Maillard reaction on peanuts, a highly allergenic food causing severe anaphylactic shocks. Roasting seems to enhance peanut allergenicity, because a stronger binding of IgE from peanut allergic patients to extracts from roasted peanuts compared to raw peanuts has been observed.(*37, 65*) This binding could be inhibited by AGE-specific antibodies and thus, could be linked to modifications by the Maillard reaction in roasted peanuts.(*65*) On the other hand, other studies suggested that the Maillard reaction attenuates the allergenic potency of peanut, because of reduced IgE-reactivity and mediator release capacity after glycation.(*66, 67*) A reduced allergenicity after modification with Maillard reaction products has also been observed for the major cherry allergen, for β–lactoglobulin in milk, as well as for tropomyosin in fish.(*27, 68-70*)

There is evidence that the Maillard reaction is not only influencing IgE-reactivity and mediator release capacity, i.e. characteristics for the elicitation of food allergy, but can also play a role earlier in the pathology, e.g. in the interaction of the allergen with an APC or in T-cell activation. In the study by Ilchmann et al. glycated OVA (AGE-OVA) activated allergen-specific T-cells to a stronger extent than the native allergen.(*71*) This enhanced $CD4^+$ T-cell activation was mediated by an enhanced uptake of AGE-OVA by DCs.(*71*) It was suggested that SR-AI/II could mediate the uptake of AGE-OVA by DCs.(*71*) These results showed that the Maillard reaction enhances the T-cell immunogenicity of OVA, which in turn might enhance the allergenic potency of the food allergen.(*71*)

All mentioned studies have in common that crude glycated foods or the respective food allergens were analyzed. The profile of the formed glycation structures is highly dependent on the chosen conditions, such as the sugar component, the temperature, the duration, the pH and the food matrix.(*26, 41*) Hence, the glycation structures contributing to this vast spectrum of results are not known. It is of great importance to investigate the influence of representative glycation structures on the immunological and allergenic properties of food allergens.

## 1.4 Dendritic cells

DCs are the unique and crucial bridge between innate and adaptive immunity.(*72, 73*) The main function of DCs is recognition, uptake and presentation of antigens followed by subsequent induction of an antigen-specific adaptive immune response.(*72*) The encounter of a DC with an antigen results in cell activation and maturation.(*74*)

The primarily occurring mechanism of antigen uptake is receptor-mediated endocytosis by pattern-recognition receptors (PRRs), like macrophage scavenger receptors, CTLs or toll-like receptors (TLRs), in addition to macropinocytosis or phagocytosis of the antigen.(*75*) The recognition of and binding of an antigen by a surface-exposed receptor via innate immune mechanisms triggers the budding of the cell membrane and the protein is transported to the cytosol in a small vesicle called endosome for intracellular processing to generate antigenic peptides.(*10*)

Some PRRs such as TLRs are involved not only in antigen uptake, but also in activation and maturation of DCs.(*61, 75*) During this transformation of the DC into a functional APC, the expression of surface PRRs is downregulated and co-stimulatory molecules, e.g. CD40, CD80 (B7.1) and CD86 (B7.2) become upregulated.(*75*) Subsequently, the cell morphology changes and antigenic peptide-loaded MHC molecules are transported to the cell surface.(*75*) The maturation process is also regulated by secretion of cytokines, e.g. IL-1, IL-6, IL-10, IL-12 and tumour necrosis factor-α (TNF-α).(*74, 75*)

The nature of the antigen determines the route of antigen processing and presentation pathway in DCs, i.e. endogenous antigens, e.g. viral or tumour antigens, are delivered to the MHC class I presentation pathway, whereas extracellular antigens, e.g. allergens or particulates, will be delivered to the MHC class II presentation pathway.(*75*) There is also the possibility of cross-presentation, which means that exogenous antigens are delivered to the MHC class I presentation pathway, but the exact mechanisms of cross-presentation are not yet completely understood.(*75*) For presentation of the antigenic peptide-MHC class I or class II complex to naive $CD8^+$ or $CD4^+$ T-cells, respectively, the mature DCs migrate to the draining lymphoid organs. There, an adaptive immune response is induced by binding of an antigen-specific TCR to the MHC complex in combination with signalling of the co-stimulatory molecules.(*74, 75*)

## 1.5 Macrophages

Macrophages are monocyte-derived cells with important functions in innate as well as in adaptive immunity.(*76*) Although there is an exceptionally high diversity of resident macrophages due to intrinsic differentiation pathways in the tissues, two main classes of activated cells mediating the majority of immune responses, i.e. M1 and M2 macrophages, have been described.(*76, 77*) In the literature, M1 macrophages are also referred to as classically activated macrophages with a mainly pro-inflammatory phenotype, whereas M2 macrophages, or alternatively activated macrophages, basically are involved in tissue repair and homeostasis as well as $T_H2$-type immune responses.(*76, 78*) Like in DCs, activation of resting macrophages is induced by a so-called danger signal, like the recognition of a pathogen or the presence of a specific cytokine.(*77*) PRRs, like some TLRs, CTLs and scavenger receptors, are expressed on the surface of macrophages and mediate endocytosis of exogenous ligands.(*79*)

The uptake of microbial related structures, like LPS, or the presence of interferon-γ (IFN-γ) leads to differentiation into M1 macrophages. M1 macrophages participate as inducer or effector cells in $T_H1$-type immune responses and thus, surface expression of co-stimulatory molecules together with MHC class II molecules is upregulated.(*76, 79*) The high level of MHC class II expression is accompanied by strong antigen-presentation to $CD4^+$ T-cells.(*78*) For an effective clearance of viral and microbial infections, M1 macrophages produce the pro-inflammatory cytokines IL-1β, IL-6, IL-12 and TNF-α.(*76, 77*) The microbicidal activity of these cytokines is assisted by the production of reactive nitrogen and oxygen species.(*78*)

The pro-inflammatory activities of M1 macrophages can be suppressed by M2 macrophages, which become activated by the cytokines IL-4 or IL-13.(*76, 80*) Like M1 cells, also M2 macrophages have a

high pre-disposition to function as APCs and activation leads to high expression of MHC class II molecules.(*79*) In M2 cells, contributing to the function as APC is the enhanced density of scavenger, mannose and galactose receptors on the cell surface for efficient parasite recognition.(*78, 79*) Besides assistance in parasitic and allergic $T_H2$ responses, M2 cells are also important for the suppression of inflammation and for tissue repair. As part of these functions M2 cells produce the anti-inflammatory cytokines IL-10 and TGF-β.(*76, 78*)

Because of the high plasticity of macrophages, the role of macrophages in food allergy and many other AGE-associated diseases, e.g. diabetic complications and Alzheimer's disease, is heavily discussed.(*44, 81, 82*) However, the association of M1 and M2 cells with AGEs has not yet been investigated.

## 1.6 T-cells

T-cells play a crucial role in adaptive immunity.(*10, 11*) The cells are divided upon their bearing co-receptors into $CD4^+$ and $CD8^+$ T-cells.(*10, 11*) The main function of $CD4^+$ T-cells, which are also called $T_H$ cells, is the activation of other leukocytes, whereas that of $CD8^+$ T-cells, which are also called cytotoxic T-lymphocytes, is clearance of microbial infections as well as killing of virus-infected and tumour cells.(*10*) Activated $CD4^+$ T-cells are the prerequisite for the activation of B-cells and their subsequent differentiation into immunoglobulin-secreting plasma cells.(*7, 10*)

Two signals are required for the activation of both T-cell classes if they are in their naive state.(*10, 74*) First, a peptide-MHC complex presented by an APC is bound by a specific TCR.(*10, 74*) Thereby peptides presented on MHC class II molecules are recognized by $CD4^+$ T-cells, whereas peptides presented on MHC class I molecules are recognized by $CD8^+$ T-cells.(*10*) The second signal is provided by co-stimulatory molecules, like CD80 or CD86 expressed by the APC and CD28 on the surface of the T-cell.(*74*) These two signals are sufficient for triggering T-cell clonal expansion, i.e. proliferation, and IL-2 production by the T-cell, which provides the last signal.(*10, 74*) High levels of IL-2 promote T-cell clonal expansion.(*11*)

The determining factor for T-cell differentiation is the cytokine milieu.(*10*) IFN-γ and IL-12 lead to the development of $T_H1$-cells, which assist infected macrophages in pathogen killing or provide help for the clearance of extracellular pathogens by activating antibody production by B-cells.(*10, 11*) Differentiation into $T_H2$-cells is induced by IL-4.(*7*) $T_H17$-cells, another subset, which has been recently identified, are responsible for autoimmunity and are induced by IL-6 and TGF-β.(*83*) Disruption of the natural balance among the T-cell subsets leads to disease.(*11*) Allergic inflammation is caused by excessive numbers of $T_H2$-cells.(*7, 11*) This response can be suppressed by high amounts

of IFN-γ produced by $T_H1$-cells.(*7, 11*) Recent studies have suggested that $T_H17$ cells could play a role in allergic inflammation, e.g. by recruitment of neutrophils, another type of inflammatory leukocytes, and by induction of the release of inflammatory mediators by resident tissue cells, like epithelial cells.(*83*) Another mechanism controlling the immune response is the induction of $T_{Reg}$s, which are able to suppress $T_H$ responses by secretion of the suppressive cytokines IL-10 and TGF-β.(*7*)

# 2 Objective

The aim of this thesis is to investigate molecular mechanisms of the influence of the Maillard reaction, which occurs during thermal processing of foods, on the immunogenic and allergenic properties of food allergens. The previous study by Ilchmann et al. showed that $CD4^+$ T-cell immunogenicity of OVA, a model food allergen, is enhanced, when it is glycated by the Maillard reaction during thermal incubation with glucose.(*71*) This Maillard reaction product of OVA with glucose contained various glycation structures.(*71*) Notably, several studies showed that receptors binding to crude products of the Maillard reaction, e.g. SR-AI/II and CD36, could bind only to distinct glycation structures.(*84*, *85*) Based on this background, the working hypothesis for this thesis was that distinct glycation structure(s) contribute to the enhanced $CD4^+$ T-cell immunogenicity of crude glycated OVA (AGE-OVA). To verify the hypothesis, OVA was selectively modified with the glycation structures $N^{\varepsilon}$-carboxyethyllysine (CEL), CML, methylglyoxal-induced hydroimidazolones (MG-H1) or pyrraline, which are representative glycation structures found in processed foods. The following experimental aims were set up:

(1) To investigate the immunogenic properties of these OVA samples modified with distinct glycation structures using cultured murine DCs and T-cells.

(2) To investigate the allergenic properties of the glycated OVAs using a murine model of food allergy.

(3) To investigate the immunogenic properties of the glycated OVAs using cultured human DCs and macrophages.

First, a detailed characterization of the modified OVAs with chromatographic methods or by means of enzyme-linked immunosorbent assay (ELISA) was performed. The immunogenic properties of the modified OVA samples in comparison to AGE-OVA or native OVA were then investigated using *in vitro* cell culture assays. The ability of the allergens to activate transgenic allergen-specific $CD4^+$ T-cells and $CD8^+$ T-cells, which is crucial for provoking immune responses, was assessed using a co-culture system of these T-cells with bone marrow-derived DCs. The capacity of the modified OVAs to induce DC maturation as well as uptake of fluorescent-labelled OVA samples by DCs was assessed by flow cytometric analyses. Afterwards, the molecular uptake mechanism was investigated by inhibiting putative receptors playing a central role in endocytosis of OVA or AGE-modified proteins, or using DCs deficient for the putative receptor. Immunocytochemistry was performed to identify the intracellular compartment containing the glycated allergen by confocal microscopy, which could elucidate a pathway of receptor-mediated antigen delivery for antigen presentation.

In the second part of this thesis, the allergenic potency of AGE-OVA and selectively modified OVAs with enhanced T-cell immunogenicity was investigated using an *in vivo* mouse model of intestinal food allergy. BALB/c mice were sensitized with either form of OVA in combination with a $T_H2$-directing adjuvant and afterwards orally challenged with the allergen. As a measure of immunogenicity, T-cell responses of $CD4^+$ T-cells isolated from the mesenteric lymph nodes, the gut draining lymphoid organ, were assessed *in vitro*. In addition, the humoral immune response was elucidated by determining the levels of IgE, IgG1 and IgG2a antibodies in the sera of the mice. Allergenic potency of the modified OVAs was investigated by monitoring clinical symptoms, like loss of bodyweight, drop in body temperature and diarrhoea, during the challenge.

Finally, a system of human cell culture for studying the influence of the Maillard reaction on the immunogenic properties of OVA should be established, because tissue samples of egg allergic patients are very limited as most patients are small children. For this purpose, assays for investigating antigen uptake or DC maturation were transferred to cell culture of peripheral blood mononuclear cell (PBMC)-derived human DCs or macrophages.

All parts of this thesis will contribute to a better understanding of the molecular mechanisms of food allergy.

# 3 Materials and Methods

## 3.1 Materials

### 3.1.1 Commonly used equipment

**Table 1: Commonly used devices and equipment in this thesis.**

| equipment | model | company |
|---|---|---|
| circular dichroism-(CD-) spectrometer | J-810S | JASCO (Groß-Umstadt) |
| centrifuges | centrifuge 5417C/R<br>multifuge 1S-R<br>Heraeus Varifuge 3.0R | Eppendorf (Hamburg)<br>Heraeus (Langenselbold)<br>Heraeus (Langenselbold) |
| ELISA reader | Spectra Max 340 PC | Molecular Devices (München) |
| flow cytometers | BD™ LSR II<br>BD™ LSR II SORP | Becton Dickinson (Heidelberg)<br>Becton Dickinson (Heidelberg) |
| incubator for cells | BBD6220 $CO_2$ incubator<br>Labotect C-200 | Thermo Scientific (Nidderau)<br>Labotect (Göttingen) |
| laminar flow | SterilGARD SG-400 | The Baker Company (Sanford, ME, USA) |
| magnetic stirrer | IKAMAG® RCT basic | IKA (Staufen) |
| orbital shaker | KS 130 control | IKA (Staufen) |
| power supply | PowerPac™ 300 | Bio-Rad Laboratories (München) |
| scales | Explorer Pro<br>EK-300i | Ohaus (Pin Brook, NJ, USA)<br>AND (Abingdon, UK) |
| seesaw shaker | DUOMAX 1030 | Heidolph Instruments (Schwalbach) |
| thermo mixer | Thermomixer Compact | Eppendorf (Hamburg) |
| vortex | Vortex Genie 2 | Scientific Industries (New York, USA) |
| water bath | Grant GD 100 | Grant Instruments Ltd. (Cambridge, UK) |

Special equipment which was used for a single method is listed in the relevant method.

### 3.1.2 Chemicals

All chemicals were provided from Carl Roth (Karlsruhe), Sigma-Aldrich (Steinheim) or Merck (Darmstadt) if not stated otherwise.

### 3.1.3 Buffers

All buffers were prepared using deionized water unless stated otherwise and were either autoclaved or sterile filtered.

**Table 2: General buffers used.**

| buffer | composition | pH |
|---|---|---|
| CD-buffer A | 100 mmol/l $KH_2PO_4$ | 4.5 |
| CD-buffer B | 100 mmol/l $Na_2HPO_4$ | 9.0 |
| EDTA/trypsin | phosphate buffered saline (PBS) (see below)<br>+ 0.1 % (w/v) ethylenediaminetetraacetic acid (EDTA)<br>+ 0.25 % (w/v) trypsin | |
| ELISA blocking buffer | PBS<br>+ 2 % (w/v) bovine serum albumin (BSA) | |
| ELISA coating buffer | 16 mmol/l $Na_2CO_3$<br>34 mmol/l $NaHCO_3$ | 9.6 |
| ELISA washing buffer | PBS<br>+ 0.05 % (v/v) Tween 20 | 7.1 |
| ELISA assay buffer | PBS<br>+ 1 % (w/v) BSA<br>+ 0.05 % (v/v) Tween 20 | |
| FACS-buffer | PBS<br>+ 1 % (w/v) BSA<br>+ 20 mmol/l EDTA<br>+ 0.03 % (w/v) $NaN_3$ | |
| HEPES | 1 mol/l 2-[4-(2-hydroxyethyl)-piperazin-1-yl]ethane sulphonic acid | 7.9<br>adjusted with NaOH |
| ICC-assay buffer | PBS<br>+ 1 % (v/v) normal mouse serum<br>+ 0.1 % (v/v) Triton® X-100 | |
| MACS-buffer | PBS<br>+ 2 mmol/l EDTA<br>+ 5 % (w/v) BSA | 7.2<br>adjusted with HCl |
| penicillin/ streptomycin/ L-glutamine | 3.14 g/l penicillin G potassium salt<br>5 g/l streptomycin sulphate<br>15 g/l L-glutamine | |

| buffer | composition | pH |
|---|---|---|
| permeabilization-buffer | PBS<br>+ 5 % (w/v) skim milk powder<br>+ 1 % (v/v) normal mouse serum<br>+ 0.1 % (v/v) Triton® X-100<br>+ 1 µg/ml normal mouse IgG | |
| phosphate buffer A | 200 mmol/l $NaH_2PO4$ | |
| phosphate buffer B | 200 mmol/l $Na_2HPO4$ | |
| phosphate-buffered saline (PBS) | 137 mmol/l NaCl<br>2.7 mmol/l KCl<br>1.45 mmol/l $KH_2PO_4$<br>8.1 mmol/l $Na_2HPO_4$ | 7.1<br>adjusted with HCl |
| SDS loading buffer 4x | 0.25 mol/l tris(hydroxymethyl)amino-methane (TRIS)<br>4.2 % (w/v) sodium dodecyl sulphate (SDS)<br>20 % (v/v) glycerin<br>2 % (w/v) bromophenolblue<br>optional: + 10 % (v/v) 2-mercaptoethanol | |
| SDS running buffer 10x | 250 mmol/l TRIS<br>1.92 mol/l glycine<br>10 % (w/v) SDS | |
| separation gel buffer | 1.5 mol/l TRIS<br>0.4 % (w/v) SDS | 8.8<br>adjusted with HCl |
| stacking gel buffer | 0.5 mol/l TRIS<br>0.4 % (w/v) SDS | 6.8<br>adjusted with HCl |

### 3.1.4 Cell culture media and reagents

**Table 3: Media composition and other reagents used for cell culture application in this thesis.**

| medium | composition | application |
|---|---|---|
| DC medium | RPMI 1640 (Gibco®; Invitrogen, Darmstadt)<br>+ 10 % (v/v) foetal calf serum (FCS) (Lot: 1088G) (Biochrom, Berlin)<br>+ 10 mmol/l HEPES<br>+ 1 mmol/l sodium pyruvate<br>(Sigma-Aldrich, Steinheim)<br>+ 1 % (v/v) penicillin/ streptomycin/ L-glutamine<br>+ 0.1 mmol/l 2-mercaptoethanol<br>(Sigma-Aldrich, Steinheim) | murine BMDCs |
| Ficoll | Biocoll density 1.077 g/ml<br>(Biochrom, Berlin) | iDCs, mDCs |
| human DC medium | CellGro® GMP serum-free DC-medium<br>(CellGenix, Freiburg) | iDCs, mDCs |
| LSM 1077 | Lymphocyte Separation Medium<br>(PAA Laboratories GmbH, Cölbe) | human macrophages |
| macrophage medium | RPMI<br>+ 10 % (v/v) FCS<br>+ 1 % (v/v) penicillin/streptomycin/L-glutamine<br>+ 10 mmol/l HEPES<br>+ 0.05 mmol/l 2-mercaptoethanol | human macrophages |
| macrophage wash medium | PBS<br>+ 5 % (v/v) macrophage medium | human macrophages |
| proliferation medium | RPMI 1640<br>+ 5 % (v/v) FCS (Lot: 105K3396)<br>(Sigma-Aldrich, Steinheim)<br>+ 1 % (v/v) penicillin/streptomycin/L-glutamine<br>+ 0.05 mmol/l 2-mercaptoethanol | murine T-cells and APCs |
| red blood cell lysis buffer 1x | 10x Lysing buffer BD Pharm lyse<br>diluted 1:10 with water | all murine cells |

| medium | composition | application |
|---|---|---|
| wash medium | RPMI 1640<br>+ 5 % (v/v) FCS (Lot: 0434H)<br>(Biochrom, Berlin)<br>+ 1 % (v/v) penicillin/streptomycin/L-glutamine<br>+ 0.05 mmol/l 2-mercaptoethanol | murine T-cells and APCs |

### 3.1.5 Proteins

**Table 4: Proteins used for cell culture or as ELISA standard in this study.**

| protein | application | origin |
|---|---|---|
| mIFN-γ | ELISA | self-prepared standard from cell culture supernatants |
| mitomycin C | APCs | Sigma-Aldrich (Steinheim) |
| prostaglandin $E_2$ ($PGE_2$) | mDC culture | Cayman Chemical (Ann Arbor, MI, USA) |
| rhGM-CSF | human macrophage culture | Leukine |
| rhGM-CSF | iDC culture | CellGenix (Freiburg) |
| rhIL-1β | mDC culture | Peprotech (Hamburg) |
| rhIL-4 | iDC culture | CellGenix (Freiburg) |
| rhM-CSF | human macrophage culture | R&D Systems (Wiesbaden) |
| rhTNF-α | mDC culture | Peprotech (Hamburg) |
| rmGM-CSF | BMDC culture | R&D Systems (Wiesbaden) |
| rmIL-2 | ELISA | Peprotech (Hamburg) |
| rmIL-4 | ELISA | Peprotech (Hamburg) |
| rmIL-6 | ELISA | BD Biosciences (Heidelberg) |
| rmIL-10 | ELISA | BD Biosciences (Heidelberg) |
| rmIL-17A | ELISA | Peprotech (Hamburg) |

### 3.1.6 Antibodies

#### 3.1.6.1 Primary antibodies

**Table 5: Primary antibodies used in this thesis.**

| antibody | clone | application | origin |
|---|---|---|---|
| anti-CD36 antibody | JC63.1 | blocking | abcam (Cambridge, UK) |
| anti-chicken egg albumin (mouse IgG1) | OVA-14 | ELISA | Sigma-Aldrich (Steinheim) |
| anti-dinitrophenyl antibody (mouse IgE) | SPE-7 | ELISA | Sigma-Aldrich |
| anti-EEA-1 rabbit pAb | polyclonal | immunocytochemistry (ICC) | Merck Calbiochem (Darmstadt) |
| anti-human CD206 (MMR) PE | 19.2 | flow cytometry | eBioscience (Frankfurt a.M.) |
| anti-human CD36 FITC | NL07 | flow cytometry | eBioscience |
| anti-human CD80 (B7-1) PE | 2D10.4 | flow cytometry | eBioscience |
| anti-human CD86 (B7-2) PE | IT2.2 | flow cytometry | eBioscience |
| anti-human HLA-DR PE | L243 | flow cytometry | eBioscience |
| anti-human SR-AI/MSR1-PE | 351615 | flow cytometry | R&D Systems (Wiesbaden) |
| anti-mouse CD11b PE | M1/70 | flow cytometry | eBioscience |
| anti-mouse CD11c APC | N418 | flow cytometry | eBioscience |
| anti-mouse CD16/CD32 purified | 93 | flow cytometry | eBioscience |
| anti-mouse CD4 PE | GK1.5 | flow cytometry | eBioscience |
| anti-mouse CD80 (B7-1) FITC | 16-10A1 | flow cytometry | eBioscience |
| anti-mouse CD86 (B7-2) FITC | GL1 | flow cytometry | eBioscience |
| anti-mouse CD8a PE | 53-6.7 | flow cytometry | eBioscience |
| anti-mouse IFN-γ purified | R4-6A2 | ELISA | eBioscience |
| anti-mouse IFN-γ Biotin | XMG1.2 | ELISA | eBioscience |
| anti-mouse IL-17A Biotin | eBio17B7 | ELISA | eBioscience |
| anti-mouse IL-17A purified | eBio17CK15A5 | ELISA | eBioscience |
| anti-mouse IL-4 Biotin | BVD-24G2 | ELISA | eBioscience |
| anti-mouse IL-4 purified | 11B11 | ELISA | eBioscience |

| antibody | clone | application | origin |
|---|---|---|---|
| anti-mouse IL-6 Biotin | MP5-32C11 | ELISA | eBioscience |
| anti-mouse IL-6 purified | MP5-20F3 | ELISA | eBioscience |
| anti-mouse MHC Class II (I-A/I-E) FITC | M5/114.15.2 | flow cytometry | eBioscience |
| anti-mouse/rat CD40 FITC | HM40-3 | flow cytometry | eBioscience |
| Biotin anti-mouse IL-2 | JES6-5H4 | ELISA | BioLegend (Fell) |
| Biotin rat anti-mouse IgE | R35-118 | ELISA | BD Pharmingen (Heidelberg) |
| goat anti-mouse IgG1-HRP | polyclonal | ELISA | Invitrogen (Darmstadt) |
| goat anti-mouse IgG2a-HRP | polyclonal | ELISA | Invitrogen |
| mouse anti-CEL | 4F5 | ELISA | kind gift of Prof. Ryoji Nagai (Tokyo, Japan) |
| mouse anti-CML | 6D12 | ELISA | kind gift of Prof. Ryoji Nagai |
| mouse anti-GA-pyridine | 2A2 | ELISA | kind gift of Prof. Ryoji Nagai |
| mouse IgG1 κ isotype control PE | P3.6.2.8.1 | flow cytometry | eBioscience |
| mouse IgG2a κ isotype control PE | eBM2a | flow cytometry | eBioscience |
| mouse IgG2b κ isotype control PE | eBMG2b | flow cytometry | eBioscience |
| mouse IgM isotype control FITC | 11E10 | flow cytometry | eBioscience |
| normal mouse IgG | polyclonal | immunocytochemistry | Santa Cruz (Heidelberg) |
| purified anti-mouse IL-2 | JES6-1A12 | ELISA | BioLegend (Fell) |
| rabbit IgG isotype control FITC | polyclonal | flow cytometry | eBioscience |
| rat IgG1 isotype control FITC | eBRG1 | flow cytometry | eBioscience |
| rat IgG2a κ isotype control FITC | eBR2a | flow cytometry | eBioscience |
| rat IgG2b κ isotype control FITC | eB149/10H5 | flow cytometry | eBioscience |
| SR-BI antibody [DyLight488] | polyclonal | flow cytometry | Novus Biologicals (Cambridge, UK) |

### 3.1.6.2 Secondary antibodies

**Table 6: Secondary antibodies used in this thesis.**

| antibody | application | origin |
|---|---|---|
| anti-mouse IgG-HRP | ELISA | Sigma-Aldrich (Steinheim) |
| anti-mouse IgA-FITC | flow cytometry | abcam (Cambridge, UK) |
| AlexaFluor®488 goat anti-rat IgG (H+L) | flow cytometry | Invitrogen (Darmstadt) |
| Cy3-goat F(ab') fragment anti-rabbit IgG | immunocyto-chemistry | Jackson ImmunoResearch (Suffolk, UK) |
| Streptavidin-HRP | ELISA | eBioscience (Frankfurt a.M.) |

### 3.1.7 Mice

**Table 7: Mice strains used in this thesis.**

| genotype | short form | genetic background | reference |
|---|---|---|---|
| BALB/c | | wild type (wt) | |
| C57BL/6J | | wt | |
| C.Cg-Tg(DO11.10)10Dlo/J | DO11.10 | BALB/c | Murphy et al.(*86*) |
| C57BL6-Tg(TcraTcrb)1100Mjb/J | OT-I | C57BL/6 | Hogquist et al.(*87*) |
| B6.Cg-Tg(TcraTcrb)425Cbn/J | OT-II | C57BL/6 | Barnden et al.(*88*) |
| B6.Cg-Msr1$^{tm1Csk}$/J | SR-A$^{-/-}$ | C57BL/6 | Suzuki et al.(*89*) |

BALB/c mice and C57BL/6J mice were purchased from Charles River Laboratories (Kisslegg). Breeding pairs of the genetically modified mice were originally bought at Jackson Laboratories (Bar Harbour, ME, USA) and bred in the mouse breeding facility of the Paul-Ehrlich-Institut according to the German legislation.

### 3.1.8 Software

The analysis of the data, excluding flow cytometric analyses, was done using the program GraphPad Prism 5.04 (GraphPad Software Inc., La Jolla, CA, USA)

The data generated by the flow cytometers with BD FACSDiva Software v6.1.3 (BD Biosciences, Heidelberg) were exported and analyzed with FlowJo v7.6.3 (TreeStar Inc., Ashland, OR, USA).

SoftMax Pro 5.2 (Molecular Devices Corp., Sunnyvale, CA, USA) was used for measurement of plates at the ELISA reader.

Densitometric analysis of Coomassie-stained gels after SDS-PAGE was performed with Totallab TL120 v2006.

Statistical analysis of the data was performed with IBM SPSS statistics (IBM, Chicago, IL, USA) and either analysis of variance followed by Dunnett's test or for data of individual mice Mann-Whitney test was used. A *p* value below 0.05 was considered significant.

## 3.2 Methods

### 3.2.1 Preparation of AGE-OVA and AGE-BSA

Crude glycated ovalbumin (AGE-OVA) and crude glycated bovine serum albumin (AGE-BSA) were prepared using a protocol established by Gasic-Milenkovic et al.(*90*) In detail, 1 mmol/l endotoxin-free OVA (Seikagaku Corporation, Tokyo, Japan) or 1 mmol/l BSA (Sigma-Aldrich, Steinheim) were incubated with 1 mol/l glucose (VWR, Darmstadt) in 100 mmol/l sodium phosphate buffer for six weeks at 50 °C. Afterwards, excess glucose was removed by extensive dialysis against PBS. OVA or BSA incubated under the same conditions but without glucose served as controls and is referred to as incubated OVA (inc. OVA) or incubated BSA (inc. BSA) in the following.

100 mmol/l sodium phosphate buffer pH 7.4: 19 ml phosphate buffer A
+ 81 ml phosphate buffer B
+ 100 ml $H_2O$

### 3.2.2 Selective modification of OVA with distinct glycation structures

The selective modification of endotoxin-free OVA with the glycation structures CEL, CML, MG-H1 or pyrraline was performed by Dr. Anne Wellner from Technische Universität (TU) Dresden.

Modification of OVA with CEL or CML as well as arginine modification with MG-H1 was performed according to Glorieux et al.(*91*) Briefly, to a solution of 20 mg/ml OVA in 0.2 mol/l sodium phosphate buffer 15 mol pyruvic acid per mol lysine for carboxyethylation or 5 mol glyoxylic acid per mol lysine for carboxymethylation were added. After adjusting the pH to 7.4 with 0.5 mol/l NaOH and addition of 41 mmol $NaBH_3CN$ for CEL- or 8.8 mmol $NaBH_3CN$ for CML-modification, respectively, the solution was heated for 20 h at 40 °C.

Arginine modification with MG-H1 was carried out by incubating a solution of 10 mg/ml OVA and 2 mol methylglyoxal (MGO) per mol arginine residues in OVA in 0.067 mol/l sodium phosphate buffer for 30 min at 40 °C.

The method for modification of OVA with pyrraline was established by Henle and Bachmann.(*92*) Briefly, 4 mg/ml OVA were dissolved in 0.1 mol/l sodium acetate buffer and 3-desoxyglucosulose (3-DG) was added, resulting in a molar ratio of 3-DG to lysine of 4:1. The solution was lyophilized and the mixture was incubated in a dry state at 70 °C for 10 min, 30 min or 4 h, respectively.

Before analysis, all samples were extensively dialyzed against water and lyophilized. Overall modification of lysine and arginine residues was assessed with amino acid analysis as described by Henle et al.(*93, 94*) This method was also applied for determining the level of MG-H1 conjugated to OVA. The levels of CEL or CML were determined with gas chromatography-mass spectrometry (GC-MS) analysis after acid hydrolysis as described by Wellner et al.(*95*) The glycation structure pyrraline was detected using reversed phase high performance liquid chromatography with diode array detector (RP-HPLC/DAD) as described by Förster et al.(*96*)

### 3.2.3 Determination of protein concentration with BCA

The principle for quantification of proteins using bicinchoninic acid (BCA) is based on the Biuret reaction.(*97*) In alkaline solution $Cu^{2+}$ ions are reduced by proteins to $Cu^{+}$ ions. In a second step, $Cu^{+}$ ions form violet coloured complexes with BCA, which can be detected using a photometer.(*97*)

The protein concentration was determined using BCA Protein Assay Kit (Thermo Scientific, Nidderau) according to the manufacturer's instructions. If necessary, protein and standard samples were diluted in PBS. Then, a volume of 25 µl per sample was transferred to a 96-well microtiter plate (NUNC, Wiesbaden) in duplicate. The working reagent was prepared by mixing 50 parts of solution A and 1 part of solution B. 200 µl working reagent were added to the samples and the plate was

incubated for 30 min at RT in the dark on an orbital shaker. The absorbance at a wavelength of 562 nm was measured by an ELISA reader.

Solution A: sodium carbonate, sodium bicarbonate, bicinchoninic acid and sodium tartrate in 0.1 mol/l NaOH

Solution B: 4 % (w/v) $Cu_2SO_4$ in $H_2O$

### 3.2.4 Gel electrophoresis

The basic principle of gel electrophoresis is the separation of different molecules by means of their different electrophoretic mobility.(*97*) The most commonly used technique for the separation of proteins is sodium dodecyl sulphate-polyacrylamide gel electrophoresis (SDS-PAGE), which separates protein-SDS complexes according to their molecular weight.(*97*) Here, the discontinuous SDS-PAGE without acrylamide gradient first described by Laemmli was used.(*98*)

The protein samples were loaded with SDS by incubation of the sample containing SDS loading buffer for 3 min at 95 °C. The cooled samples were shortly centrifuged before loading on the gel, which consisted of a 4.5 % stacking gel and either 7.5 % or 10 % separation gels. Electrophoresis was carried out at a constant voltage of 100 V in SDS running buffer. The gels were washed in water for 1 h to remove the SDS, which would be interfering with the dye Coomassie Brilliant Blue. The gels were stained with GelCode Blue Stain Reagent (Thermo Scientific, Nidderau) for 2 h. Unbound dye was removed by washing the gels in water for at least 1 h. Afterwards, the gels were scanned for documentation.

7.5 % separation gel:
- 9.0 ml $H_2O$
- 4.5 ml acrylamide (Rotiphorese® Gel 40; Carl Roth, Karlsruhe)
- 4.5 ml separation gel buffer
- 80 µl 10 % (w/v) ammoniumpersulphate (APS)
- 15 µl *N,N,N',N'*-tetramethylethylenediamine (TEMED)

10 % separation gel:
- 7.5 ml $H_2O$
- 6 ml acrylamide (Rotiphorese® Gel 40)
- 4.5 ml separation gel buffer
- 80 µl 10 % (w/v) APS
- 15 ml TEMED

4.5 % separation gel: 3.6 ml $H_2O$
0.9 ml acrylamide (Rotiphorese® Gel 40)
1.5 ml stacking gel buffer
20 µl 10 % (w/v) APS
15 µl TEMED

Molecular weight marker: PageRuler Plus Prestained Protein Ladder (#26619; Thermo Scientific, Nidderau)
PageRuler Prestained Protein Ladder (#26616; Thermo Scientific)

### 3.2.5 Enzyme-linked immunosorbent assay (ELISA)

The basic principle of an ELISA is the detection of a specific protein or structure via antigen-antibody interaction.(*99*) In the indirect ELISA system, the antigen is bound to the surface of an ELISA microtiter plate and then detected by an antigen-specific primary antibody together with a matching enzyme-conjugated secondary antibody.(*99*) In the final step, an enzyme, mainly peroxidases are used, converses a colorimetric substrate for detection by optical means.(*99*)
The detection of a specific antigen from a crude mixture of proteins can be done using a sandwich ELISA, where the plate is coated with an antigen-specific capture antibody.(*99*) In the next step, the antigen is applied and afterwards, it is detected as already described for the indirect ELISA.(*99*)

All incubation steps were carried out at RT and 80 rpm (rounds per minute) on a shaker unless stated otherwise. Between the incubation steps, the plates were washed three times with 150 µl/well ELISA washing buffer.

#### 3.2.5.1 Detection of AGE-structures with ELISA

For the detection of AGE-structures with ELISA according to Ilchmann et al., ELISA plates (Microlon600; greiner bio-one, Frickenhausen) were coated with 50 µl/well of a 5-fold dilution series (1 mg/ml to 0.5 ng/ml) of modified OVAs in ELISA coating buffer at 4 °C overnight (o/n).(*71*) Unbound binding sites of the plates were blocked by incubation with 100 µl/well ELISA blocking buffer for 1 h. Afterwards, the plates were incubated for 2 h with 50 µl/well of 1 µg/ml primary antibody recognizing the glycation structure in ELISA assay buffer. Available were mouse monoclonal antibodies (mAb) raised against the glycation structures CEL, CML or glycolaldehyde-pyridine

(GA-pyridine). These primary antibodies were detected by incubation of the plate with 50 µl/well horseradish peroxidase (HRP-)conjugated anti-mouse IgG diluted 1:20,000 in ELISA assay buffer for 1 h. Subsequently, 100 µl/well of substrate solution was added and the plates were incubated for up to 30 min on the shaker in the dark. The substrate oxidized by the peroxidase was 3,3',5,5'-tetramethylbenzidine (TMB) (555214; BD Biosciences, Heidelberg). The enzymatic reaction was stopped by addition of 50 µl/well of 0.5 mol/l $H_2SO_4$. The absorbance at a wavelength of 450 nm and a reference wavelength of 630 nm was measured by an ELISA reader. For evaluation, the reduced absorbance, i.e. the difference of the absorbance values at 450 nm and 650 nm, was used.

#### 3.2.5.2 Detection of OVA-specific IgE, IgG1 and IgG2a antibodies in the sera of mice

Detection of OVA-specific IgE, IgG1 or IgG2a antibodies in sera was performed using a sandwich ELISA system. ELISA plates were coated with 0.1 µg/ml native OVA in ELISA coating buffer o/n at 4 °C. Wells for the IgE standard curve were coated o/n at 4 °C with 0.5 µg/ml purified anti-mouse IgE mAb. After blocking of free binding sites by incubation for 1 h with 100 µl/well ELISA blocking buffer, the plates were incubated with 50 µl/well sample for 2 h. Samples were sera from mice sensitized with OVA or from sensitized and EW-diet fed mice diluted in ELISA assay buffer or standard solutions. A 2-fold dilution series in ELISA assay buffer ranging from 1 U/ml to 2 mU/ml of mouse anti-dinitrophenyl IgE was applied for the IgE standard curve. The standard curves for IgG1 and IgG2a were prepared using a 2-fold dilution series in ELISA assay buffer ranging from 62.5 mU/ml to 0.12 mU/ml of mouse anti-OVA IgG1 mAb. Afterwards, the plates were incubated for 1 h with 50 µl/well of Biotin-anti-mouse IgE (1:1000), HRP-anti-mouse IgG1 (1:4000) or HRP-anti-mouse IgG2a (1:4000) diluted in ELISA assay buffer as primary antibodies, respectively. Incubation with Streptavidin-HRP diluted 1:2000 in ELISA assay buffer for 30 min was only necessary for the detection of IgE antibodies.

Substrate reaction and the following steps were performed as already described in chapter 3.2.5.1.

#### 3.2.5.3 Detection of cytokines in cell culture supernatants

Cytokines in cell culture supernatants were detected using a sandwich ELISA system with compatible antibody pairs offered by the manufacturers. ELISA plates were coated o/n at 4 °C with 50 µl/well of 0.5 µg/ml capture antibody, a purified antibody specific for the respective cytokine, in ELISA coating buffer. Free binding sites of the plates were blocked by incubation with 100 µl/well ELISA blocking buffer for 1 h. As standards for the quantification of the cytokine levels a 2-fold dilution

series ranging from 4 ng/ml to 8 pg/ml of the respective recombinant cytokine in medium was prepared. The plates were incubated for 2 h with 50 µl/well sample in duplicate, i.e. (un)diluted cell culture supernatants or standard dilution series. The captured cytokine was detected by incubation of the plates for 1 h with 50 µl/well of 0.5 µg/ml Biotin-conjugated cytokine-specific antibody in ELISA assay buffer. Subsequently, the plates were incubated with 50 µl/well Streptavidin-HRP diluted 1:4000 in ELISA assay buffer for 30 min in the dark.

Substrate reaction and the following steps were performed as already described in chapter 3.2.5.1.

### 3.2.6 Measurement of protein secondary structure with circular dichroism spectroscopy

Circular dichroism spectroscopy (CD-spectroscopy) is based on the differential absorbance of circular polarized light by optic active substances, like proteins.(*97*) The secondary structure elements of proteins show different absorbance of the left and the right circular polarized component of circular polarized light.(*97*) The difference of both absorbance values, which is called, ellipticity, is measured by a CD-spectrometer as a function of the wavelength.(*97*)

Salt was removed by dialyzing the sample o/n against plenty 10 mmol/l phosphate buffer pH 7.4. After initialization of the spectrometer, baseline correction was performed by measuring the spectrum of 10 mmol/l phosphate buffer pH 7.4 in the range of 185 nm to 255 nm. Then a fast test measurement of the sample was run to check that salt has been efficiently removed and protein concentration was appropriate. For the regular measurement, the sample was scanned ten times with the settings listed below in table 8.

**Table 8: Settings used for measurement of CD-spectra.**

| **parameter** | **setting** |
|---|---|
| start wavelength | 255 nm |
| end wavelength | 185 nm |
| scanning mode | continuous |
| scanning speed | slow: 50 nm/min |
| | fast test: 500 nm/min |
| bandwidth | 1.0 nm |
| accumulation | 10 (or 1 for preliminary test) |

The data was evaluated by calculating the mean residual ellipticity ($\Theta_{MRW}$) according to the formula below and plotted against the wavelength.

$$\Theta_{MRW} = \frac{100 \cdot \theta}{N \cdot c \cdot d}$$

θ: measured ellipticity in mdeg
N: number of amino acid residues
c: protein concentration in mmol/l
d: path length in cm

| | |
|---|---|
| 10 mmol/l phosphate buffer pH 7.4: | 19.7 ml CD-buffer A |
| | 80.3 ml CD-buffer B |
| | ad 1 l with $H_2O$ |

### 3.2.7 Labelling of proteins with FITC

The uptake of an antigen by dendritic cells and the subsequent antigen processing inside the cell can only be elucidated if the antigen is labelled with a fluorophore. The fluorophore fluorescein isothiocyanate (FITC) can be bound to proteins by formation of a stable thiourea bond between free amino residues of the protein and the isocyanate group of the dye. The molar ratio of bound FITC to the protein, the molar FITC/protein-ratio, can be easily determined by absorbance measurements and was of great interest, because for the comparison of the antigen uptake of different proteins the FITC/protein-ratio in all samples needs to be similar.

The labelling of native OVA, inc. OVA, all modified OVA samples, native BSA, inc. BSA and AGE-BSA with FITC was performed with the FluoroTag FITC Conjugation Kit (FITC1; Sigma-Aldrich, Steinheim).

One vial of FITC was reconstituted in 0.1 mol/l sodium carbonate buffer pH 9.0 and solutions with different FITC concentrations shown in table 9 were prepared. For the small scale labelling procedure 50 µl FITC-solution were added dropwise to 200 µl of protein solution (5 mg/ml in 0.1 mol/l sodium carbonate buffer pH 9.0). The reaction mixture was incubated for 2 h at RT in the dark. The sample was applied to an equilibrated Sephadex G25M column for the separation of the labelled protein and excess dye. The flow through was collected followed by elution of the labelled protein with PBS in ten

fractions à 250 µl. During elution two distinct yellow bands were visible, the lower one containing the labelled protein and the upper one the unreacted dye.

The absorbance of the fractions at a wavelength of 280 nm was measured to determine protein content. Fractions with an absorbance value above 0.2 were pooled and the molar FITC/protein-ratio was determined. The samples were stored for several days at 4 °C in solution or lyophilized aliquots were stored at -80 °C for long-term storage.

**Table 9: Prepared FITC-solutions for the labelling reaction.**

| FITC concentration | 0.1 mol/l sodium carbonate buffer pH 9.0 | reconstituted FITC (20:1) |
|---|---|---|
| 20:1 | 2 ml | 1 vial |
| 10:1 | 500 µl | 500 µl |
| 5:1 | 750 µl | 250 µl |

Determination of the molar FITC/protein-ratio:

For the determination of the molar FITC/protein-ratio with the formula below the absorbance of the labelled proteins at 280 nm and at 495 nm was measured.

$$FITC/protein = \frac{M_{protein}}{M_{FITC}} \cdot \frac{A_{495} \cdot P_{280}^{0.1\%}}{F_{495}^{0.1\%} \cdot [A_{280} - 0.35 \cdot A_{495}]} = C \cdot \frac{A_{495}}{A_{280} - 0.35 \cdot A_{495}}$$

Where: $C = \frac{M_{protein}}{M_{FITC}} \cdot \frac{P_{280}^{0.1\%}}{F_{495}^{0.1\%}}$ is a protein-specific absolute term.

$M_{protein}$ is the molecular weight of the protein.

$M_{FITC}$: is the molecular weight of FITC and is 389 g/mol.

$P_{280}^{0.1\%}$: is the absorbance of 1 mg/ml protein at 280 nm and is 0.686 for OVA or 0.6 for BSA.

$F_{495}^{0.1}$: is the absorbance of bound FITC at 495 nm at pH 13.0 and is 195.

$A_{495}$: measured absorbance at 495 nm.

$A_{280}$: measured absorbance at 280 nm.

### 3.2.8 Cell culture

All cell culture works were carried out under sterile conditions in a laminar flow cabinet. The cells were incubated at 37 °C with 5 % $CO_2$ and a relative humidity of 80 % if not stated otherwise.

#### 3.2.8.1 Culture of murine cells

##### 3.2.8.1.1 Preparation of murine bone marrow-derived dendritic cells (BMDCs)

The sacrificed mice were disinfected using 70 % ethanol. The bones were carefully removed from the hind legs. Using a fresh pair of forceps, the bones were shortly disinfected in 70 % ethanol and afterwards washed in RPMI 1640. The ends of the bones were cut off with a fresh scissor and the bone marrow was rinsed out using a syringe with a 26G needle filled with 5 ml DC medium. A single cell suspension was prepared by pipetting and then given through a 70 µm cell strainer (BD Biosciences, Heidelberg). The cells of one leg were pooled and centrifuged at 1100 rpm and 4 °C for 6 min. All following centrifugation steps were carried out with these settings. The supernatant was discarded and the pellet was loosened by shaking. Lysis of erythrocytes was performed by addition of 1.5 ml red blood cell lysis buffer 1x per leg followed by incubation for 1 min at RT. To stop lysis, 10 ml DC medium were added and the cells were centrifuged. The cells were washed twice with DC medium. In a final volume of 5 ml DC medium $5 \cdot 10^6$ cells were seeded in a T25 cell culture flask (NUNC, Wiesbaden) and 100 ng/ml rmGM-CSF (recombinant murine granulocyte macrophage-colony stimulating factor) were added.

The media needed to be exchanged at day 3, day 6 and day 7 of culture.

The differentiated bone marrow-derived dendritic cells (BMDCs) were harvested on day 8 of culture using a cell scraper (TPP, Trasadingen, CH). The cells were washed once with DC medium and the cell number was determined.

##### 3.2.8.1.2 Assessment of BMDC maturation

The maturation of BMDCs upon antigen stimulation was assessed by culturing $1 \cdot 10^6$ BMDCs from C57BL/6 mice, generated as described in chapter 3.2.8.1.1, in the presence of 50 µg/ml antigen in a cell culture plate (greiner bio-one, Frickenhausen) for 20 h. Antigens used in this assay were all forms of OVA as well as 1 µg/ml LPS, which served as positive control. The cell culture supernatants were collected for cytokine measurement with ELISA according to chapter 3.2.5.3 and the cells were stained for expression of the co-stimulatory molecules CD40, CD80, CD86 as well as for MHC class II

molecules as described in chapter 3.2.9.2. Afterwards, the cells were stained for the DC cell surface markers CD11b and CD11c according to chapter 3.2.9.4.

#### 3.2.8.1.3 Assessment of antigen uptake by BMDCs with flow cytometric analysis

BMDCs from C57BL/6 mice or B6.Cg-Msr1 mice were prepared as described in chapter 3.2.8.1.1 and for this assay $1 \cdot 10^6$ cells in a volume of 200 µl were seeded into a 24-well cell culture plate (greiner bio-one, Frickenhausen). After the addition of 200 µl of antigen solution, the cells were incubated for 15 min at 37 °C. As antigens FITC-labelled forms of all OVA samples as well as FITC-labelled native BSA, inc. BSA and AGE-BSA were used. Then, the cells were scraped and transferred into a FACS-tube (BD Biosciences, Heidelberg). The cell culture plate was washed twice with PBS, the washing solution was added to the respective cells and then the cells were centrifuged at 1100 rpm and 4 °C for 5 min. After blocking of $F_c$-receptor binding according to chapter 3.2.9.1, the cells were stained for the surface markers CD11b and CD11c as described in chapter 3.2.9.4 and analyzed with flow cytometry on the same day.

The contribution of several receptors in antigen uptake was analyzed with specific ligands inhibiting antigen-binding. Therefore, BMDCs were pre-incubated with the respective inhibitor listed in table 10 for 30 min at 37 °C before addition of the antigen.

**Table 10: Receptors, their inhibitors and the respective inhibitor concentration used to elucidate receptor contribution to antigen uptake.**

| receptor | inhibitor | amount of inhibitor used |
|---|---|---|
| CD36 | blocking antibody | 2 µg/ml |
| galectin-3 | lactose | 150 mmol/l |
| MR (CD206) | mannan | 3 mg/ml |
| SR-BI | phosphatidylserine | 100 µmol/l |
| SR-BI | BLT-1 | 10 µmol/l or 1 µmol/l |

#### 3.2.8.1.4 Cell preparation for analysis with a confocal microscope

A confocal microscope, also called laser scanning microscope (LSM), is used to investigate (co-)localisations of proteins inside cells.(*97*) Before microscopic analysis, the proteins are directly conjugated with a fluorescent dye or stained directly or indirectly with antibodies labelled with a fluorophore.(*97*)

In an LSM, a high resolution is achieved by focussing the laser light in one point of the sample.(*97*) The emitted fluorescence of the target passes through a confocal pinhole before reaching the detector, which is usually a photomultiplier.(*97*) Confocal means that the pinhole is in the conjugate plane of the focus point in the sample.(*97*) Hence, emitted light outside the focus plane is rejected by the pinhole and does not reach the detector.(*97*) The images are generated by point-to-point scattering of the sample followed by a reconstruction of the detector signals by a computer.(*97*)

For cell analysis with a confocal microscope, 12 mm round cover slips (Carl Roth, Karlsruhe) were placed in a 24-well cell culture plate and 400 µl $1.25 \cdot 10^6$ BMDCs/ml in DC medium, were added. During 1 h incubation at 37 °C, the cells could adhere on the cover slips. Afterwards, fresh DC medium was added and BMDCs were incubated with 10 µg/ml of FITC-labelled OVA sample for 15 min at 37 °C. All following steps were carried out in the dark at RT and between all single steps the cells were washed three times with plenty PBS. The cells were fixed after washing by incubation for 20 min with 4 % (w/v) paraformaldehyde (PFA) (Thermo Scientific, Nidderau) in PBS. Then blocking and permeabilization was performed by incubation of the cells for 1 h in permeabilization-buffer. The cells were incubated with 5 µg/ml primary antibody for 1 h and afterwards with 5 µg/ml secondary antibody for 30 min, both diluted in ICC-assay buffer. For staining of endosomal compartments, polyclonal rabbit anti-early endosomal antigen-1 (EEA-1) IgG together with Cy3-goat F(ab') fragment anti-rabbit IgG as secondary antibody were used. The nucleus was stained by incubation of the cells with 0.125 µg/ml 4',6-diamidino-2-phenylindole (DAPI) in ICC-assay buffer for 7 min. The cover slips were mounted with fluorescence mounting medium (S3023; DAKO, Hamburg) on SuperFrost® microscope slides (VWR, Darmstadt). After drying, the slides were stored at 4 °C in the dark until analysis with a LSM 510 (Carl Zeiss, Jena).

#### 3.2.8.1.5 Preparation of splenocyte or lymph node cell suspension for T-cell isolation

The sacrificed mice were disinfected in 70 % ethanol. The spleen or the lymph nodes (LN) of interest were removed and placed in a petri dish containing wash medium. The cells were mechanically released by pressing the organ with the plunger of a syringe. The cell suspension was filtered through a 70 µm cell strainer and centrifuged. All centrifugation steps were carried out at 1300 rpm and 4 °C for 10 min. After centrifugation, red blood cell lysis was carried out for spleens only by adding 1.5 ml red blood cell lysis buffer 1x per spleen and incubating for 1 min to 2 min at RT. The lysis was stopped by addition of 10 ml wash medium and the cells were centrifuged. Splenocytes and LN cells were washed twice with 10 ml wash medium, respectively, and afterwards resuspended in 5 ml MACS-buffer before determining the cell number.

#### 3.2.8.1.6 Magnetic separation of $CD4^+$ or $CD8^+$ T-cells

The basic principle of magnetic cell sorting (MACS) is the separation of magnetically labelled cells from unlabelled ones. Therefore, cells become labelled with specific magnetic beads before the actual separation in a strong magnetic field using a special column is performed. The principle of positive selection was applied for $CD4^+$ T-cell separation, i.e. $CD4^+$ T-cells were retained in the magnetic field, whereas the flow-through and washing fractions contained non-$CD4^+$ cells. For elution of the labelled $CD4^+$ T-cells, the column needed to be removed from the magnetic field. The opposite, namely negative selection, was used for $CD8^+$ T-cell separation.

For T-cell isolation, either splenocyte or LN cell suspension (see 3.2.8.1.5) was centrifuged at 1300 rpm at 4 °C for 10 min and the supernatant was completely removed by pipetting.

Labelling of $CD4^+$ T-cells was performed by resuspending the cells in 90 µl MACS-buffer per $10^7$ cells and addition of 10 µl CD4 (L3T4) MicroBeads (130-049-201; Miltenyi Biotec, Bergisch-Gladbach) per $10^7$ cells. The mixture was incubated for 15 min in the fridge.

For $CD8^+$ T-cell isolation, the $CD8a^+$ T-cell isolation kit (130-090-859; Miltenyi Biotec, Bergisch-Gladbach) was used. Non-$CD8^+$ T-cells were labelled by resuspension of splenocytes in 40 µl MACS-buffer per $10^7$ cells followed by incubation with 10 µl Biotin-Antibody Cocktail per $10^7$ cells for 10 min in the fridge. After addition of 30 µl MACS-buffer per $10^7$ cells and 20 µl Anti-Biotin MicroBeads per $10^7$ cells, the cells were incubated for additional 15 min in the fridge.

The labelling reaction was stopped by addition of 1 ml to 2 ml MACS-buffer per $10^7$ cells and centrifugation at 1300 rpm and 4 °C for 10 min. The supernatant was completely removed by pipetting and the cells were resuspended in 500 µl MACS-buffer per $10^8$ cells. The suspension was applied to an equilibrated MACS LS column (130-042-401; Miltenyi Biotec, Bergisch-Gladbach) placed in the strong magnetic field of a QuadroMACS Separator (130-080-976; Miltenyi Biotec, Bergisch-Gladbach). The column was washed with plenty MACS-buffer. The flow-through and washing fractions contained unlabelled $CD8^+$ T-cells. For collection of $CD4^+$ T-cells, the column was removed from the magnetic field and labelled $CD4^+$ T-cells were eluted with 5 ml MACS-buffer. After washing once with cell culture medium, the cells were used in the respective assays.

The isolated $CD4^+$ T-cells and $CD8^+$ T-cells had a purity of over 90 % as was determined by flow cytometry as described in chapter 3.2.9.

#### 3.2.8.1.7 Co-culture of BMDCs with OVA-specific $CD4^+$ T-cells

This assay was used to assess the $CD4^+$ T-cell immunogenicity of the modified OVAs. BMDCs were prepared as described in chapter 3.2.8.1.1 and OVA-specific OT-II-derived or DO11.10-derived $CD4^+$ T-cells were prepared according to chapter 3.2.8.1.6. In the wells of a 96-well flat bottom cell culture plate (NUNC, Wiesbaden) $1.6 \cdot 10^5$ BMDCs/ml and $8 \cdot 10^5$ $CD4^+$ T-cells/ml were seeded and antigen solution was applied. The cells were stimulated with final concentrations of 2 µg/ml or 20 µg/ml of all modified OVAs including native OVA and inc. OVA as controls. Cells treated with medium only served as negative control.

Cell culture supernatants after 24 h and 72 h incubation were used for the determination of cytokine expression by ELISA as described in chapter 3.2.5.3

#### 3.2.8.1.8 Co-culture of BMDCs with OVA-specific $CD8^+$ T-cells

A co-culture of C57BL/6-derived BMDCs with OVA-specific OT-I-derived $CD8^+$ T-cells was used to investigate the $CD8^+$ T-cell immunogenicity of the modified OVAs.

The method of Burgdorf et al. was adapted with minor modifications.(*59*) Briefly, BMDCs, generated as described in chapter 3.2.8.1.1, were stimulated with 10 µg/ml LPS for 2 h at 37 °C. Afterwards, the cells were scraped, washed three times with DC medium and $6.25 \cdot 10^5$ BMDCs/ml were seeded into a 96-well round bottom cell culture plate (NUNC, Wiesbaden). Then the antigen solution, which has already been described in chapter 3.2.8.1.7, was added resulting in a final concentration of 20 µg/ml or 200 µg/ml of OVA and BMDCs were primed with antigen for 3 h at 37 °C. The cells were washed three times with plenty PBS (prewarmed to 37 °C in a water bath) and afterwards, the cells were re-equilibrated in 100 µl/well warm DC medium (37 °C). To this suspension, $1.25 \cdot 10^6$ $CD8^+$ T-cells/ml, isolated according to chapter 3.2.8.1.6, were added. The resulting co-culture was incubated at 37 °C for 20 h to 72 h. Cytokine expression in the cell culture supernatants was determined by ELISA as described in chapter 3.2.5.3.

#### 3.2.8.1.9 Assessment of $CD4^+$ T-cell proliferation using CFSE

Staining of cells with carboxyfluorescein diacetate succinimidyl ester is often used for analysis of cell proliferation.(*99*) The molecule is colourless extracellular and after diffusion into cells it is transformed into highly fluorescent carboxyfluorescein succinimidyl ester (CFSE).(*99*) This fluorescent dye is retained inside the cells by formation of conjugates with intracellular amines, mainly

proteins.(*99*) Upon cell division or proliferation approximately half of the conjugated proteins are transferred to the new cell and this can be detected with flow cytometry as shown in figure 5.(*99*)

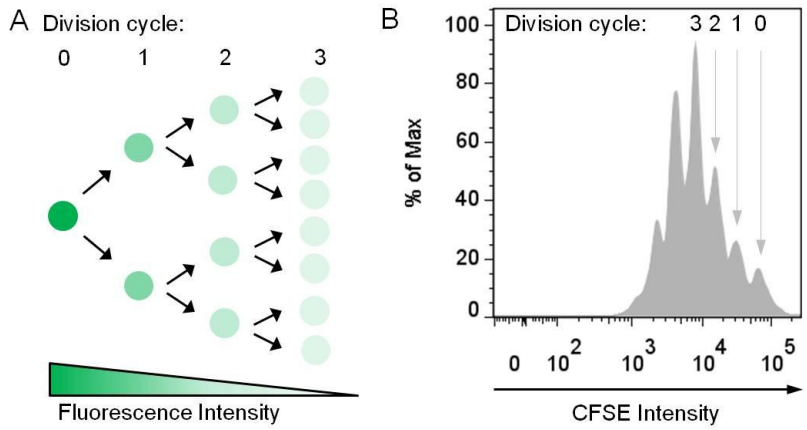


**Figure 5: Mechanism of CFSE division.** (A) Schematic illustration of CFSE dilution upon cell division. (B) Example of flow cytometric analysis of CFSE-stained proliferating cells. In the histogram, the parent generation (0) and five daughter generations are shown.

The proliferation of OVA-specific OT-II-derived or DO11.10-derived $CD4^+$ T-cells was analyzed using the CellTrace™ CFSE Cell Proliferation Kit (C34554; Life Technologies GmbH, Darmstadt) according to the manufacturer's instructions. Briefly, magnetically separated $CD4^+$ T-cells, prepared as described in chapter 3.2.8.1.6, were washed once with 5 ml PBS + 0.1 % (w/v) BSA (Sigma-Aldrich, Steinheim). The cell concentration was adjusted to $1 \cdot 10^6$ cells/ml with PBS + 0.1 % (w/v) BSA and 2 µl CFSE 5 mmol/l in dimethyl sulphoxide (DMSO) were added per 1 ml cell suspension. The mixture was incubated for 10 min at 37 °C in a water bath and the staining reaction was quenched by addition of 5 volumes of ice-cold DC medium followed by incubation of the cells for 5 min on ice. The cells were washed three times with 10 ml DC medium, respectively.

For the assessment of $CD4^+$ T-cell proliferation, $8 \cdot 10^5$ CFSE-stained $CD4^+$ T-cells/ml together with $1.6 \cdot 10^5$ BMDCs/ml were seeded into a 96-well flat bottom cell culture plate (NUNC, Wiesbaden) and the antigen solution was added. As antigens all forms of OVA in a final concentration of 2 µg/ml were used. After 96 h incubation, the cells were detached from the plate by short incubation with 25 µl/well of EDTA/trypsin at 37 °C followed by addition of 250 µl/well of cold DC-medium. The cells were transferred to a FACS tube and 1 ml FACS-buffer was added. Unspecific binding to $F_c$-receptors of the cells was blocked as described in chapter 3.2.9.1. The cells were then stained for CD4 according to chapter 3.2.9.2 and analyzed by flow cytometry on the same day.

#### 3.2.8.1.10 Assessment of $CD4^+$ T-cell proliferation using [methyl-$^3$H]thymidine

Proliferation of $CD4^+$ T-cells was also assessed by incorporation of the radioactive-labelled nucleotide thymidine.

For this assay, splenic antigen-presenting cells (APCs) were prepared from spleens of naive syngeneic mice as described in chapter 3.2.8.1.5 without lysis of the red blood cells. Incubation of $1 \cdot 10^8$ splenocytes with 50 µg/ml mitomycin C for 30 min at 37 °C in a water bath inhibited their proliferation ability and retained the antigen-presenting capacity. After washing three times with proliferation medium, $2 \cdot 10^6$ APCs/ml were seeded into a 96-well cell culture plate (NUNC, Wiesbaden) together with $5 \cdot 10^5$ $CD4^+$ T-cells/ml, which were isolated as described in chapter 3.2.8.1.6. The cells were stimulated with 100 µg/ml or 1000 µg/ml of native OVA, Pyr-OVA or AGE-OVA. After 72 h of culture, [methyl-$^3$H]thymidine (Perkin Elmer, Rodgau) was added to the cells at a final concentration of 0.025 nmol/l (equiv. to 0.5 µCi) and the cells were incubated for additional 20 h. The cells were transferred onto printed filter mats A (Perkin Elmer, Rodgau) and MeltiLex™A melt-on scintillator sheets (Perkin Elmer, Rodgau) for signal amplification were melted on. The filter mats were sealed in sample bags (Perkin Elmer, Rodgau), transferred into a cassette and the frequency of radioactive-labelled cells was counted by a scintillation counter (1450 Microbeta Liquid Scintillation and Luminescence counter; Perkin Elmer, Rodgau).

### 3.2.8.2 Culture of human cells

#### 3.2.8.2.1 Preparation of human dendritic cells

The preparation of human DCs is divided into two steps, first, the isolation of $CD14^+$ monocytes and second, the differentiation of monocytes into immature dendritic cells (iDCs).

For the isolation of human monocytes by Ficoll gradient centrifugation, 15 ml Ficoll were given into a 50 ml centrifugation tube. The disinfected blood bag was opened and the buffy coat was transferred into a T75 cell culture flask. The blood was diluted with PBS up to a volume of 200 ml. Then, Ficoll was carefully overlayed with 25 ml of diluted buffy coat. After centrifugation at 900 xg for 20 min without brake, different layers were visible as shown in figure 6. The small white one was composed of the cells of interest and was carefully transferred into a fresh centrifugation tube. MACS-buffer was added up to a volume of 50 ml and the cells were centrifuged at 2000 rpm and 4 °C for 10 min. The pellets were resuspended in 5 ml MACS-buffer and the cells of two tubes were pooled. Again, the cells were washed by addition of 40 ml MACS-buffer and centrifugation at 1200 rpm and 4 °C for 10 min. The pellets were pooled in 20 ml MACS-buffer and the cell number was determined.

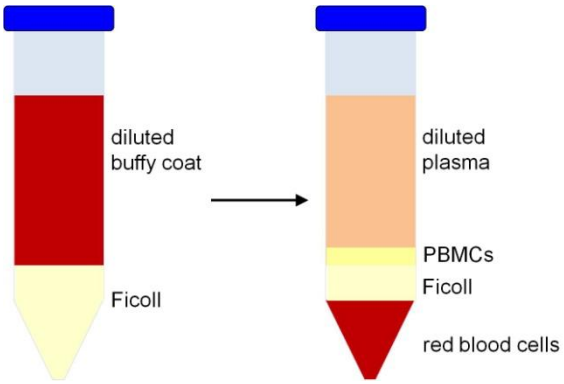


**Figure 6: Schematic picture of Ficoll gradient centrifugation for the separation of human PBMCs from buffy coat.**

The yield of the following MACS separation is about 5 %, so 20-times more cells than needed were used. The appropriate amount of cells was centrifuged at 300 xg and 4 °C for 10 min. After complete removal of the supernatant by pipetting, the cells were resuspended in 40 µl MACS-buffer per $10^7$ cells. Then 10 µl of CD14 MicroBeads (130-050-201; Miltenyi Biotec, Bergisch-Gladbach) per $10^7$ cells were added and the mixture was incubated for 15 min in the fridge. The reaction was stopped by addition of 500 µl MACS-buffer per $10^7$ cells and centrifugation at 300 xg and 4 °C for 10 min. The cells were resuspended in 500 µl MACS-buffer per $10^8$ cells and separation of $CD14^+$ cells was performed using an autoMACS® Pro Separator (Miltenyi Biotec, Bergisch-Gladbach) and the pre-installed method POSSELD. After addition of 4.5 ml human DC medium per 500 µl separated cells, the cell number was determined.

The cells were centrifuged at 1200 rpm and 4 °C for 5 min and afterwards 1 ml of a cell suspension with $1 \cdot 10^6$ cells/ml in human DC medium supplemented with 1000 U/ml rhIL-4 and 1000 U/ml rhGM-CSF was given into the wells of a 24-well cell culture plate (greiner bio-one, Frickenhausen). During 5 d incubation the cells differentiated into iDCs.

Some studies were also performed with mature human dendritic cells (mDCs). For maturation, iDCs were centrifuged at 1200 rpm for 5 min and the medium was replaced by 1 ml of human DC medium supplemented with 10 ng/ml rhIL-1β, 10 ng/ml rhTNF-α and 1 µg/ml $PGE_2$. The cells were cultured for additional 2 d and maturation was confirmed by measuring the expression levels of CD80 and CD86 with flow cytometry according to chapter 3.2.9.

#### 3.2.8.2.2 Preparation of human macrophages

The isolation and generation of human macrophages from buffy coat were performed using a similar protocol as for human dendritic cells including density gradient centrifugation and a magnetic separation.

Onto the top of 15 ml pre-warmed (37 °C) lymphocyte separation medium 25 ml of buffy coat diluted 1:3 in pre-warmed PBS was layered. After centrifugation at 1600 rpm and RT for 30 min, the white interface was collected and macrophage wash medium was added up to a volume of 50 ml. The cells were centrifuged at 2200 rpm and RT for 8 min and the pellet was resuspended in 50 ml macrophage wash medium before centrifugation at 1600 rpm and RT for 8 min. Thrombocytes were removed by an additional washing of the pellet, centrifugation at 800 rpm and RT for 8 min and the supernatant was discarded. For lysis of red blood cells, 10 ml of cold 0.15 mol/l $NH_4Cl$ in water were added and incubated for 10 min to 15 min. Lysis was stopped by adjusting the volume to 50 ml with macrophage wash medium and the cells were centrifuged at 800 rpm and RT for 8 min. The cell number was determined and the magnetic separation of monocytes was performed as described in chapter 3.2.8.2.1. Around $4 \cdot 10^7$ to $5 \cdot 10^7$ PBMCs in 5 ml macrophage medium + 1 % (v/v) autologous plasma were seeded in a cell culture flask and incubated for 90 min at 37 °C and 5 % $CO_2$. The non-adherent cells were removed by washing twice with 4 ml macrophage wash medium.

The differentiation into M1 macrophages was carried out by addition of 5 ml macrophage medium supplemented with 10 ng/ml rhGM-CSF, whereas 4 ml macrophage medium supplemented with 30 ng/ml rhM-CSF (rh macrophage colony-stimulating factor) were used for the generation of M2 macrophages. The cells were harvested after 5 d to 7 d incubation.

#### 3.2.8.2.3 Assessment of receptor expression by human DCs or macrophages

To analyze surface receptor expression by DCs or macrophages, adherent human DCs or macrophages were generated as described in the chapters 3.2.8.2.1 and 3.2.8.2.2. The cells were harvested and directly stained for the co-stimulatory molecules CD80, CD86 or HLA-DR (human leukocyte antigen-DR; the homologue to mouse MHC class II) as well as for the receptors SR-AI/II, SR-BI, CD36 and the MR according to chapter 3.2.9.2.

#### 3.2.8.2.4 Assessment of antigen uptake by human DCs or macrophages

Antigen uptake by human iDCs as well as by human M1 or M2 macrophages was assessed according to Hilmenyuk et al.(*100*). Briefly, the cells were incubated with 0.5 µg/ml or 5 µg/ml of FITC-labelled OVA samples in the respective cell culture medium for 15 min, 60 min or 240 min, extensively washed, fixed with 1 % (w/v) PFA in PBS and afterwards analyzed with flow cytometry according to chapter 3.2.9. *In vitro* differentiation of PBMCs in DCs or macrophages resulted in highly homologous cell populations and therefore, it was not necessary to stain for specific cell surface markers.

### 3.2.9 Flow cytometry

Flow cytometry is a powerful tool for cell analysis and is used to study the properties of specific cell subsets.(*99*) The cells of interest are identified by staining of specific cell markers and molecules of interest on the cell surface with monoclonal antibodies labelled with a fluorescent dye.(*99*) Inside the flow cytometer, these marked cells are detected by passing through a laser beam and so-called fluorescence-activated cell sorter (FACS) are able to separate labelled from unlabelled cells.(*99*)

For analysis, a very fine laminar stream of the cell suspension is created by forcing it with high pressure through a needle.(*99*) The encounter of a cell in the laminar stream with the laser beam causes light scattering as well as excitation of the dye leading to fluorescence.(*99*) The scattered light as well as the fluorescence is guided through a set of filters and splitters and is then detected by several photomultiplier tubes.(*99*) The detected signals become processed by a connected computer.(*99*) The forward and the sideward scattered light provide information about the cell size and the granularity of the cell, respectively.(*99*) The detected fluorescence resembles the expression levels of the stained cell surface molecules.(*99*)

Flow cytometry was used in this thesis for many different purposes, like analysis of the maturation status of DCs, determination of antigen uptake by DCs and analysis of $CD4^+$ T-cell proliferation.

#### 3.2.9.1 Blocking of $F_c$-receptor binding

Receptors, which bind to the $F_c$-domain of antibodies, so-called $F_c$-receptors are present on the surface of many cells, like DCs and macrophages. False-positive signals by unspecific binding of the antibodies to $F_c$-receptors were excluded by blocking of $F_c$-receptors before staining of the respective surface molecules.

All cells were washed twice with plenty FACS-buffer or PBS to remove residual cell culture medium, which can inhibit the staining. BMDCs used for direct staining according to chapter 3.2.9.2 were

incubated for 30 min at 4 °C with 50 µl anti-mouse CD16/CD32 diluted in FACS-buffer before staining.

Blocking of human cells for detection of SR-BI was performed by incubation of the cells with 5 µl Human TruStain FcX™ (BioLegend; Fell) per 100 µl cell suspension for 5 min to 10 min at RT or with 20 µl of Human Fc Receptor Binding Inhibitor (eBioscience; Frankfurt a.M.) for 20 min on ice according to the manufacturer's instructions.

Afterwards, it was directly continued with the staining protocol.

#### 3.2.9.2 Direct staining of cell surface molecules

Direct staining of cell surface molecules was performed for staining of the maturation markers CD40, CD80 and CD86, and of MHC class II molecules on BMDCs. Also staining of CD4 or CD8 on T-cells either for proliferation analysis with CFSE or for determination of T-cell purity was performed using the direct staining approach. For characterization of human DCs, direct staining of CD80, of CD86 and of HLA-DR was performed. Both human DCs and macrophages were stained for the receptors SR-AI/II, CD36, SR-BI and the MR.

After blocking of the $F_c$-receptors, 50 µl of the appropriate antibody diluted in FACS-buffer were added to the blocking solution and the cells were incubated for additional 30 min at 4 °C in the dark. Plenty FACS-buffer was added and the cells were centrifuged at 1100 rpm and 4 °C for 5 min. Stained BMDCs were washed again with FACS-buffer and afterwards stained for CD11b and CD11c as described in chapter 3.2.9.4.

All other cells were washed three times with plenty FACS-buffer. The cells were resuspended in a small volume of FACS-buffer and fixed by addition of 1 % (w/v) PFA in PBS. The cells were stored at 4 °C in the dark until analysis.

#### 3.2.9.3 Indirect staining of cell surface receptors

For staining of cell surface receptors where no specific fluorophore-antibody conjugate was available, an indirect staining by using a specific primary antibody and a dye-conjugated secondary antibody was mandatory.

After blocking of the cells as described in chapter 3.2.9.1, the primary antibody was added to the cells and the sample was incubated for 30 min at 4 °C in the dark. The cells were washed twice with plenty PBS or FACS-buffer. The cells were resuspended in 100 µl of the respective blocking solution and the dye-conjugated secondary antibody was added. The cells were incubated for 30 min at 4 °C in the

dark. The staining reaction was quenched by addition of plenty PBS or FACS-buffer followed by washing once with FACS-buffer.

BMDCs were afterwards stained for CD11b and CD11c as described in chapter 3.2.9.4 and human cells were extensively washed with FACS-buffer, fixed with 1 % (w/v) PFA in PBS and stored at 4 °C in the dark until analysis.

#### 3.2.9.4 Staining of BMDCs for CD11b and CD11c

To distinguish the population of fully differentiated BMDCs from other cells, like remaining bone marrow cells, the cells were stained for CD11b and CD11c, which are specific markers for myeloid dendritic cells.

The staining was performed by resuspending the washed cells in 50 µl of a cocktail containing anti-CD11c allophycocyanin (APC) mAb and anti-CD11b phycoerythrin (PE) mAb diluted in FACS-buffer and incubation for 30 min at 4 °C in the dark. The cells were washed once by addition of FACS-buffer. After centrifugation at 1200 rpm and 4 °C for 5 min, the cells were washed three times with FACS-buffer. The cells were resuspended in a small volume of FACS-buffer and fixed with 1 % (w/v) PFA in PBS. The samples were stored in the fridge until analysis on the same day.

### 3.2.10 Animal experimental methods

The animal experiments were performed in agreement with the German legislation and guidelines of the Paul-Ehrlich-Institut. All mice were kept in the experimental animal facility at the Paul-Ehrlich-Institut under specified pathogen free conditions. The mice received water and a special diet *ad libitum*.

#### 3.2.10.1 Sensitization of mice with i.p. injection

Mice are usually not exposed to allergens that induce allergic reaction in humans. Therefore, the first allergen contact, which is termed sensitization, can be achieved by injection of the allergen together with a $T_H2$-directing adjuvant into the mice.

BALB/c mice (n = 6) were sensitized twice in a two week interval with 10 µg of either native OVA, Pyr-OVA or AGE-OVA in PBS together with 1 mg of aluminium hydroxide (ALUM) (Imject® ALUM; Thermo Scientific, Nidderau) as an adjuvant by intraperitoneal (i.p.) injection. As a control, mice (n = 3) were injected with 1 mg of ALUM suspended in PBS.

#### 3.2.10.2 Blood withdrawal from the tail

Blood was taken from the tail vein of the mice one week after i.p. sensitization for the analysis of antigen-specific IgE, IgG1 and IgG2a antibodies in the sera. To stimulate the blood flow, the mice were warmed under an infrared lamp. The mice were fixated and the tail vein was cut with a razorblade. The blood was collected in a special tube for serum isolation (Sarstedt, Nümbrecht) and afterwards, the bleeding at the tail was stopped. The collected blood was clotted for 30 min at RT and the serum was separated by centrifugation at 10,000 xg for 3 min and stored at -20 °C until analysis.

#### 3.2.10.3 Induction of clinical symptoms

The induction of clinical symptoms, also called challenge, in sensitized animals can be performed in different ways, e.g. by injection, feeding, supplementation to the drinking water, oral gavage or inhalation. In this food allergy model, which has been established by Burggraf et al., two weeks after the second sensitization mice were challenged by feeding a diet containing high amounts of OVA (EW-diet; ssniff Spezialdiäten GmbH, Soest) for one week.(*101*) During challenge, clinical symptoms, like loss of body weight and drop in body temperature, were monitored. After challenge, the mice were euthanized using gaseous $CO_2$ to take blood as well as the mesenteric lymph nodes (MLN), which is the gut draining lymphoid organ. Proliferation of MLN-derived $CD4^+$ T-cells was analyzed according to chapter 3.2.8.1.10 and the antibody levels in the sera were determined by ELISA as described in chapter 3.2.5.2.

# 4 Results and Discussion

## 4.1 Identification of glycation structures to enhance the immunogenic and allergenic potency of ovalbumin using murine immune cells

### 4.1.1 Introduction

In this chapter, the immunogenic and allergenic properties of OVA modified with the representative glycation structures CEL, CML, MG-H1 or pyrraline were investigated. These glycation structures are present in industrially roasted peanuts and their composition in AGE-OVA is also known. To identify glycation structures contributing to the enhanced immunogenic properties of AGE-OVA, the $CD4^+$ T-cell immunogenicity as well as the DC uptake of each modification was assessed. Finally, the potential allergenicity of AGE-OVA, of the glycation structure(s) with enhanced T-cell immunogenicity, and of native OVA were compared in a mouse model of intestinal allergy.

### 4.1.2 Characterization of the modified OVAs with glycation structures

To identify glycation structures enhancing the T-cell immunogenicity of a food allergen, OVA was modified with CEL, CML, pyrraline or MGO-derivatives of arginine, such as MG-H1 (figure 7A). Crude glycated OVA (AGE-OVA) was prepared by thermal incubation of OVA with glucose at 50 °C for six weeks, following a protocol used in a previous study.(*71*) The modification levels of the glycation structures were determined by GC-MS or RP-HPLC-DAD after acid hydrolysis and are shown in tables 11 and 12. AGE-OVA as well as OVA thermally incubated without glucose (inc. OVA) and the native protein served as controls. Chemical modification of OVA and analysis of glycation structures were performed by Dr. Anne Wellner under supervision of Prof. Thomas Henle (TU Dresden).

**Table 11: Levels of specific modification by glycation structures in OVA samples.**

| sample | CEL | CML | MG-H1 | argpyrimidine | pyrraline | 3DG-H |
|---|---|---|---|---|---|---|
| CE-OVA | 363.3 | - | - | - | - | - |
| CM-OVA | - | 334.5 | - | - | - | - |
| MGO-OVA | - | - | 53.6 | 38.0 | - | - |
| Pyr-OVA | - | - | - | - | 236.4 | 116.2 |
| AGE-OVA | - | 28 | - | - | 0.9 | - |

data are given in µmol/g OVA determined with RP-HPLC

- : not analyzed

**Table 12: Levels of modification of lysine and arginine residues in OVA samples.**

| sample | specific modification | | total modification | |
|---|---|---|---|---|
| | Lys [%] | Arg [%] | Lys [%] | Arg [%] |
| CE-OVA | 80.1 | - | 77.2 | - |
| CM-OVA | 73.8 | - | 81.2 | - |
| MGO-OVA | - | 30.1 | - | 71.1 |
| Pyr-OVA | 51.1 | 25.1 | 72.4 | 39.7 |
| AGE-OVA | 41.3 | - | 69.8 | - |

The modification of OVA with CEL or CML was very selective resulting in 77 % lysine modification with CEL in OVA modified with CEL (CE-OVA) or 81 % lysine modification with CML in OVA modified with CML (CM-OVA), respectively (table 12). Additionally, the presence of these glycation structures in CE-OVA, CM-OVA and AGE-OVA could be detected by ELISA using specific antibodies (figures 8A and 8B). The reactions of OVA with 3-DG to form pyrraline or with MGO to form MG-H1 are less selective. OVA modified with pyrraline (Pyr-OVA) contained 3-DG derived hydroimidazolones (3DG-H) (table 11 and figure 7B include all identified by-products) on 25 % of arginine residues as well as modification with unknown AGEs on 14 % of arginine residues and 11 % of lysine residues, respectively. In the reaction of OVA with MGO, arginine residues were modified with MG-H1 (53 µmol/g OVA) and argpyrimidine (38 µmol/g OVA), a common by-product of this reaction. The levels of MG-H1 and argpyrimidine in MGO-OVA modified 30.1 % of arginine residues. This result suggests that the majority, approximately 41 % of arginine residues, was modified with unknown AGE structures. Presence of GA-pyridine in OVA samples was detected by ELISA using a specific antibody. Pyr-OVA and MGO-OVA did not contain GA-pyridine modification (figures 8C and 8D). Detectable levels of GA-pyridine were only found in AGE-OVA.

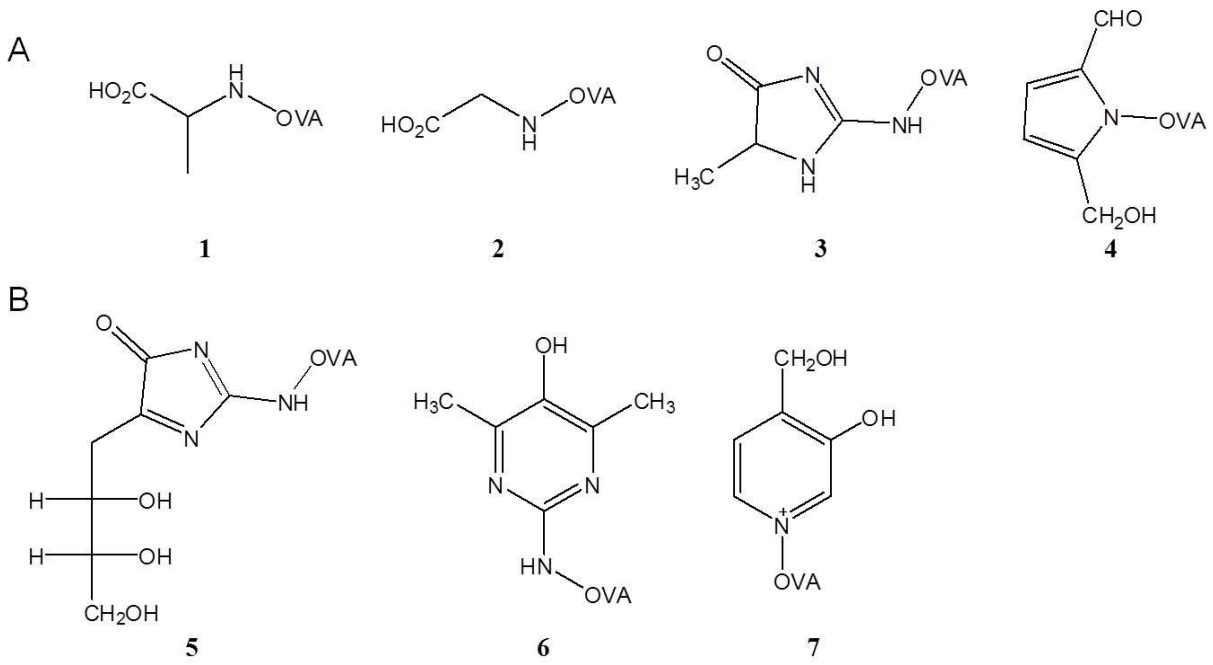


**Figure 7: Scheme of glycation structures.** (A) Main products: 1: OVA with CEL (CE-OVA); 2: OVA with CML (CM-OVA), 3: OVA with MG-H1 (MGO-OVA), 4: OVA with pyrraline (Pyr-OVA). (B) By-products: 5: OVA with 3-desoxyglucosulose induced hydroimidazolone (3DG-H) 6: OVA with argpyrimidine, 7: OVA with GA-pyridine.

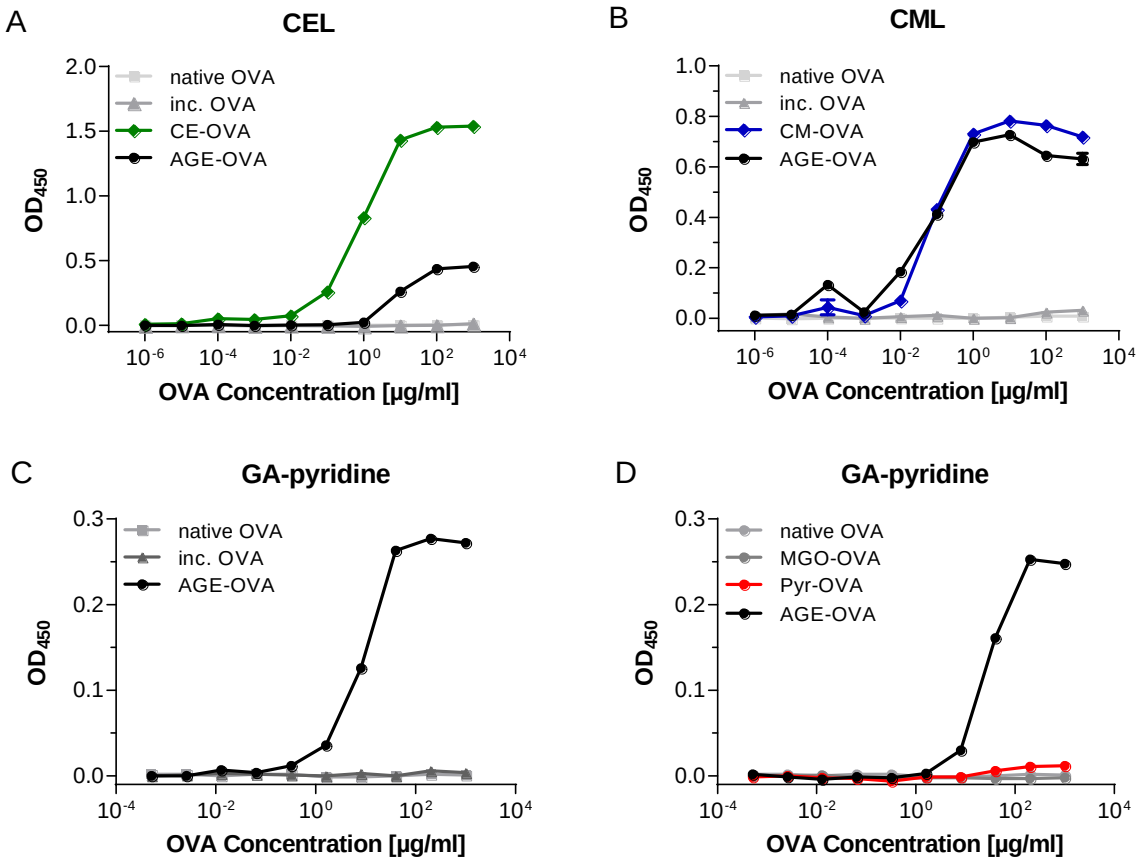


**Figure 8: Detection of glycation structures in OVA by ELISA.** (A) CEL, (B) CML and (C, D) GA-pyridine in OVA samples were detected by ELISA using antibodies specific for the indicated glycation structure.

To assess whether modification induces a molecular shift (e.g. aggregation) in the proteins, the OVA samples were subjected to SDS-PAGE under reducing conditions. For native OVA, shown in lane 1 in figure 9, one distinct band with an apparent molecular weight of around 45 kDa was visible. For inc. OVA, shown in lane 2, a second band of low intensity at a molecular weight of about 35 kDa was observed. This result suggests that the majority of OVA stays intact and only a small part degrades during thermal processing. CE-OVA, CM-OVA and MGO-OVA, shown in lane 3 to lane 5, seem to have a slightly higher molecular weight than native OVA due to modification. For Pyr-OVA, shown in lane 6, and AGE-OVA, shown in lane 7, broad smears around a molecular weight of 45 kDa, 100 kDa to 130 kDa and above are visible. The smear bands of AGE-OVA suggest that OVA could be modified with many different glycation structures. More than 100 kDa bands of Pyr-OVA and AGE-OVA indicate that aggregates formed by cross-linking AGEs are present in these samples.

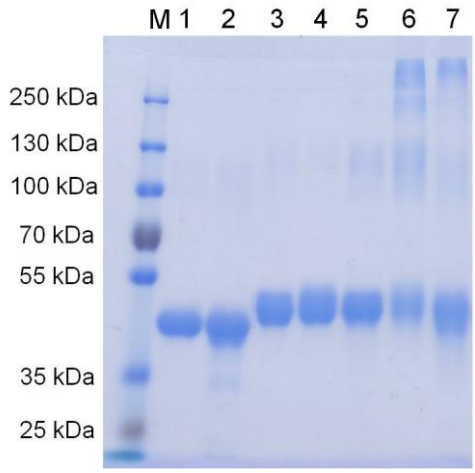


**Figure 9: Analysis of the modified OVAs with SDS-PAGE.** OVA samples (5 µg/lane) were loaded on a reducing 7.5 % TRIS-glycine gel and stained with Coomassie Brilliant Blue after electrophoresis. Lane M: molecular weight marker, lane 1: native OVA, lane 2: inc. OVA, lane 3: CE-OVA, lane 4: CM-OVA, lane 5: MGO-OVA, lane 6: Pyr-OVA, lane 7: AGE-OVA.

Next, the secondary structure of all OVA samples was analyzed with CD-spectroscopy. The CD-spectra of all forms of OVA look similar (figure 10). The shape of the curves with two minima at approximately 221 nm and 210 nm and a maximum at approximately 190 nm indicate that the structure is composed mainly of α-helices, as it is known for the native form of OVA.(*17*) These results suggest that there seem to be only minor changes in the secondary structure elements of OVA due to modification.

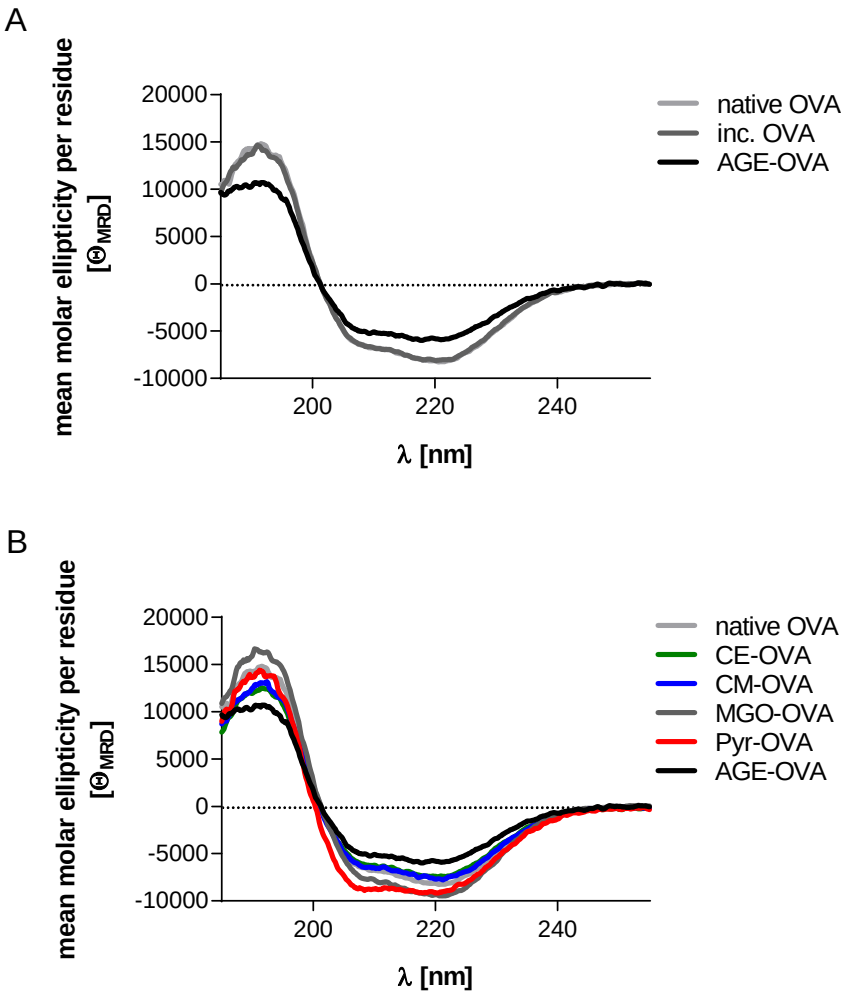


**Figure 10: CD-spectra of (A) native OVA, inc. OVA and AGE-OVA as well as of (B) all modified OVAs.**

### 4.1.3 Characterization of AGE-BSA

As a control for some experiments, crude glycated BSA (AGE-BSA) was prepared under the same conditions as used for AGE-OVA, i.e. by incubation of BSA with glucose at 50 °C for six weeks. The presence of the glycation structures CEL, CML and GA-pyridine was assessed by ELISA.

As seen in AGE-OVA, CEL, CML and GA-pyridine were detected in AGE-BSA (figure 11). SDS-PAGE analysis showed the distinct band of native BSA or inc. BSA in lane 1 and lane 2 in figure 12. The band of AGE-BSA in lane 3 was a broad smear. The smear was also observed for AGE-OVA. Taken together, the results suggest that AGE-BSA could have a similar glycation profile as detected in AGE-OVA and is a suitable control for AGE-OVA.

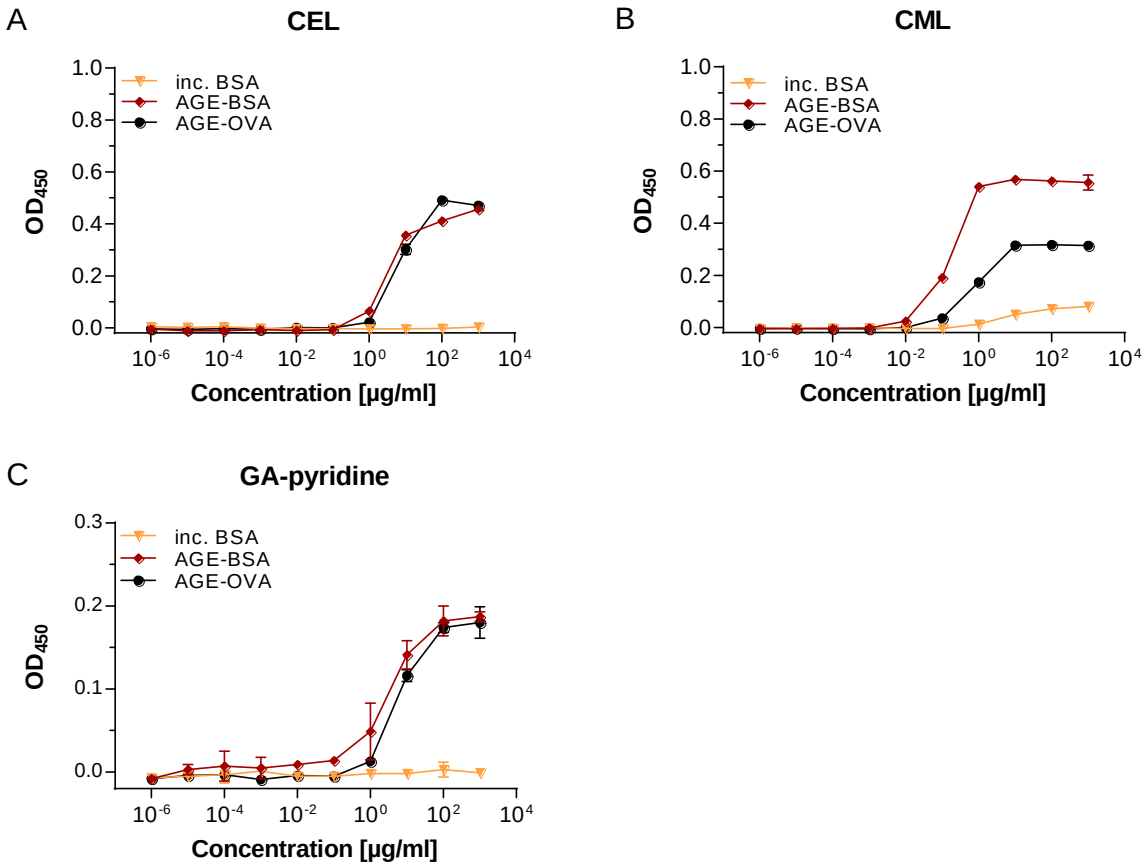


**Figure 11: Detection of glycation structures in the BSA samples by ELISA.** (A) CEL, (B) CML and (C) GA-pyridine in inc. BSA and AGE-BSA were detected by ELISA using antibodies specific for the indicated glycation structure.

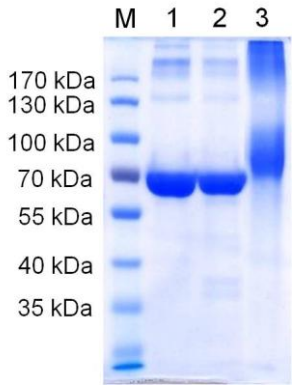


**Figure 12: Analysis of AGE-BSA by SDS-PAGE.** BSA samples (5 µg/lane) were loaded on a 10 % reducing TRIS-glycine gel and stained with Coomassie Brilliant Blue after electrophoresis. Lane M: molecular weight marker, lane 1: native BSA, lane 2: inc. BSA, lane 3: AGE-BSA.

### 4.1.4 Assessment of the T-cell immunogenicity of the modified OVAs with glycation structures *in vitro*

Next, the $CD4^+$ and the $CD8^+$ T-cell immunogenicity of OVA was assessed. The $CD4^+$ T-cell immunogenicity was assessed, because $CD4^+$ T-cells play a crucial role to induce food allergies. The $CD8^+$ T-cell immunogenicity was also assessed as it is known that OVA activates not only $CD4^+$ T-cells, but also $CD8^+$ T-cells due to its natural mannose residues. Several studies have shown that OVA binds to the mannose receptor (MR) expressed on the cell surface of DCs, which leads to cross-presentation of OVA to $CD8^+$ T-cells. (*59, 64*)

T-cell immunogenicity was assessed by measuring IL-2 production and proliferation of T-cells upon stimulation with OVA samples in a co-culture system with bone marrow-derived dendritic cells (BMDCs).

#### 4.1.4.1 IL-2 production by OVA-specific $CD4^+$ T-cells stimulated by the OVAs modified with glycation structures

The analysis of IL-2 production, also an indicator for T-cell activation, by OVA-specific $CD4^+$ T-cells stimulated with the OVAs modified with glycation structures was performed using an *in vitro* co-culture system of OVA-specific $CD4^+$ T-cells with BMDCs. BMDCs have been generally used as a model for antigen presenting cells (APCs). OVA-specific $CD4^+$ T-cells were isolated from OT-II mice on a C57BL/6 background, or from DO11.10 mice on a BALB/c background. In homozygous OT-II mice and DO11.10 mice, around 80 % to 85 % of $CD4^+$ T-cells express monoclonal TCR recognizing the amino acid region 323 to 339 in OVA.(*102*) This region corresponds to the sequence ISQAVHAAHAEINEAGR in the one letter notation for amino acids. $CD4^+$ T-cells from OT-II mice are specific for the MHC class II haplotype $I\text{-}A^b$, whereas those from DO11.10 mice are specific for the haplotype $I\text{-}A^d$.

In this thesis, both mouse strains are compared, because C57BL/6 mice tend to develop $T_H1$ and $T_H17$ immune responses in contrast to BALB/c mice, which tend to develop $T_H2$ responses. Another reason for the use of OT-II mice is that many genetically modified mouse strains are on a C57BL/6 background.

A co-culture system of OVA-specific $CD4^+$ T-cells and syngeneic BMDCs (i.e. cells generated from mice on the same genetic background) was used to assess IL-2 production by T-cells. The cells were stimulated with 2 µg/ml or 20 µg/ml of either form of OVA. Stimulation with OVA leads to activation of the $CD4^+$ T-cells, which subsequently produce the cytokine IL-2. The concentration of IL-2 in the cell culture supernatants was measured by ELISA.

AGE-OVA induced production of higher amounts of IL-2 by OT-II-derived $CD4^+$ T-cells (OT-II cells) compared to native OVA (figure 13A). Of the modified OVAs, only Pyr-OVA induced significantly higher levels of IL-2 production by OT-II cells compared to native OVA. CE-OVA, CM-OVA or MGO-OVA induced comparable IL-2 production by OT-II cells as the one by native OVA and inc. OVA. A similar result was observed when BALB/c-derived BMDCs and DO11.10-derived $CD4^+$ T-cells (DO11.10 cells) were used for the co-culture system (figure 13B). Pyr-OVA and AGE-OVA induced production of enhanced amounts of IL-2 by DO11.10 cells compared to native OVA. CE-OVA, CM-OVA and MGO-OVA slightly enhanced IL-2 production, but it was not remarkable, when the cells were stimulated with the lower concentration of 2.0 µg/ml. These results suggest that of the modifed OVA samples assessed in this experiment, Pyr-OVA induces significantly higher $CD4^+$ T-cell activation.

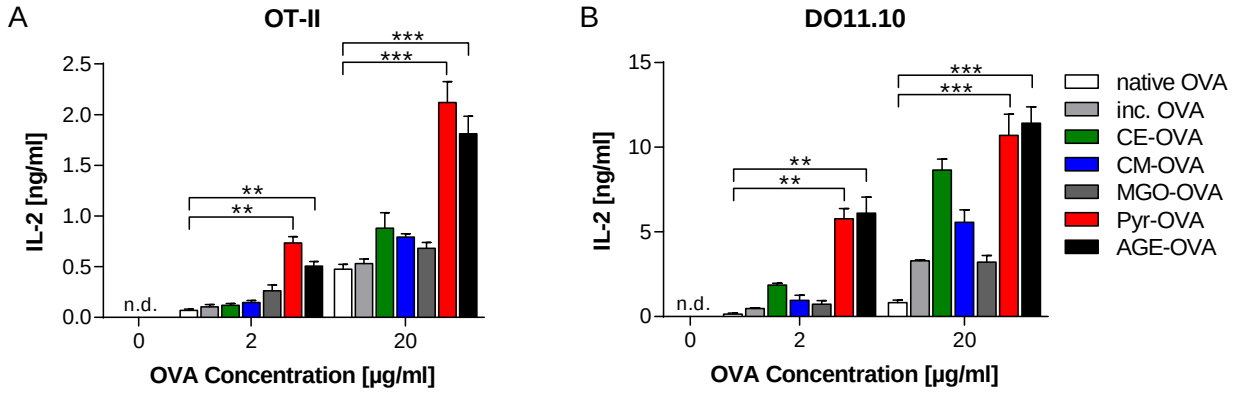


**Figure 13: IL-2 production by OT-II- or DO11.10-derived $CD4^+$ T-cells upon stimulation with OVA samples.** $CD4^+$ T-cells were isolated from (A) OT-II mice or (B) DO11.10 mice and co-cultured with syngeneic BMDCs in the presence of 2 µg/ml or 20 µg/ml of OVA samples. After 24 h of co-culture, the concentration of IL-2 in the cell culture supernatants was determined by ELISA. * $p < 0.05$, ** $p < 0.01$, *** $p < 0.001$ (n.d.: not detectable; below detection limit of 0.05 pg/ml).

As mentioned above, Pyr-OVA contained not only pyrraline but also 3DG-H and other unknown glycation structures (see Pyr-OVA 3 in table 13). Protein aggregation was also induced during formation of Pyr-OVA by incubation of OVA with 3-DG (figures 9 and 14). To examine whether the enhanced $CD4^+$ T-cell activation by Pyr-OVA was due to pyrraline, OVA was incubated with 3-DG at 70 °C for shorter duration to reduce the levels of unspecific modification. Pyr-OVA 1 and Pyr-OVA 2 prepared by 10 min and 30 min incubation, respectively, reduced the levels of unspecific by-products (table 13) and protein aggregation (figure 14) compared to Pyr-OVA 3 prepared by 4 h incubation, which has been used in the former experiments.

**Table 13: Levels of modification in Pyr-OVA samples.**

| sample | pyrraline | 3DG-H | specific modification | | total modification | |
|---|---|---|---|---|---|---|
| | [µmol/g protein] | | Lys [%] | Arg [%] | Lys [%] | Arg [%] |
| Pyr-OVA 1 | 50.7 | 7.8 | 10.9 | 1.7 | 12.6 | 0.6 |
| Pyr-OVA 2 | 143.5 | 33.8 | 31.0 | 7.3 | 36.4 | 11.8 |
| Pyr-OVA 3 | 236.4 | 116.2 | 51.1 | 25.1 | 72.4 | 39.7 |

modification levels of Pyr-OVA samples with Pyr and 3-DG in µmol/g OVA determined with RP-HPLC as well as percentage of total lysine and arginine modification assessed with amino acid analysis.

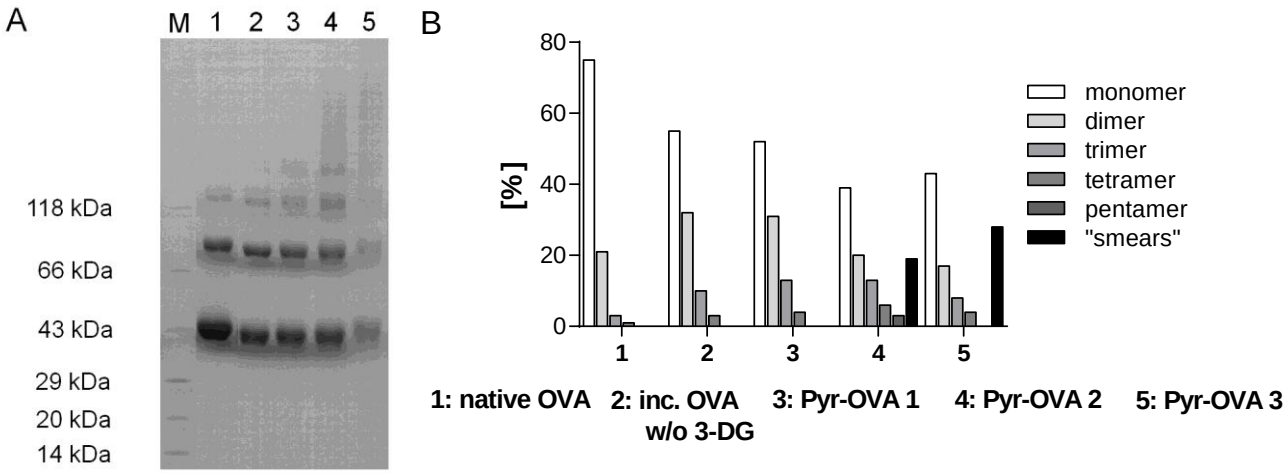


**Figure 14: Aggregation of Pyr-OVA samples.** Pyr-OVA samples (5 - 10 µg/lane) were loaded on a 4 % to 20 % acrylamide gradient gel for SDS-PAGE under non-reducing conditions and (A) stained with Coomassie Brilliant Blue followed by (B) densitometric analysis. M: molecular weight marker, 1: native OVA, 2: OVA incubated w/o 3-DG, 3: Pyr-OVA 1, 4: Pyr-OVA 2, 5: Pyr-OVA 3.

Pyr-OVA 1 and Pyr-OVA 2 still induced higher IL-2 production by OT-II cells and DO11.10 cells compared to native OVA, as can be seen in figure 15. Enhanced $CD4^+$ T-cell activation by Pyr-OVAs depended on pyrraline modification levels. OVA incubated at 70 °C without 3-DG, a control for Pyr-OVA, induced only basal levels of $CD4^+$ T-cell activation as did native OVA (data not shown). Figure 15 shows that Pyr-OVA 1 induced production of lower levels of IL-2 compared to Pyr-OVA 3. In addition, the results indicate that Pyr-, but not 3DG-H-modification, causes the enhanced T-cell activation, because levels of 3DG-H in Pyr-OVA 1 are nearly at the detection level and significantly lower compared to Pyr-OVA 3. Thus, these results suggest that pyrraline could contribute to the enhanced $CD4^+$ T-cell activation of Pyr-OVA.

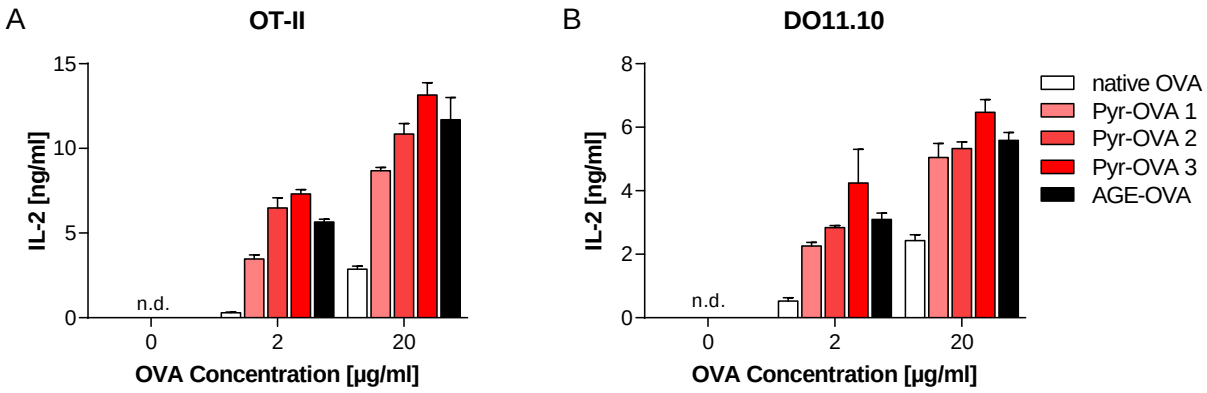


**Figure 15: IL-2 production by OT-II- or DO11.10-derived CD4$^+$ T-cells upon stimulation with Pyr-OVAs.** CD4$^+$ T-cells were isolated from (A) OT-II or (B) DO11.10 mice and co-cultured with syngeneic BMDCs in the presence of 2 µg/ml or 20 µg/ml of OVA samples. After 24 h of co-culture, the concentration of IL-2 in the cell culture supernatants was determined by ELISA. (n.d.: not detectable; below detection limit of 0.05 pg/ml)

### 4.1.4.2 Proliferation of OVA-specific CD4$^+$ T-cells stimulated by the OVAs modified with glycation structures

To further assess CD4$^+$ T-cell activation by OVA samples, T-cell proliferation was analyzed. Stimulation of T-cells with OVA induces T-cell activation, which is characterized by T-cell proliferation as well as cytokine production by T-cells and thus, T-cell proliferation can be used as a marker for T-cell activation.

To measure the proliferation of OVA-specific CD4$^+$ T-cells, T-cells were stained with CFSE, a chemical with green fluorescence, prior to their culture with BMDCs in the presence of 2 µg/ml of either form of OVA. Cell proliferation was analyzed by measuring CFSE intensity of the CD4$^+$ T-cells using flow cytometry.

Pyr-OVA 3, which has been used in all following experiments and is referred to as Pyr-OVA, and AGE-OVA induced higher proliferation of OT-II cells compared to native OVA (figure 16). CE-OVA induced a slightly higher T-cell proliferation compared to native OVA. All other forms of OVA, i.e. inc. OVA, CM-OVA and MGO-OVA, induced similar levels of T-cell proliferation as did native OVA. These results suggest that modification of OVA with pyrraline induces higher CD4$^+$ T-cell activation.

Like in measurements of IL-2 production, DO11.10 cells showed similar proliferation against the OVA samples as did OT-II cells (figure 17). Pyr-OVA and AGE-OVA induced higher proliferation of DO11.10 cells than other OVAs. Here, a slightly enhanced proliferation by CE-OVA was also observed.

Enhanced IL-2 production and proliferation of both OT-II and DO11.10 cells by Pyr-OVA suggest that this modified OVA has a considerably higher $CD4^+$ T-cell immunogenicity than native OVA and the other OVAs modified with glycation structure.

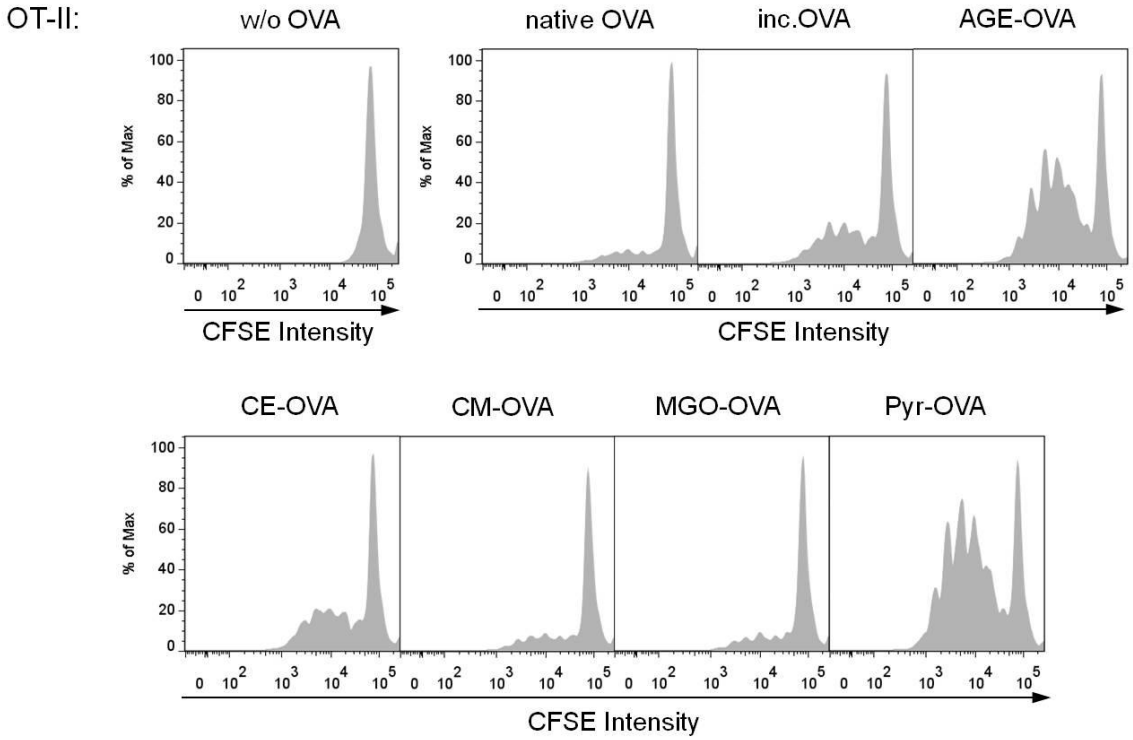


**Figure 16: Proliferation of OT-II-derived $CD4^+$ T-cells upon stimulation with OVA samples.** $CD4^+$ T-cells isolated from OT-II mice were stained with CFSE and co-cultured with syngeneic BMDCs in the presence of 2 µg/ml of OVA samples. After 96 h of co-culture, CFSE intensity of $CD4^+$ T-cells was measured with flow cytometry.

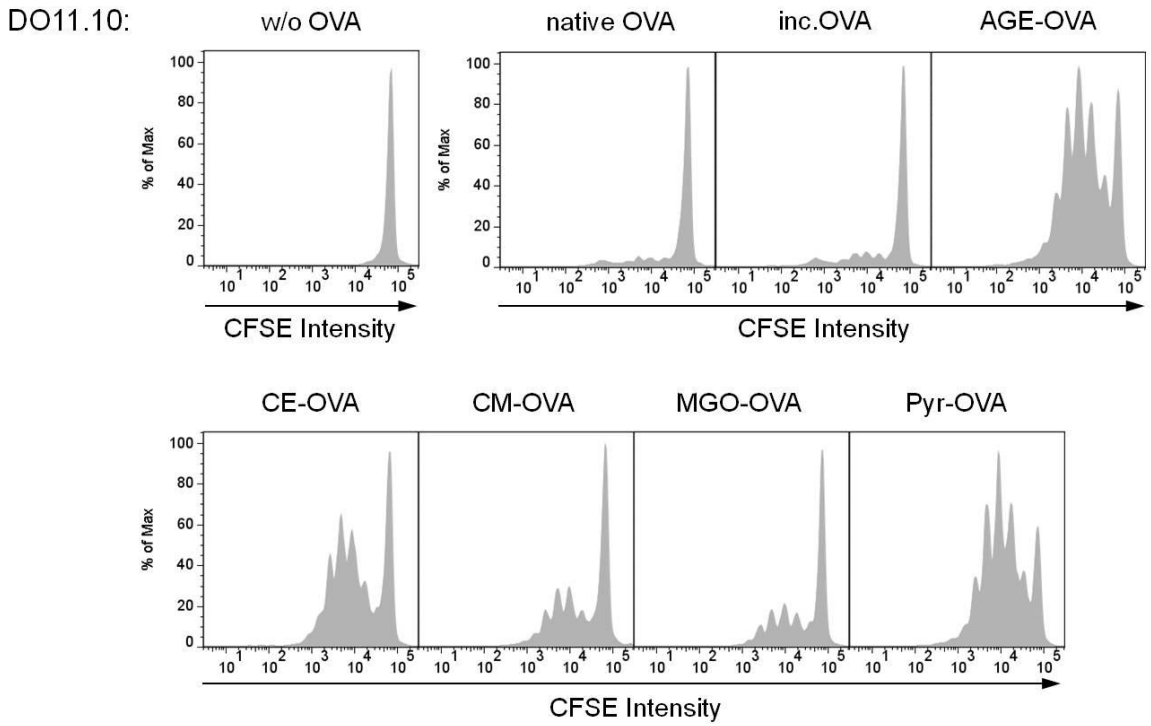


**Figure 17: Proliferation of DO11.10-derived CD4$^+$ T-cells upon stimulation with OVA samples.** CD4$^+$ T-cells isolated from DO11.10 mice were stained with CFSE and co-cultured with syngeneic BMDCs in the presence of 2 µg/ml of OVA samples. After 96 h of co-culture, CFSE intensity of CD4$^+$ T-cells was measured with flow cytometry.

#### 4.1.4.3 $T_H1$, $T_H2$ and $T_H17$ cytokine production by OVA-specific CD4$^+$ T-cells stimulated by the OVAs modified with glycation structures

Naive CD4$^+$ T-cells differentiate into three different subsets of effector cells, i.e. $T_H1$, $T_H2$ and $T_H17$ cells. It has been an important question whether AGEs influence the differentiation of T-cells. To investigate the influence of AGEs on T-cell differentiation, cytokine production by OT-II cells and DO11.10 cells upon stimulation with OVA samples was measured. OVA-specific CD4$^+$ T-cells were co-cultured with BMDCs upon stimulation with either 2 µg/ml or 20 µg/ml of modified OVAs for 72 h. The concentrations of the $T_H1$-related cytokine IFN-γ, the $T_H2$-related cytokine IL-4 and the $T_H17$-related cytokine IL-17A in the cell culture supernatants were determined by ELISA.

Results of IFN-γ and IL-17A production by OT-II cells are shown in figure 18. IL-4 was not detected in the cell culture supernatants of OT-II cells due to the C57BL/6 background of the mice. Pyr-OVA induced the highest levels of IFN-γ and IL-17A production by OT-II cells. AGE-OVA induced higher levels of IFN-γ and IL-17A production at a concentration of 2 µg/ml, but not at 20 µg/ml. A possible explanation might be that the viability of the CD4$^+$ T-cells might be weakened after 72 h of co-culture due to overstimulation of the T-cells by AGE-OVA or toxicity of this crude glycation product at higher concentrations. The putative toxicity of AGE-OVA may also be an explanation for the strong levels of

IL-2 induced by AGE-OVA compared to native OVA and the lower levels of IFN-γ and IL-17A induced by AGE-OVA compared to native OVA, because levels of IL-2 were measured after 24 h of cell culture compared to the levels of IFN-γ and IL-17A, which were measured after 72 h of cell culture. The other modified OVAs tended to induce slightly higher levels of IFN-γ and IL-17A by OT-II cells compared to native OVA.

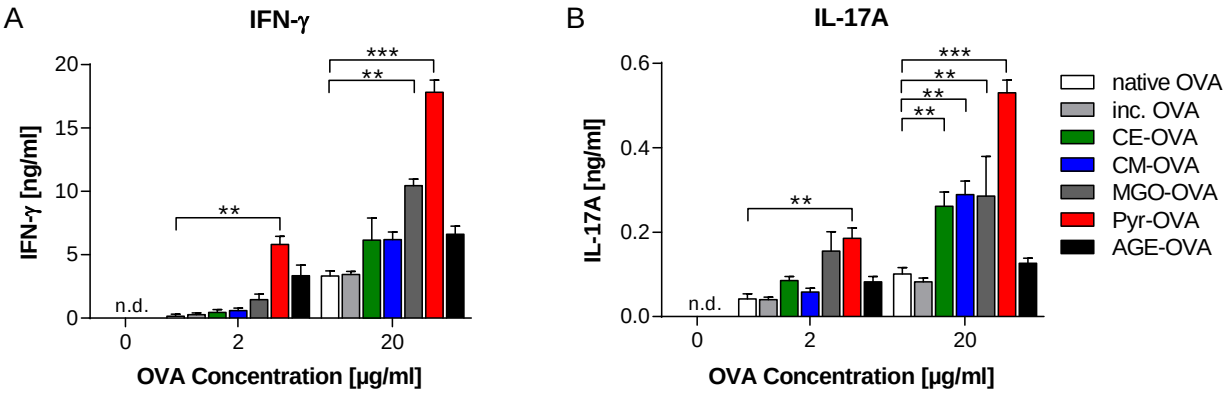


**Figure 18: $T_H1$ and $T_H17$ cytokine production by OT-II-derived $CD4^+$ T-cells upon stimulation with OVA samples.** $CD4^+$ T-cells were isolated from OT-II mice and co-cultured with syngeneic BMDCs in the presence of 2 µg/ml or 20 µg/ml of OVA samples. After 72 h of co-culture, the concentrations of (A) IFN-γ or (B) IL-17A in the cell culture supernatants were determined by ELISA. * $p < 0.05$, ** $p < 0.01$, *** $p < 0.001$ (n.d.: not detectable; below detection limit of 0.01 pg/ml).

DO11.10 cells produced detectable levels of IL-4 and IL-17A, but not of IFN-γ, in the co-culture system with BMDCs. Of the OVA samples, Pyr-OVA and AGE-OVA induced higher levels of IL-4 production by DO11.10 cells at 2 µg/ml, the low concentration used, compared to native OVA and the other modified OVAs (figure 19A). However, IL-4 production by DO11.10 cells was reduced when the cells were stimulated with 20 µg/ml of Pyr-OVA or AGE-OVA. In contrast, native OVA and the other modified OVAs induced higher IL-4 production by DO11.10 cells at a concentration of 20 µg/ml. DO11.10 cells also induced detectable levels of IL-17A, which are shown in figure 19B. IL-17A production by DO11.10 cells was remarkably enhanced when the cells were stimulated with 20 µg/ml of Pyr-OVA compared to the other OVA samples including native OVA. These results suggest first, that the threshold to induce IL-4 production could be lower than that to induce IL-17A production by DO11.10 cells, second, that the reduced IL-4 production of DO11.10 cells by 20 µg/ml of Pyr-OVA could be an over-dosation of this material, and third, that Pyr-OVA is capable of inducing higher T-cell stimulation than the other modified OVAs and native OVA.

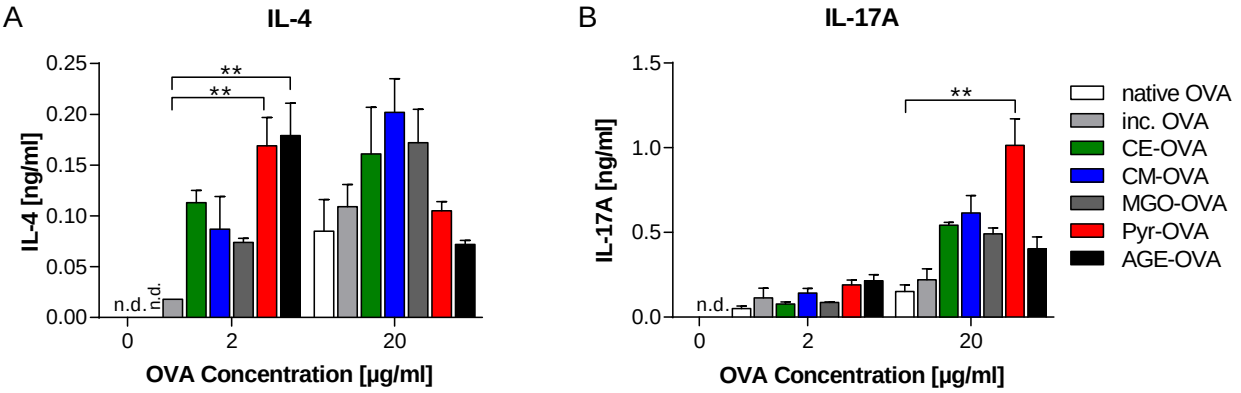


**Figure 19: $T_H2$ and $T_H17$ cytokine production by DO11.10-derived $CD4^+$ T-cells upon stimulation with OVA samples.** $CD4^+$ T-cells were isolated from DO11.10 mice and co-cultured with syngeneic BMDCs in the presence of 2 µg/ml or 20 µg/ml of OVA samples. After 72 h of co-culture the concentrations of (A) IL-4 or (B) IL-17A in the cell culture supernatants were determined by ELISA. (n.d.: not detectable; below detection limit of 0.01 pg/ml)

Taken together, Pyr-OVA enhanced both the production of the $T_H1$-related cytokine IFN-γ and the $T_H2$-related cytokine IL-4 by OT-II cells and DO11.10 cells, respectively. Furthermore, Pyr-OVA enhanced production of IL-17A, a $T_H17$-related cytokine, by both cell types. These results suggest that Pyr-OVA does not bias the differentiation of $CD4^+$ T-cells into a specific $T_H$ subset.

#### 4.1.4.4 IL-2 and IFN-γ production by OVA-specific $CD8^+$ T-cells stimulated by the OVAs modified with glycation structures

Next, the $CD8^+$ T-cell immunogenicity of the OVA samples was assessed. For the assessment, a co-culture system of OT-I-derived $CD8^+$ T-cells (OT-I cells) with syngeneic BMDCs was used following a protocol established by Burgdorf et al.(*59*) The genetically modified mouse strain OT-I is on a C57BL/6 background and expresses an OVA-specific TCR. This TCR recognizes complexes of the MHC class I molecule $K^b$ with an OVA peptide containing the amino acid region 257 to 264 (SIINFEKL). In this assay, BMDCs were stimulated with LPS before co-culture, because this enhances cross-presentation of exogenous antigens by MHC class I molecules.(*103*) As a marker for $CD8^+$ T-cell activation, the concentration of IL-2 in the cell culture supernatants was determined by ELISA.

Figure 20 shows that AGE-OVA and native OVA induced similar levels of IL-2 production by OT-I cells. These results indicate that AGE-OVA was not capable of enhancing $CD8^+$ T-cell activation.

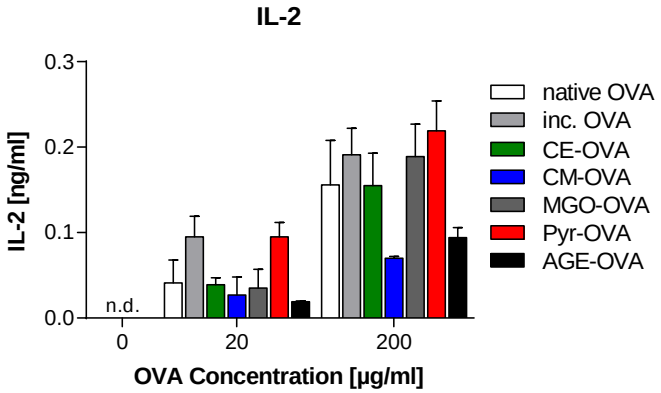


**Figure 20: IL-2 production by OT-I-derived CD8$^+$ T-cells upon stimulation with OVA samples.** CD8$^+$ T-cells were isolated from OT-I mice. Syngeneic BMDCs were treated with 10 µg/ml LPS for 2 h, incubated with 20 µg/ml or 200 µg/ml of OVA samples for 3 h and washed. OT-I cells and OVA sample-primed BMDCs were cultured for 20 h. The concentration of IL-2 in the cell culture supernatants was then determined by ELISA. (n.d.: not detectable; below detection limit of 0.01 pg/ml)

CD8$^+$ T-cell activation leads to the initiation of the natural cytotoxic effector function and the release of cytotoxic mediators. As a part of this response, the cells produce the cytokine IFN-γ. Thus, the functionality of the CD8$^+$ T-cells can be checked by measuring the IFN-γ concentration in the cell culture supernatants by ELISA. To verify the CD8$^+$ T-cell activation by OVA samples, the concentration of IFN-γ in the cell culture supernatants after 72 h of co-culture was determined by ELISA.

As expected, levels of IFN-γ production correlate well with those of IL-2 production by OT-I cells stimulated with OVA samples (figures 20 and 21). No enhanced production of IFN-γ was observed by OT-I cells stimulated with neither AGE-OVA nor Pyr-OVA. These results suggest that modification of OVA with pyrraline or other glycation structures did not influence the CD8$^+$ T-cell immunogenicity of OVA.

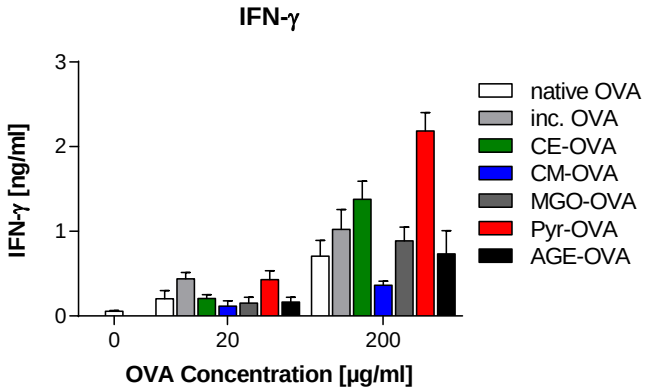


**Figure 21: IFN-γ production by OT-I-derived CD8$^+$ T-cells upon stimulation with OVA samples.** CD8$^+$ T-cells were isolated from OT-I mice. Syngeneic BMDCs were treated with 10 µg/ml LPS for 2 h, incubated with 20 µg/ml or 200 µg/ml of OVA samples for 3 h and washed. OT-I cells and OVA sample-primed BMDCs were cultured for 72 h. The concentration of IFN-γ in the cell culture supernatants was determined by ELISA.

### 4.1.5 Interaction of modified OVAs with BMDCs *in vitro*

#### 4.1.5.1 Non-effect of the OVAs modified with glycation structures on BMDC maturation

Antigen uptake and maturation of DCs is a prerequisite for efficient activation of CD4$^+$ or CD8$^+$ T-cells. Several studies have indicated that some AGEs have the potential to influence DC maturation.(*104, 105*) Hence, it was assessed whether the OVAs modified with glycation structures induce BMDC maturation.

BMDCs were stimulated with 50 µg/ml of OVA sample or 1 µg/ml of LPS, a pyrogen known to induce DC maturation, for 18 h. Expression levels of the co-stimulatory molecules CD40, CD80 and CD86 as well as of MHC class II molecules on the cell surface of BMDCs were measured with flow cytometry. Additionally, the concentration of IL-6 in the cell culture supernatants was determined by ELISA.

The expression levels of the co-stimulatory molecules on BMDCs stimulated with either OVA sample were comparable to those of non-stimulated cells (figure 22A). In contrast, incubation of BMDCs with LPS resulted in increased levels of CD40, CD80, CD86 and MHC class II molecules on the cell surface (figure 22B), showing that the BMDCs were functional. Levels of IL-6 induced by Pyr-OVA and AGE-OVA (figure 23) as well as by all other modified OVAs (data not shown) were comparable to those of native OVA and non-stimulated cells. Incubation of BMDCs in the presence of LPS induced production of higher levels of IL-6 compared to non-stimulated cells. The results suggest that maturation of BMDCs is not induced by the OVAs modified with glycation structures.

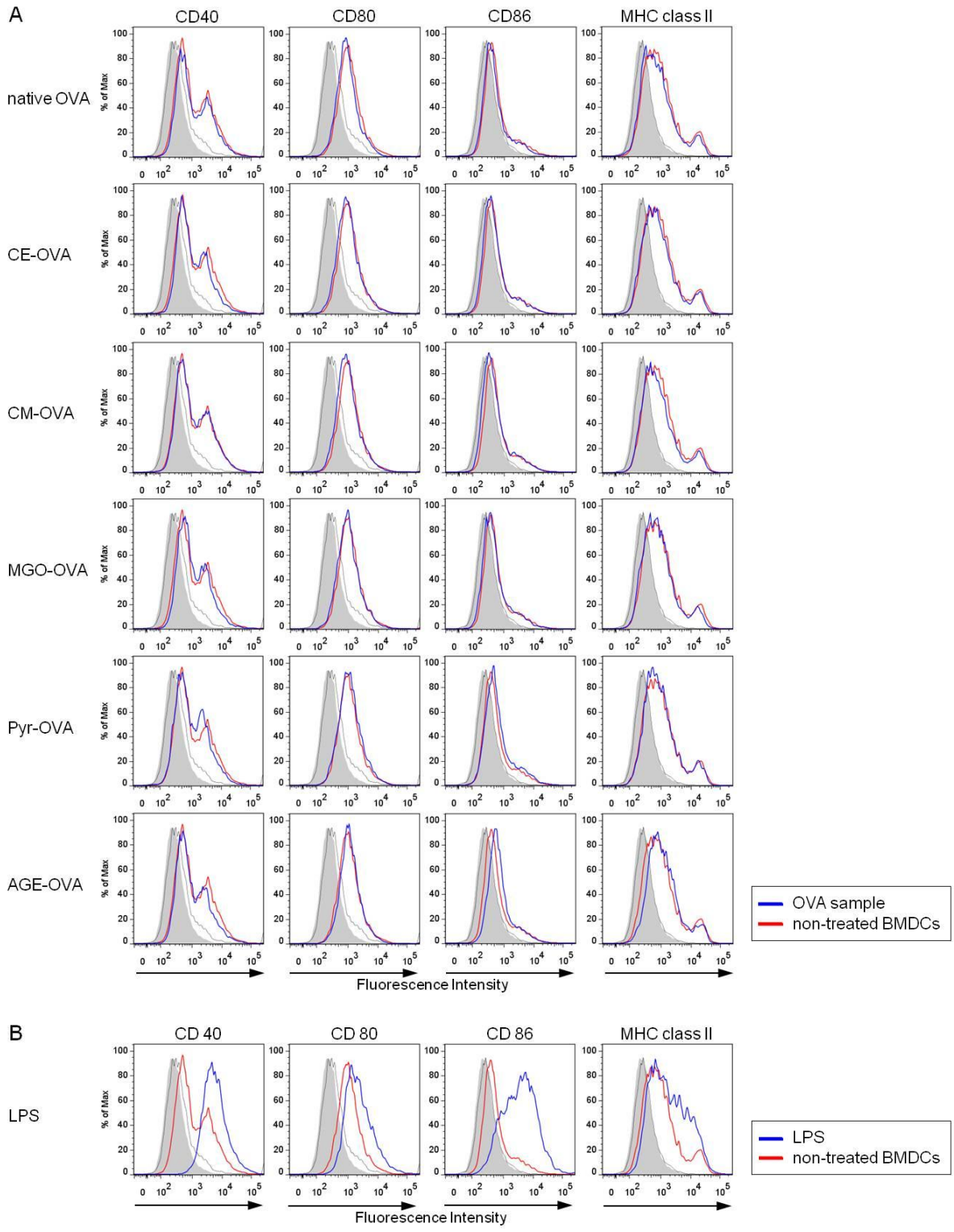


**Figure 22: Co-stimulatory molecule and MHC class II expression by BMDCs upon stimulation with OVA samples.** C57BL/6-derived BMDCs were incubated with (A) 50 µg/ml of OVA sample or (B) 1 µg/ml of LPS for 18 h (blue) or with medium only (red). The cells were then stained using anti-CD40, CD80, CD86 or MHC class II mAb for maturation markers, as well as anti-CD11b and CD11c mAbs for DC surface markers. The expression levels of the maturation markers on the cell surface of $CD11b^{+}CD11c^{+}$ cells were analyzed with flow cytometry. Grey areas represent unstained BMDCs and black lines indicate BMDCs incubated with the respective isotype control antibody.

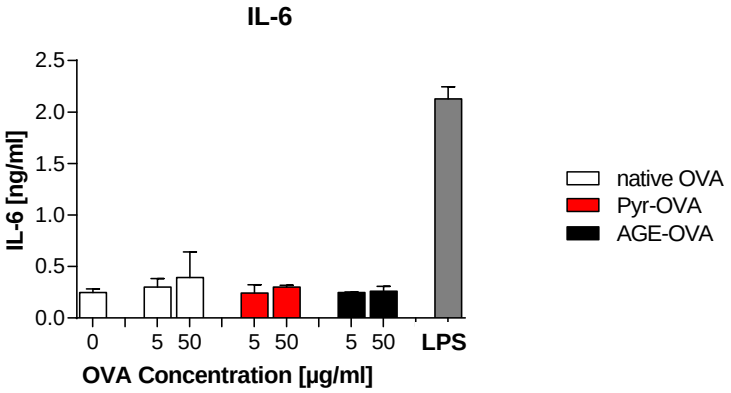


**Figure 23: IL-6 production by BMDCs upon stimulation with OVA samples.** C57BL/6-derived BMDCs were incubated with 5 µg/ml or 50 µg/ml of native OVA, Pyr-OVA, AGE-OVA or 1 µg/ml of LPS for 18 h. The concentration of IL-6 in the cell culture supernatants was determined by ELISA.

#### 4.1.5.2 Uptake of the OVAs modified with glycation structures by BMDCs

A previous study showed that AGE-OVA was highly taken up by BMDCs compared to native OVA and inc. OVA.(*71*) Therefore, the uptake of the modified OVAs was assessed, to see if the specific modification enhances the allergen uptake by BMDCs. For this assessment, the OVA samples were labelled with FITC, a green fluorescent dye, at comparable FITC/protein-ratios. For the uptake assay, also native OVA, inc. OVA and AGE-OVA as well as BSA samples labelled with FITC were used for control experiments. Typical data of FITC/protein-ratios of the OVA samples and the BSA samples are shown in tables 14 and 15, respectively. BMDCs were incubated with either 0.5 µg/ml or 5 µg/ml of FITC-labelled sample for 15 min. The FITC intensity of the $CD11b^{+}CD11c^{+}$ population of the cells was then assessed with flow cytometry.

**Table 14: Calculated molar FITC/protein-ratios of FITC-labelled OVA samples.**

| sample | molar FITC/protein |
|---|---|
| native OVA | 0.46 |
| inc. OVA | 0.42 |
| AGE-OVA | 0.42 |
| CM-OVA | 0.58 |
| CE-OVA | 0.43 |
| MGO-OVA | 0.63 |
| Pyr-OVA | 0.36 |

**Table 15: Calculated molar FITC/protein-ratios of FITC-labelled BSA samples.**

| sample | molar FITC/protein |
|---|---|
| native BSA | 1.55 |
| inc. BSA | 1.38 |
| AGE-BSA | 1.35 |

#### 4.1.5.2.1 Influence of the glycation structure on the antigen uptake by BMDCs

The observed stronger signals for BMDCs incubated in the presence of AGE-OVA compared to native OVA indicate that AGE-OVA is taken up to a stronger extent by BMDCs than native OVA (figures 24 and 25). Also for Pyr-OVA an enhanced antigen uptake by BMDCs was observed. The high uptake of Pyr-OVA and AGE-OVA is visible at both analyzed concentrations. At a concentration of 5 µg/ml a slightly enhanced uptake of CE-OVA and CM-OVA can be seen, which is absent at the antigen dose of 0.5 µg/ml. The uptake of MGO-OVA is comparable to that of native OVA. These results indicate that Pyr-OVA as well as AGE-OVA, but not the other OVAs modified with glycation structures or native OVA, are highly taken up by BMDCs.

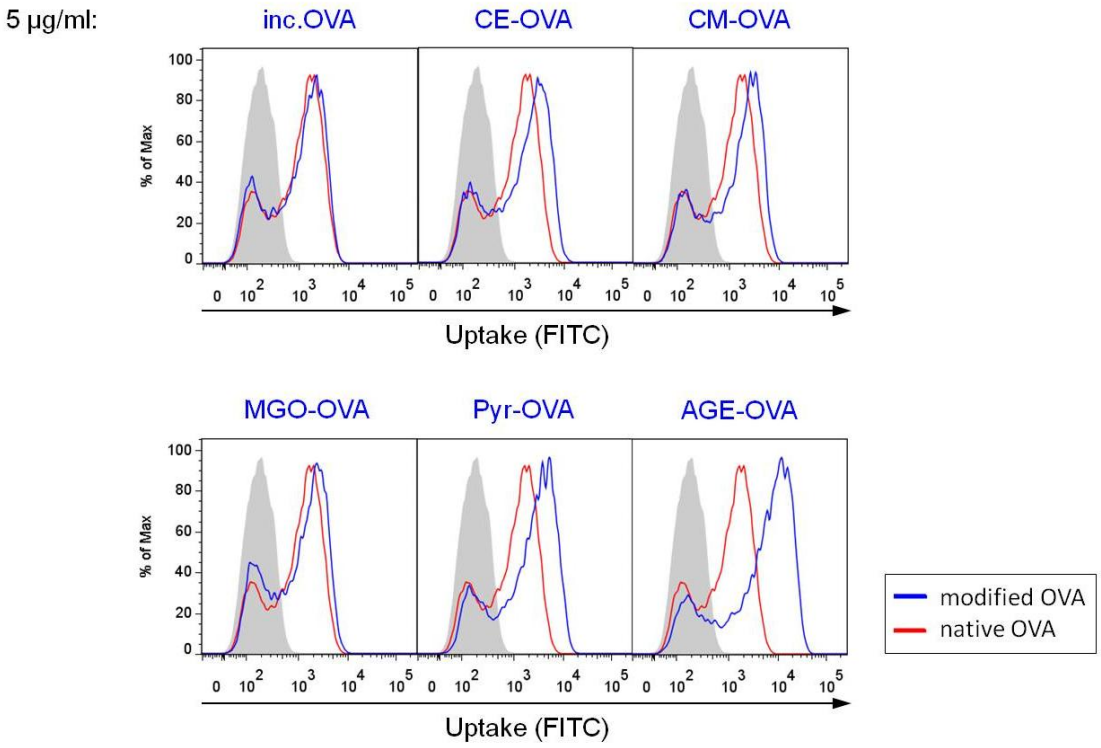


**Figure 24: Uptake of 5 µg/ml OVA samples by BMDCs.** C57BL/6-derived BMDCs were incubated with 5 µg/ml of FITC-labelled OVA samples for 15 min. The uptake of the OVA samples by $CD11b^{+}CD11c^{+}$ BMDCs was measured with flow cytometry. Grey areas represent BMDCs cultured without antigen.

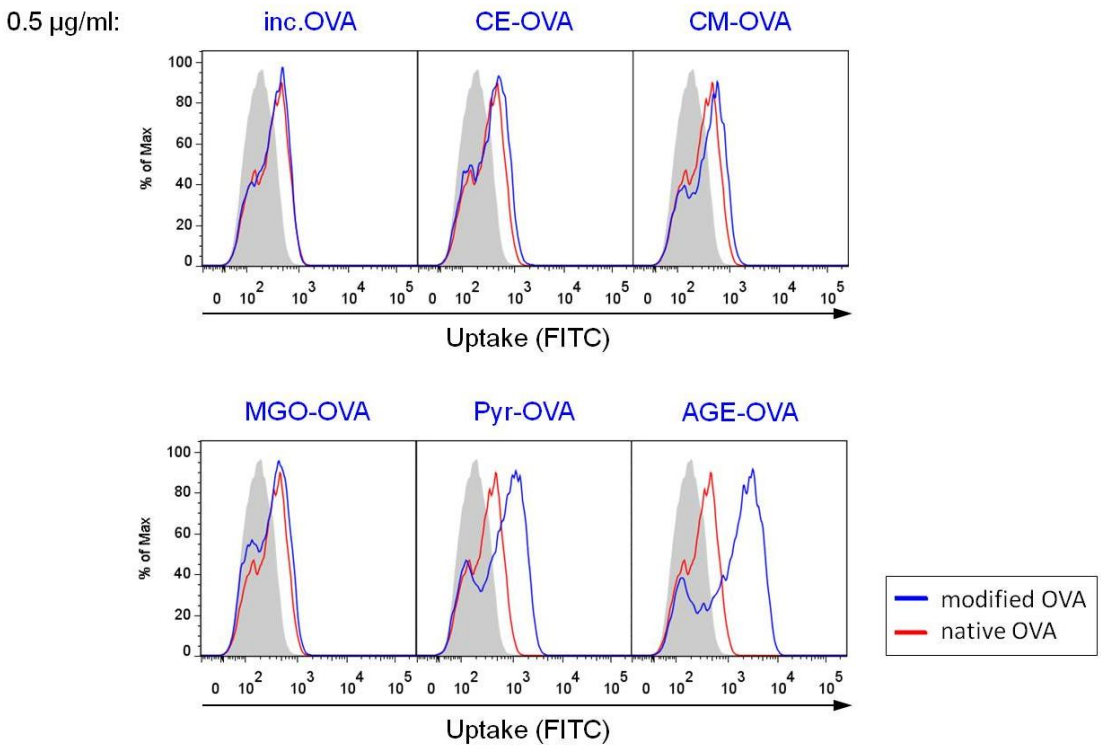


**Figure 25: Uptake of 0.5 µg/ml OVA samples by BMDCs.** C57BL/6-derived BMDCs were incubated with 0.5 µg/ml of FITC-labelled OVA samples for 15 min. The uptake of the OVA samples by $CD11b^{+}CD11c^{+}$ BMDCs was measured with flow cytometry. Grey areas represent BMDCs cultured without antigen.

#### 4.1.5.2.2 Involvement of SR-AI/II in the uptake of Pyr-OVA by BMDCs

The role of SR-AI/II (CD204) in the uptake of the modified OVAs by BMDCs was investigated by comparing the uptake of the modified OVAs with glycation structures by BMDCs derived from B6.Cg-Msr1 ($SR\text{-}A^{-/-}$) mice, which are deficient for SR-AI/II and on a C57BL/6 background, and wt mice. For this purpose, either wt or $SR\text{-}A^{-/-}$ BMDCs were incubated with 0.5 µg/ml or 5 µg/ml of OVA sample for 15 min. FITC intensity of $CD11b^{+}CD11c^{+}$ cells, namely the myeloid dendritic cell population in BMDCs, was then analyzed with flow cytometry.

As shown in the figures 26 and 27, native OVA was taken up to a comparable extent by wt and $SR\text{-}A^{-/-}$ BMDCs. In contrast, uptake of Pyr-OVA and AGE-OVA was reduced in $SR\text{-}A^{-/-}$ cells, although slight levels of uptake of Pyr-OVA and AGE-OVA by $SR\text{-}A^{-/-}$ BMDCs were observed. Uptake levels of the other OVA samples modified with glycation structures were comparable in wt and $SR\text{-}A^{-/-}$ BMDCs.

These results suggest that SR-AI/II mediates the uptake of Pyr-OVA and AGE-OVA by BMDCs. The residual uptake of AGE-OVA and Pyr-OVA by $SR\text{-}A^{-/-}$ cells indicate that other receptor(s) are involved in the uptake of Pyr-OVA and AGE-OVA by BMDCs.

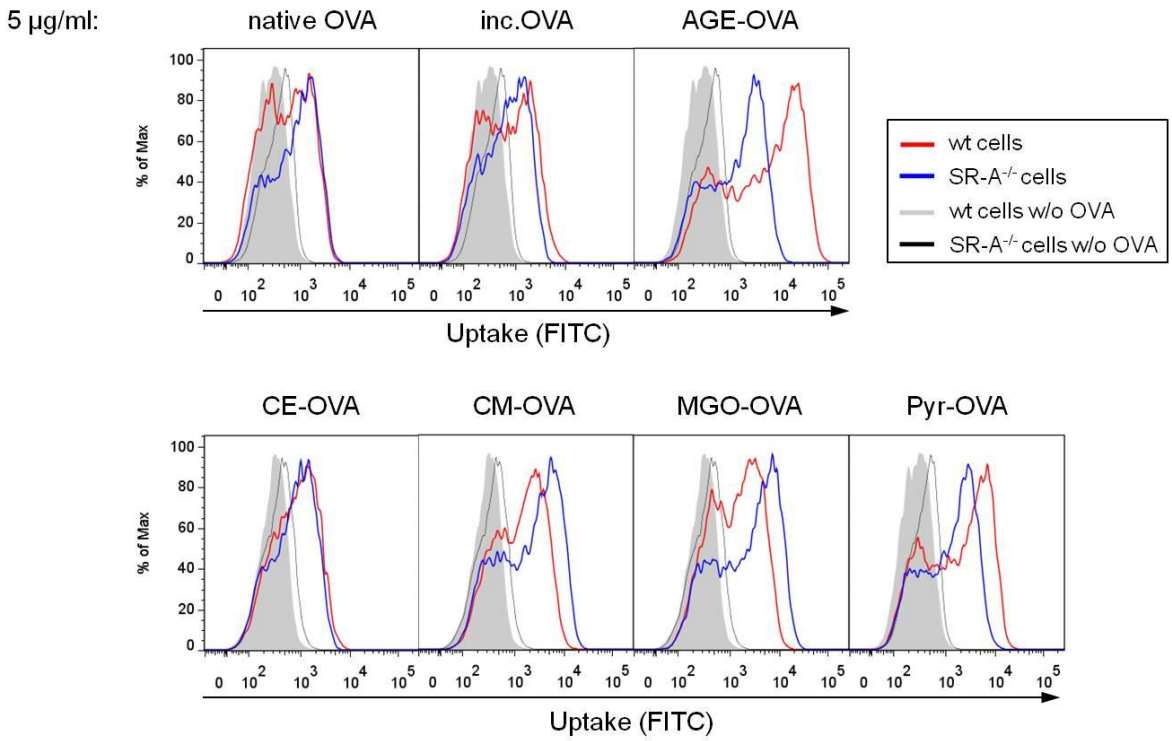


**Figure 26: Uptake of 5 µg/ml of OVA samples by SR-A$^{-/-}$ BMDCs.** Wt BMDCs (red) or SR-A$^{-/-}$ BMDCs (blue) were incubated with 5 µg/ml of FITC-labelled OVA samples for 15 min. FITC intensity of CD11b$^{+}$CD11c$^{+}$ BMDCs was measured using flow cytometry. Grey areas and the black curves represent BMDCs cultured without antigen.

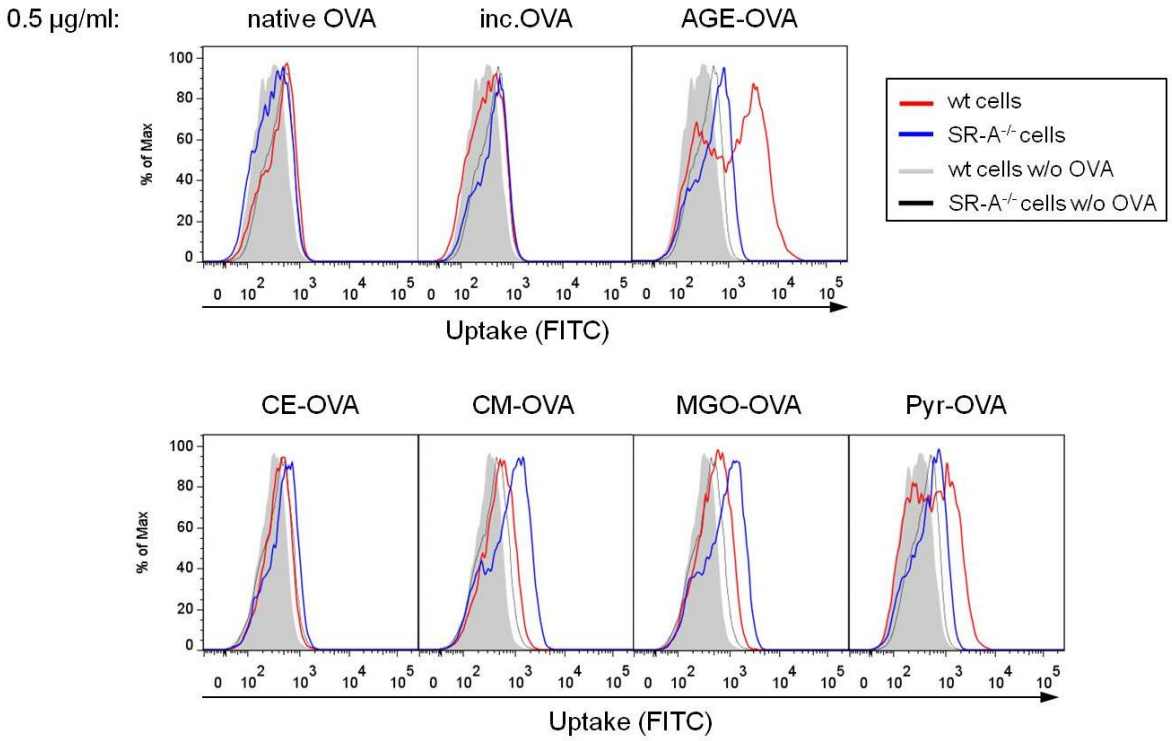


**Figure 27: Uptake of 0.5 µg/ml of OVA samples by SR-A$^{-/-}$ BMDCs.** Wt BMDCs (red) or SR-A$^{-/-}$ BMDCs (blue) were incubated with 0.5 µg/ml of FITC-labelled OVA samples for 15 min. FITC intensity of CD11b$^{+}$CD11c$^{+}$ BMDCs was measured using flow cytometry. Grey areas and the black curves represent BMDCs cultured without antigen.

#### 4.1.5.2.3 Non-involvement of galectin-3 in the uptake of Pyr-OVA by BMDCs

Next, an involvement of galectin-3 in the uptake of Pyr-OVA and AGE-OVA by BMDCs was assessed by pre-treatment of SR-A$^{-/-}$ BMDCs with 150 mmol/l of lactose, a galectin-3 inhibitor, for 30 min before incubation with the FITC-labelled OVA samples. Lactose binds to galectin-3 with high affinity and therefore, blocks binding of all other ligands to galectin-3.(*106*) Here, it was focused on assessing the uptake of Pyr-OVA and AGE-OVA in comparison to native OVA to analyze which other receptor is involved in the residual uptake of Pyr-OVA and AGE-OVA by SR-A$^{-/-}$ BMDCs.

As shown in figure 28, pre-treatment of wt and SR-A$^{-/-}$ BMDCs did not inhibit the uptake of the tested OVA samples. Similar OVA uptake was detected in pre-treated and non-treated BMDCs with lactose. These results suggest that galectin-3 is not involved in the uptake of Pyr-OVA and AGE-OVA.

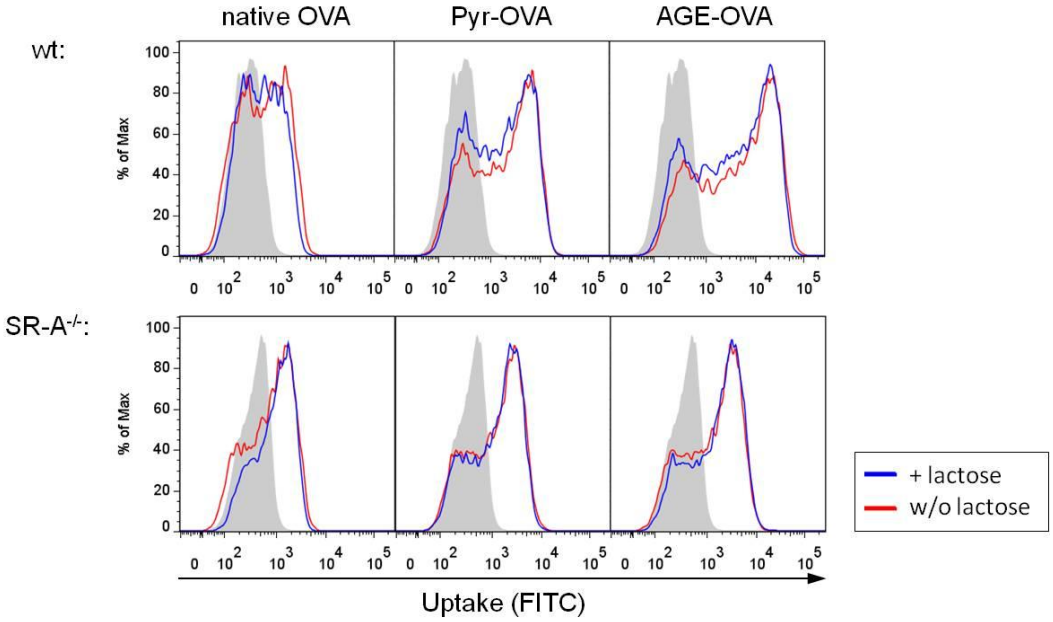


**Figure 28: Uptake of native OVA, Pyr-OVA and AGE-OVA by BMDCs after inhibition of galectin-3 with lactose.** Wt or SR-A$^{-/-}$ BMDCs were treated with 150 mmol/l of lactose 30 min prior to incubation with 5 µg/ml of FITC-labelled native OVA, Pyr-OVA or AGE-OVA for 15 min. FITC intensity of CD11b$^{+}$CD11c$^{+}$ cells was analyzed with flow cytometry. Grey areas represent BMDCs cultured without antigen.

#### 4.1.5.2.4 Non-involvement of SR-BI in the uptake of Pyr-OVA and AGE-OVA by BMDCs

An involvement of SR-BI in the uptake of the OVA samples was assessed using phosphatidylserine (PdS), a SR-BI ligand, as well as the SR-BI inhibitor BLT-1. Nieland et al. showed that both 1 µmol/l or 10 µmol/l of BLT-1 efficiently block the uptake of high density lipoprotein, a natural SR-BI ligand.(*107*) He et al. showed that 100 µg/ml of PdS efficiently inhibit binding of other ligands to SR-BI.(*108*) Hence, SR-A$^{-/-}$ BMDCs were incubated with 1 µmol/l or 10 µmol/l of BLT-1 or

100 µg/ml of PdS for 30 min before the addition of 5 µg/ml of FITC-labelled OVA samples. As control, SR-A$^{-/-}$ BMDCs were incubated with 0.2 % DMSO in DC medium, because BLT-1 was solved in DMSO according to the manufacturer's instructions.

The uptake of Pyr-OVA and AGE-OVA after pre-treatment of SR-A$^{-/-}$ BMDCs with BLT-1 was comparable to the uptake by non-treated cells (figure 29). Pre-treatment of SR-A$^{-/-}$ BMDCs with PdS also did not reduce the uptake of OVA samples (figure 30). These results suggest that SR-BI is not involved in the uptake of Pyr-OVA and AGE-OVA.

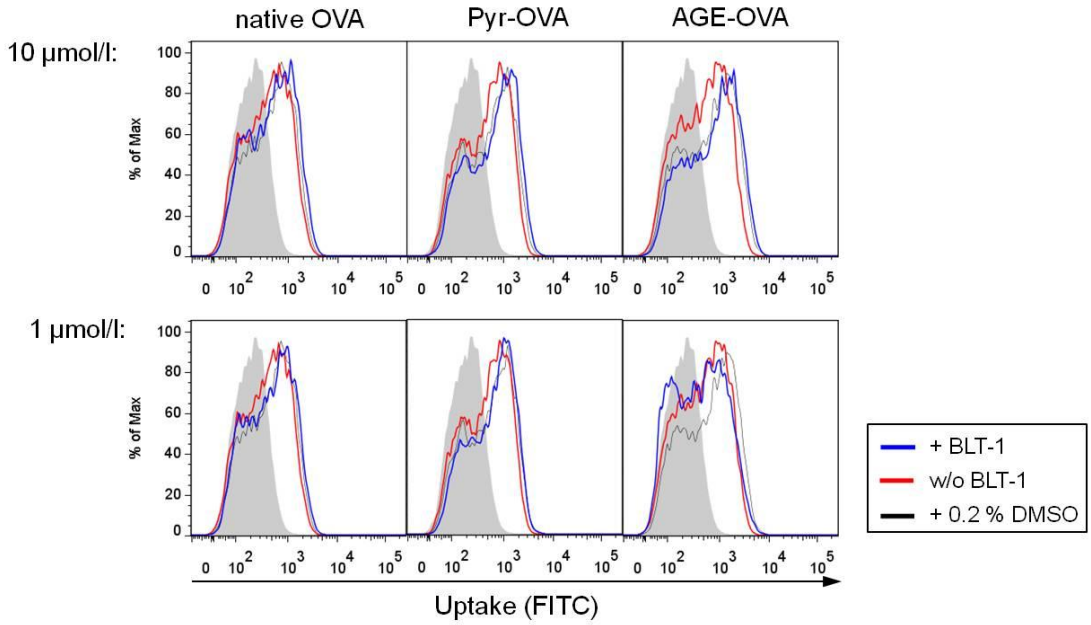


**Figure 29: Uptake of OVA samples by BMDCs after inhibition of SR-BI with BLT-1.** SR-A$^{-/-}$ BMDCs were incubated with or without 1 µmol/l or 10 µmol/l of BLT-1 in 0.2 % DMSO for 30 min and then incubated with 5 µg/ml of FITC-labelled native OVA, Pyr-OVA or AGE-OVA for 15 min. FITC intensity of CD11b$^{+}$CD11c$^{+}$ cells was analyzed with flow cytometry. Grey areas represent BMDCs cultured without antigen.

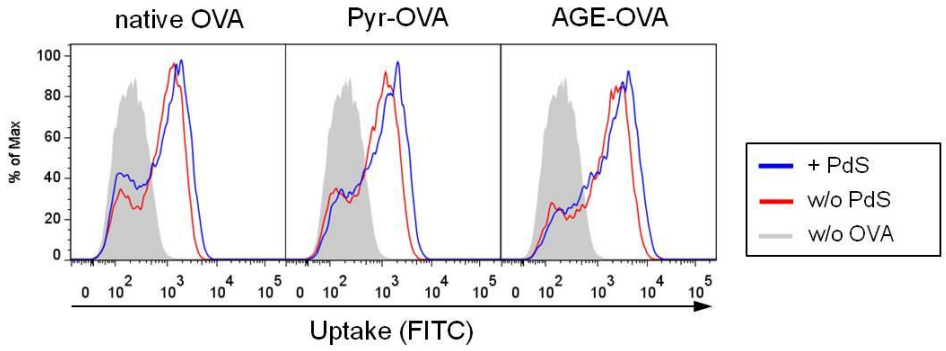


**Figure 30: Uptake of OVA samples by BMDCs after inhibition of SR-BI with PdS.** SR-A$^{-/-}$ BMDCs were incubated with or without 100 µg/ml of phosphatidylserine (PdS) for 30 min and then incubated with 5 µg/ml of FITC-labelled native OVA, Pyr-OVA or AGE-OVA for 15 min. FITC intensity of CD11b$^{+}$CD11c$^{+}$ cells was analyzed with flow cytometry. Grey areas represent BMDCs cultured without antigen.

#### 4.1.5.2.5 Non-involvement of CD36 in the uptake of Pyr-OVA and AGE-OVA by BMDCs

CD36, another member of the SR-B family, was shown to bind AGEs.(*51*) Therefore, CD36 was an interesting target for this study. A specific inhibitor for CD36 had not been available. Thus, involvement of CD36 in the uptake of Pyr-OVA or AGE-OVA by BMDCs was assessed by neutralizing antibodies to block interaction of CD36 with ligands. To exclude an involvement of SR-AI/II in the uptake of OVA samples in this assessment, SR-A$^{-/-}$ BMDCs were used. The cells were pre-treated with 2 µg/ml of anti-CD36 antibodies for 30 min and then incubated with 5 µg/ml of FITC-labelled OVA sample for 15 min.

Pre-treatment with antibodies against CD36 did not reduce the uptake of native OVA, Pyr-OVA and AGE-OVA by SR-A$^{-/-}$ BMDCs, as can be seen in figure 31A. Binding of these antibodies against CD36 expressed on the cell surface of BMDCs was confirmed with flow cytometry, as shown in figure 31B. These results suggest that CD36 does not play a role in the uptake of Pyr-OVA and AGE-OVA.

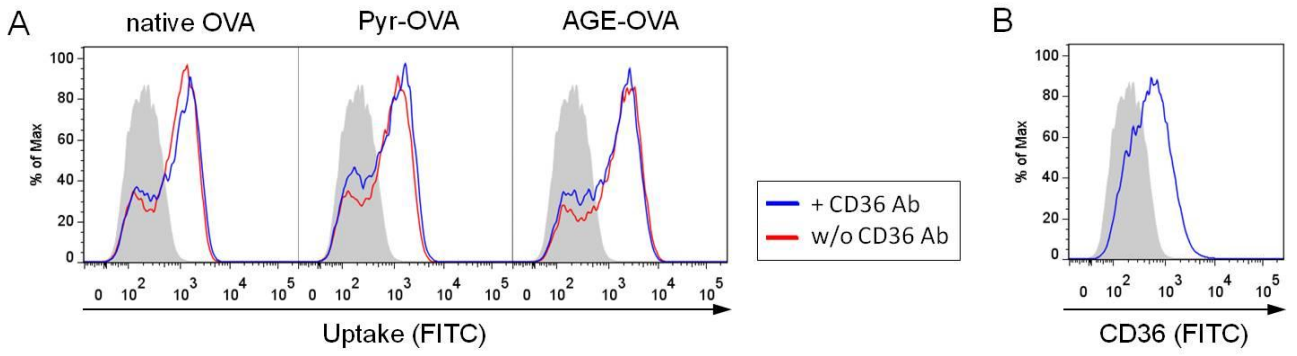


**Figure 31: Uptake of OVA samples after blocking of CD36 and binding of anti-CD36 antibodies to BMDCs.** SR-A$^{-/-}$ BMDCs were incubated with 2 µg/ml of anti-mouse CD36 IgA antibodies for 30 min and (A) then incubated with 5 µg/ml of FITC-labelled native OVA, Pyr-OVA or AGE-OVA for 15 min or (B) incubated with of FITC-labelled goat anti-mouse IgA antibody. FITC intensity of CD11b$^{+}$CD11c$^{+}$ BMDCs was analyzed with flow cytometry.

#### 4.1.5.2.6 Involvement of the mannose receptor in the uptake of Pyr-OVA by BMDCs

The uptake of the modified OVAs by the MR needed to be considered, because native OVA is a glycosylated protein and possess natural mannose residues binding to the MR.(*19, 59*) Indeed, mannan, a mannose-containing polysaccharide, has been utilized as an inhibitor for the MR. To investigate an involvement of the MR in the uptake of Pyr-OVA and AGE-OVA, wt or SR-A$^{-/-}$ BMDCs were treated with 3 mg/ml of mannan before incubation with 5 µg/ml of FITC-labelled OVA samples. BSA does not contain natural carbohydrate residues and therefore, the uptake of native BSA, inc. BSA or AGE-BSA served as a control in this experiment.

The uptake of native OVA, Pyr-OVA and AGE-OVA by mannan-treated BMDCs was essentially reduced compared to non-treated cells (figure 32). Pre-treatment of SR-A$^{-/-}$ cells with mannan nearly completely inhibited the uptake of all OVA samples, although slight levels of Pyr-OVA and AGE-OVA uptake were observed. The difference in the reduction of uptake after mannan-treatment by wt and SR-A$^{-/-}$ BMDCs in figure 32 might be explained by a strong uptake of Pyr-OVA and AGE-OVA by the SR-AI/II and thus, SR-AI/II seems to be compensating for the block of the MR.

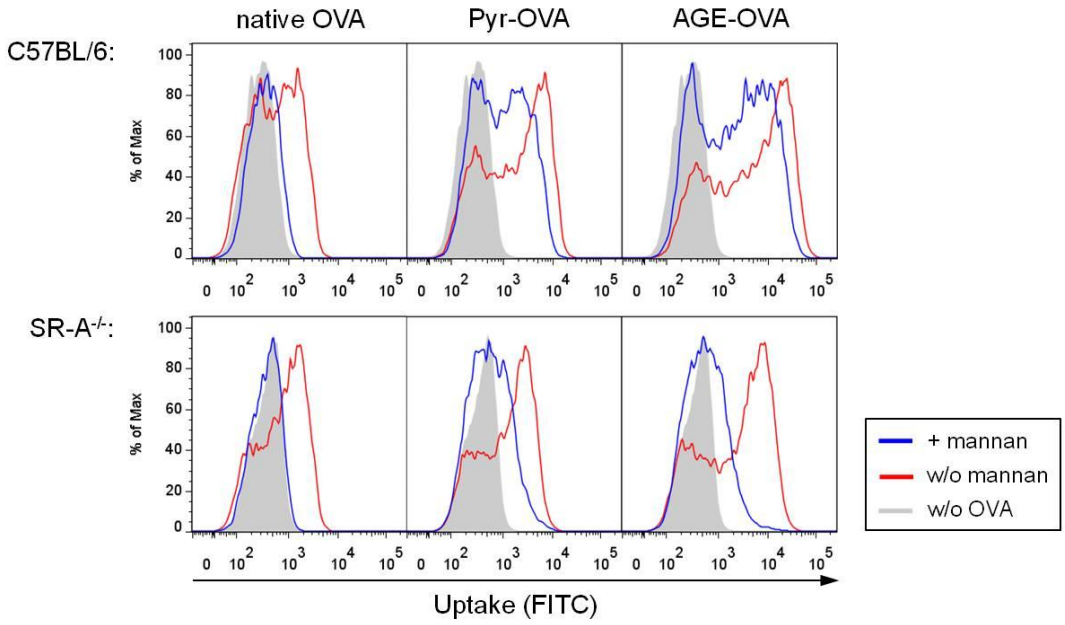


**Figure 32: Uptake of OVA samples by BMDCs after inhibition of the MR with mannan.** Wt or SR-A$^{-/-}$ BMDCs were treated with 3 mg/ml of mannan for 30 min prior to incubation with 5 µg/ml of FITC-labelled native OVA, Pyr-OVA or AGE-OVA for 15 min. FITC intensity of CD11b$^{+}$CD11c$^{+}$ cells was analyzed with flow cytometry. Grey areas represent BMDCs cultured without antigen.

To examine whether mannan inhibit the interaction of natural mannose residues in native OVA with the MR specifically, BSA samples were used, as this protein does not possess mannose residues. A strong uptake of AGE-BSA by non-treated BMDCs was observed, whereas native BSA and inc. BSA were not taken up by the cells (figure 33). Thus, the uptake of AGE-BSA by BMDCs is only mediated by AGE-binding receptors. Unexpectedly, pre-treatment of wt BMDCs with mannan reduced the uptake of AGE-BSA. The reduced uptake of AGE-BSA was also observed in SR-A$^{-/-}$ BMDCs pre-treated with mannan. These results suggest that the MR could be involved in the uptake of AGE-BSA and AGE-OVA by association with glycation structures.

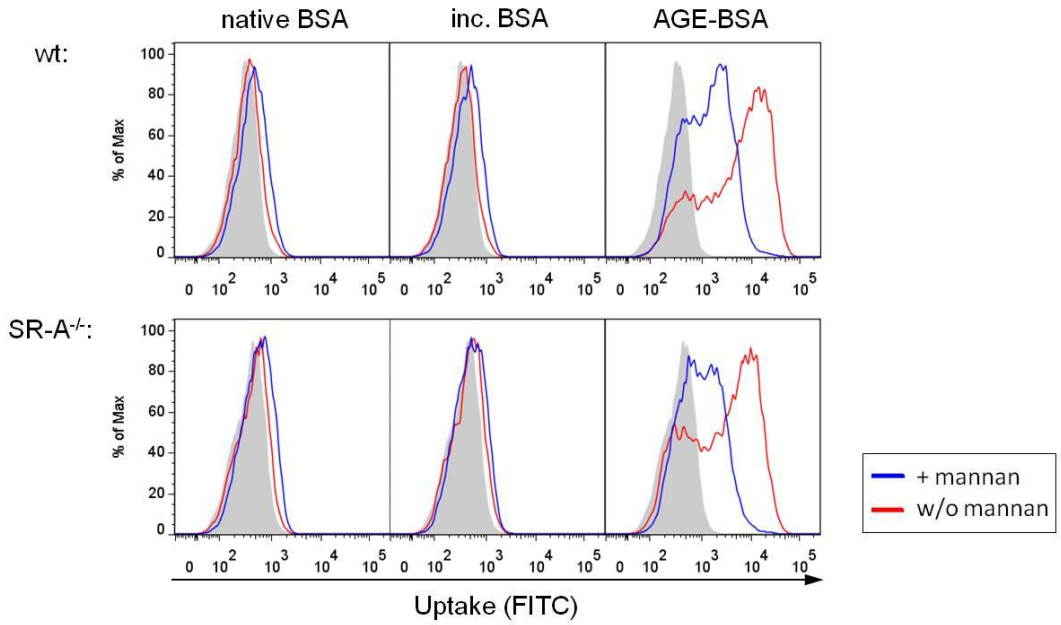


**Figure 33: Uptake of BSA samples by BMDCs after inhibition of the MR with mannan.** Wt or SR-A$^{-/-}$ BMDCs were treated with 3 mg/ml of mannan for 30 min prior to incubation with 5 µg/ml of FITC-labelled native BSA, inc. BSA or AGE-BSA for 15 min. FITC intensity of CD11b$^{+}$CD11c$^{+}$ cells was analyzed with flow cytometry. Grey areas represent BMDCs cultured without antigen.

### 4.1.6 Role of SR-AI/II in the activation of OVA-specific CD4$^{+}$ T-cells by Pyr-OVA

The results obtained so far suggest that the uptake of Pyr-OVA by BMDCs is in part mediated by SR-AI/II. Next, the impact of the SR-AI/II-mediated uptake of the OVA samples by DCs on CD4$^{+}$ T-cell activation was investigated. To investigate the impact, a co-culture system of SR-A$^{-/-}$ BMDCs and OVA-specific CD4$^{+}$ T-cells isolated from OT-II mice was used. Either wt or SR-A$^{-/-}$ BMDCs were primed with native OVA, Pyr-OVA or AGE-OVA before the addition of OT-II cells to avoid the putative interaction of antigen with CD4$^{+}$ T-cells. IL-2 production served as an indicator for T-cell activation.

As shown in figure 34, BMDCs primed with Pyr-OVA or AGE-OVA induced higher levels of IL-2 production in their culture supernatants compared to those primed with native OVA. This strong T-cell activation by Pyr-OVA and AGE-OVA was reduced by the use of SR-A$^{-/-}$ BMDCs, instead of wt BMDCs. These results suggest that SR-AI/II plays a crucial role in the uptake of Pyr-OVA and AGE-OVA by BMDCs and subsequent CD4$^{+}$ T-cell activation.

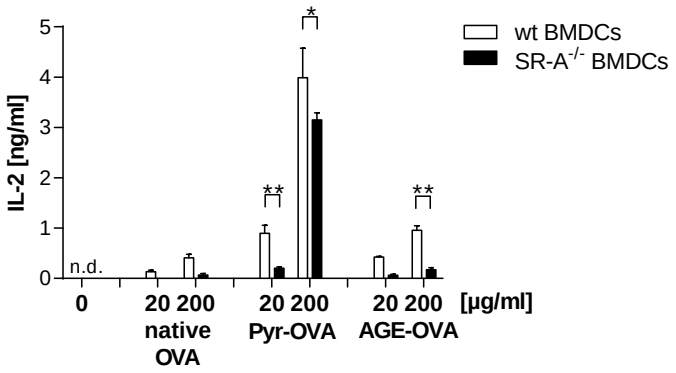


**Figure 34: IL-2 production by OT-II cells cultured with SR-A$^{-/-}$ or wt BMDCs primed with OVA samples.** CD4$^{+}$ T-cells were isolated from OT-II mice. Syngeneic BMDCs were incubated with 20 µg/ml or 200 µg/ml of native OVA, Pyr-OVA or AGE-OVA for 3 h and washed. OT-II cells and OVA sample-primed BMDCs were cultured for 20 h. The concentration of IL-2 in the cell culture supernatants was then determined by ELISA. * $p < 0.05$, ** $p < 0.01$ (n.d.: not detectable; below detection limit of 0.02 pg/ml).

### 4.1.7 Localization of Pyr-OVA and AGE-OVA in intracellular compartments after antigen uptake

Antigens taken up by receptor-mediated endocytosis, as in the case of OVA, are processed for antigen-presentation in intracellular compartments, like endosomes or lysosomes. Next, it was tried to verify the receptor-mediated endocytosis of OVA samples by BMDCs.

For this purpose, wt BMDCs were incubated with FITC-labelled Pyr-OVA or AGE-OVA for 15 min. After fixation and permeabilization, the cells were stained for early endosomes using a mAb specific for the early endosomal antigen-1 (EEA-1) followed by staining of the cell nucleus with DAPI. The analysis of the putative co-localization of the modified OVAs with EEA-1 was performed using a confocal microscope.

The yellow spots in figure 35 show co-localization of EEA-1 with Pyr-OVA or AGE-OVA, respectively. These findings suggest that Pyr-OVA and AGE-OVA are transported to endosomal compartments in BMDCs after antigen uptake.

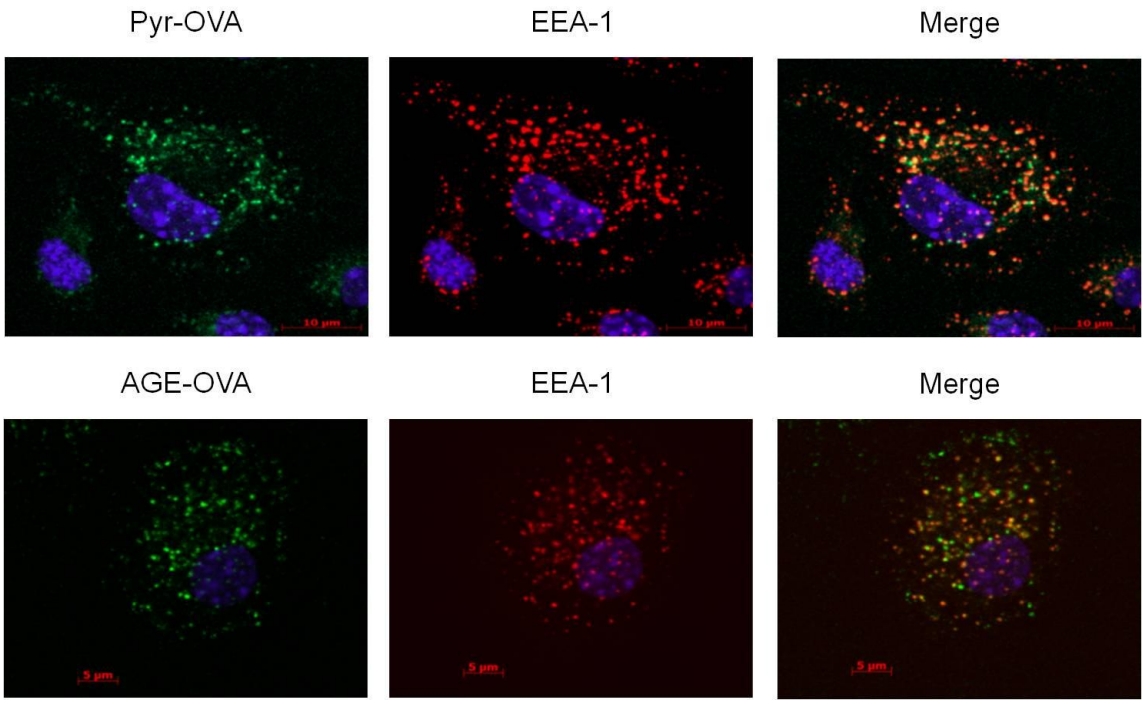


**Figure 35: Co-localization of Pyr-OVA or AGE-OVA with EEA-1 in BMDCs.** Wt BMDCs were incubated with FITC-labelled Pyr-OVA or AGE-OVA (green) for 15 min, then fixed with 4 % PFA and stained using anti-EEA-1 mAb (red). The cell nucleus was stained with DAPI (blue). The cells were analyzed using a confocal microscope.

### 4.1.8 Influence of glycation on the potential allergenicity of OVA using a mouse model of intestinal allergy

Next, it was investigated whether glycation also influences the potential allergenicity (i.e. ability to induce sensitization by triggering IgE production and to cause clinical symptoms in an allergic individual) of OVA using a mouse model of intestinal allergy. The immunization protocol of the model, which was established by Burggraf et al., is shown in figure 36.(*101*) Briefly, BALB/c mice were intraperitoneally (i.p.) sensitized with native OVA, Pyr-OVA or AGE-OVA in combination with ALUM, an adjuvant inducing $T_H2$-directed immune responses, twice at a two week interval. Two weeks after the last sensitization, the mice were fed with a diet containing egg white (EW-diet) for one week.

After the i.p. sensitization, the levels of OVA-specific IgE, IgG1 and IgG2a antibodies in the sera were determined by ELISA. During feeding the EW-diet, clinical symptoms, i.e. loss of body weight and drop in body core temperature, of the mice were monitored. Furthermore, after the feeding, the mice were euthanized for isolation of $CD4^+$ T-cells from the gut draining lymphoid organ, i.e. the mesenteric lymph nodes (MLN). The isolated MLN-derived $CD4^+$ T-cells were used to assess OVA-specific T-cell responses in the tissues.

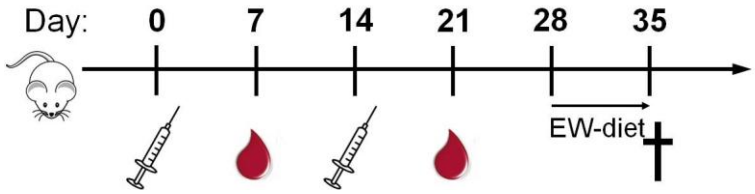


**Figure 36: Immunization protocol of a mouse model of intestinal allergy.** BALB/c mice (n=6) were i.p. sensitized with 10 µg of native OVA, Pyr-OVA or AGE-OVA together with 1 mg of ALUM twice. One week after each sensitization blood was taken from the mice. Two weeks after the last sensitization, the mice were fed with a diet containing egg white (EW-diet). On day 7 of the EW-diet, the mice were euthanized to harvest the MLN for T-cell assays.

#### 4.1.8.1 Levels of OVA-specific IgE, IgG1 and IgG2a in mice sensitized with OVA modified with glycation structure

In mice, IL-4, a $T_H2$-related cytokine, induces antibody class switch to IgE and IgG1 in B-cells, while IFN-γ, a $T_H1$-related cytokine, induces class switch to IgG2a. To assess the potential allergenicity of the OVAs modified with glycation structures, the serum levels of IgE, IgG1 and IgG2a antibodies in mice, who received i.p. sensitization with native OVA, Pyr-OVA or AGE-OVA were measured by ELISA.

After the first i.p. sensitization with OVA samples, IgE antibodies were not detectable in all groups. However, by the second sensitization, serum IgE levels of mice sensitized with Pyr-OVA or AGE-OVA were remarkably enhanced and were higher than those of mice sensitized with native OVA (figure 37A). The result suggests that Pyr-OVA and AGE-OVA could have a higher ability to induce sensitization than native OVA.

OVA-specific IgG1 antibodies were detected in the sera of mice from all groups after the first i.p. sensitization. The serum IgG1 levels of mice sensitized with Pyr-OVA or AGE-OVA were higher than those of mice sensitized with native OVA (figure 38A). After the second sensitization, serum IgG1 levels of mice sensitized with Pyr-OVA or AGE-OVA were rather reduced, compared to those of mice sensitized with native OVA. The result suggest that, in the i.p. sensitization setting, production of IgG1 antibodies was saturated by the second sensitization with Pyr-OVA and AGE-OVA due to its high immunogenicity. Serum OVA-specific IgG2a antibodies were detected in mice from all groups only after the second sensitization. The serum levels of IgG2a antibodies in mice sensitized with Pyr-OVA or AGE-OVA tended to be higher than those of mice sensitized with native OVA, although only marginal levels were detected (figure 39A). These results suggest that Pyr-OVA and AGE-OVA are capable of inducing higher antibody production than native OVA in the sensitization phase of allergy.

Next, the serum antibody levels in the sensitized mice after EW-diet feeding were measured. EW-diet feeding induced a strong boost in the levels of OVA-specific IgE and IgG1 antibodies (figures 37B and

38B), whereas OVA-specific IgG2a antibodies stayed at marginal levels (figure 39B). Here, no significant differences in the levels found after sensitization were observed. This could be due to the high amount of native OVA contained in the EW-diet, which could trigger a strong booster effect on the OVA-specific antibody production and therefore, the levels of IgE and IgG1 antibodies became comparable among all groups.

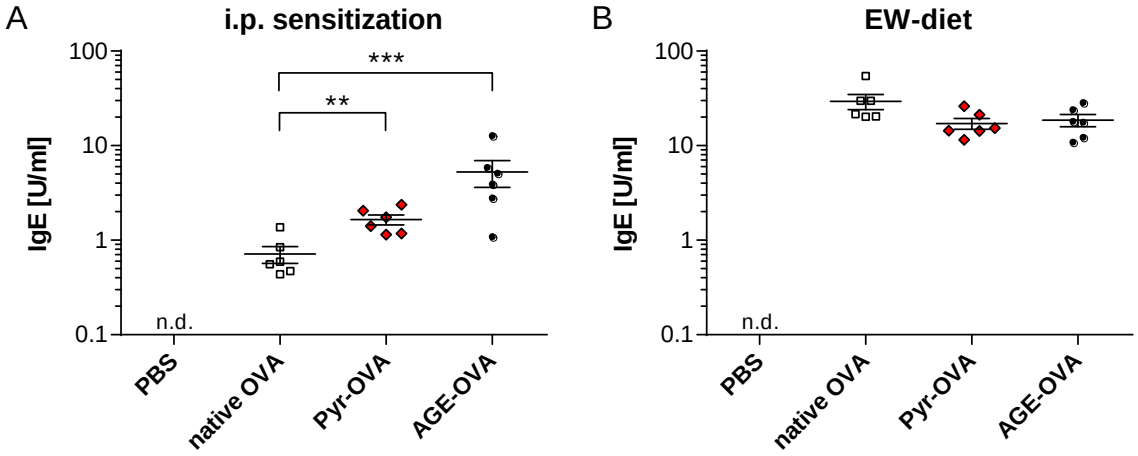


**Figure 37: OVA-specific IgE antibody production in mice sensitized with OVA samples and fed EW-diet.** (A) Mice were i.p. sensitized with native OVA, Pyr-OVA or AGE-OVA together with ALUM as an adjuvant twice. (B) Two weeks after the last sensitization, the mice were fed a diet containing egg white (EW-diet). Sera were collected one week after each sensitization and after 7d of feeding. Levels of OVA-specific IgE antibodies were determined by ELISA. Each symbol represents the data of one individual mouse. * $p < 0.05$, ** $p < 0.01$, *** $p < 0.001$ (n.d.: not detectable; below detection limit of 0.1 U/ml).

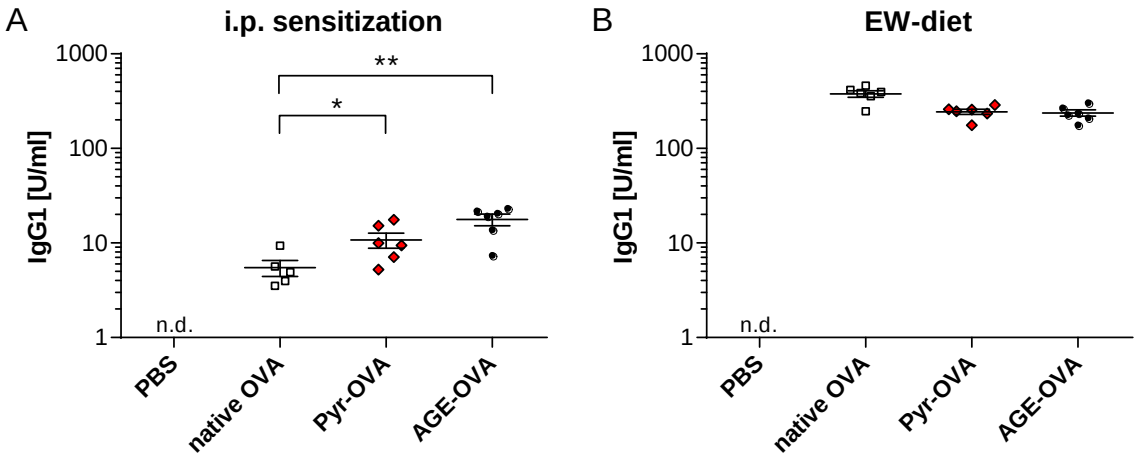


**Figure 38: OVA-specific IgG1 antibody production in mice sensitized with OVA samples and fed EW-diet.** (A) Mice were i.p. sensitized with native OVA, Pyr-OVA or AGE-OVA together with ALUM as an adjuvant twice. (B) Two weeks after the last sensitization, the mice were fed a diet containing egg white (EW-diet). Sera were collected one week after each sensitization and after 7d of feeding. Levels of OVA-specific IgG1 antibodies were determined by ELISA. Each symbol represents the data of one individual mouse. * $p < 0.05$, ** $p < 0.01$ (n.d.: not detectable; below detection limit of 0.005 U/ml).

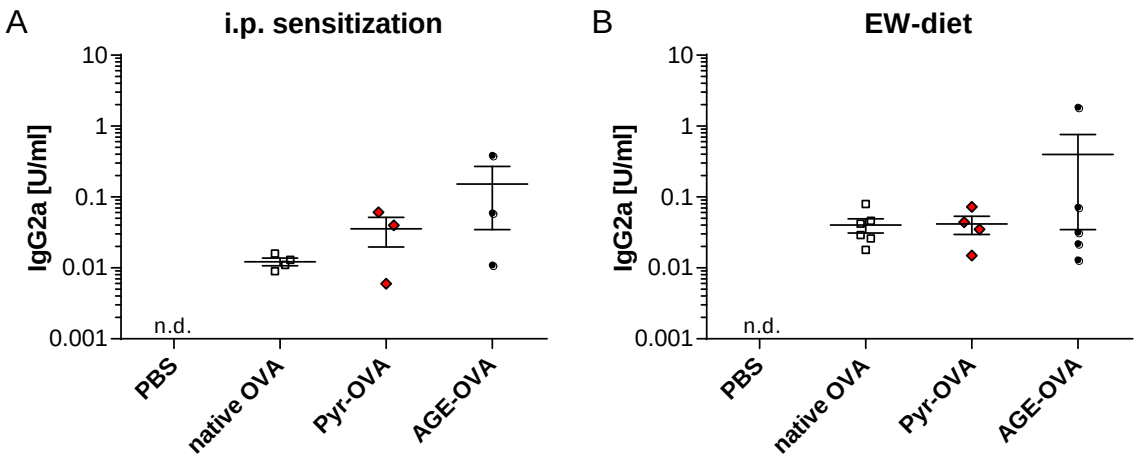


**Figure 39: OVA-specific IgG2a antibody production in mice sensitized with OVA samples and fed EW-diet.** (A) Mice were i.p. sensitized with native OVA, Pyr-OVA or AGE-OVA together with ALUM as an adjuvant twice. (B) Two weeks after the last sensitization, the mice were fed a diet containing egg white (EW-diet). Sera were collected one week after each sensitization and after 7d of feeding. Levels of OVA-specific IgG2a antibodies were determined by ELISA. Each symbol represents the data of one individual mouse. (n.d.: not detectable; below detection limit of 0.005 U/ml).

#### 4.1.8.1.1 Binding of IgE in sera of Pyr-OVA- or AGE-OVA-sensitized mice to glycation structures

Next, it was investigated whether sensitization of BALB/c mice with Pyr-OVA or AGE-OVA, induces production of IgE antibodies specific for glycation structure(s). For this purpose, ELISA was performed using plates coated with 100 µg/ml of AGE-OVA or AGE-BSA. Protein conformation and the primary sequence of OVA and BSA are different. Therefore, by using AGE-BSA it is possible to examine whether sera in AGE-OVA-sensitized mice contained antibodies binding to glycation structure(s).

As shown in figure 40, higher levels of IgE in AGE-OVA-sensitized mice and slightly increased levels of IgE in Pyr-OVA-sensitized mice were detected compared to IgE levels in native OVA-sensitized mice when ELISA plates coated with native OVA or AGE-OVA were used. No IgE binding to AGE-BSA was detected when ELISA plates were coated with this control glycation product without OVA protein (data not shown). The result suggests that Pyr-OVA and AGE-OVA would not induce antibodies specific for glycation structures.

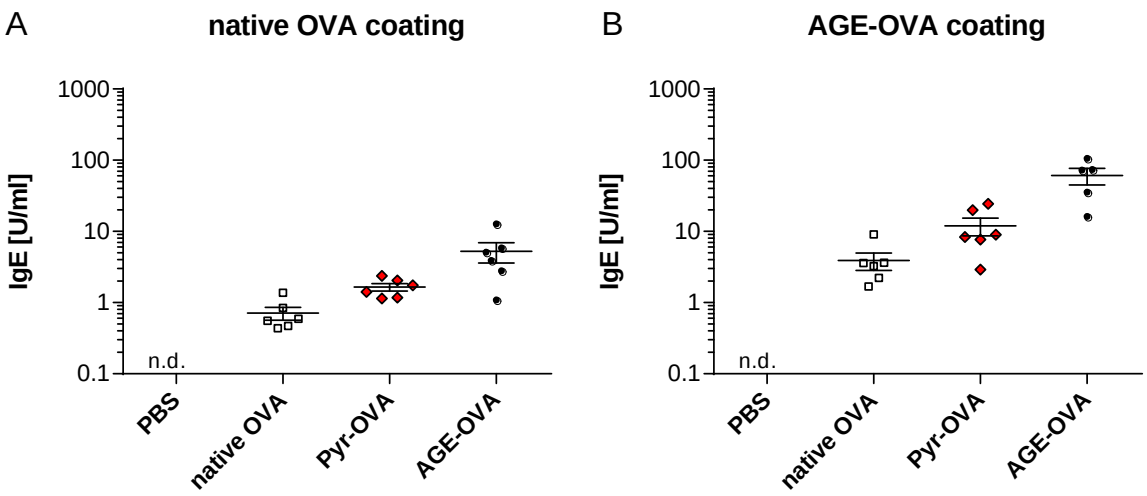


**Figure 40: Detection of IgE antibodies binding to glycation structures by ELISA.** After the second i.p. sensitization with native OVA, Pyr-OVA or AGE-OVA together with ALUM, blood was taken from the mice and the sera were prepared. The sera were then applied to ELISA plates coated with (A) native OVA or (B) AGE-OVA. IgE binding to coated materials was detected using Biotin-anti-mouse IgE mAb in combination with Streptavidin-HRP. Each symbol represents the data of one individual mouse. (n.d.: not detectable; below detection limit of 0.1 U/ml).

#### 4.1.8.2 Clinical symptoms in mice sensitized with Pyr-OVA or AGE-OVA

It was of particular importance to investigate whether the elevated levels of IgE antibodies by Pyr-OVA or AGE-OVA sensitization enhance clinical symptoms. Therefore, the sensitized animals were fed with EW-diet and their body weight as well as their body core temperature was monitored.

EW-diet feeding for four days induced strong loss of body weight in all sensitization groups (figure 41A). Although the differences were not remarkable, there was a tendency that a stronger weight loss was induced in Pyr-OVA- or AGE-OVA-sensitized mice compared to native OVA-sensitized mice. Moreover, on day four of EW-diet feeding the lowest body core temperature was detected in all sensitized mice (figure 41B). Body core temperature of Pyr-OVA- or AGE-OVA-sensitized mice was considerably lower than that of native OVA-sensitized mice.

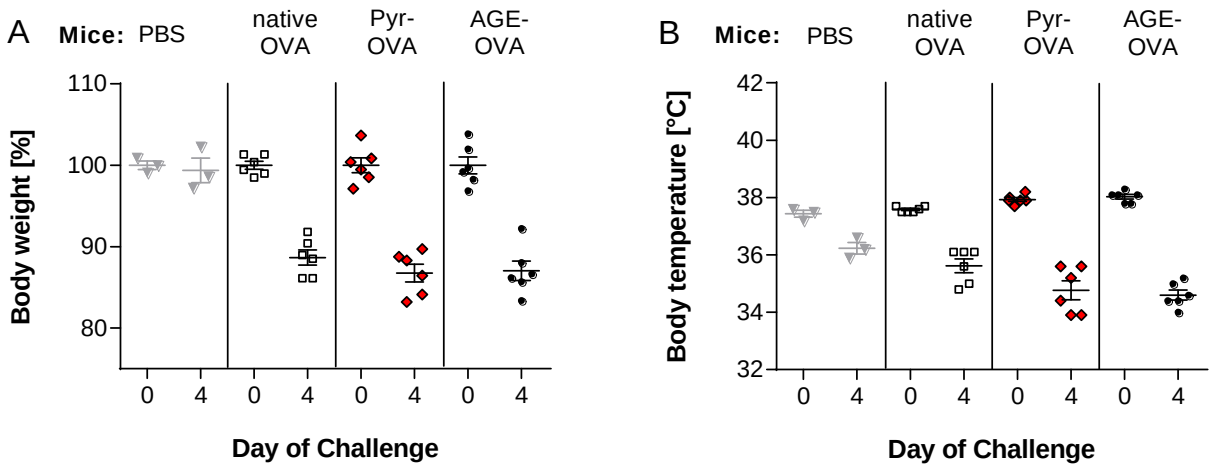


**Figure 41: Changes of (A) body weight and (B) body core temperature in mice sensitized with OVA samples and fed EW-diet.** Two weeks after the second i.p. sensitization with native OVA, Pyr-OVA or AGE-OVA together with ALUM, BALB/c mice were fed EW-diet. (A) Body weight and (B) body core temperature of sensitized and fed mice were monitored. Each symbol represents the data of one individual mouse.

Taken together, strong clinical symptoms were observed in mice sensitized with OVA samples during feeding the EW-diet and the strongest symptoms were found in Pyr-OVA- and AGE-OVA-sensitized mice. These results suggest that modification with pyrraline or glycation structures could enhance the allergenic potency of OVA.

#### 4.1.8.3 Influence of glycation structure on the activation of MLN-derived CD4$^+$ T-cells from allergic mice

Besides humoral immune responses and clinical symptoms, the T-cell immune response in the mice sensitized with the OVAs modified with glycation structures was assessed. The mice were sacrificed after one week of EW-diet feeding and their MLN were isolated. Proliferation as well as cytokine production by MLN-derived CD4$^+$ T-cells upon *in vitro* stimulation with OVA samples was then measured.

CD4$^+$ T-cells from mice sensitized with native OVA, Pyr-OVA or AGE-OVA showed higher proliferation in response to Pyr-OVA or AGE-OVA (figure 42). The proliferation levels of MLN CD4$^+$ T-cells in response to OVA samples were similar among the groups. Enhanced IL-4 production, particular against Pyr-OVA, was observed by MLN CD4$^+$ T-cells from mice sensitized with native OVA or Pyr-OVA (figure 43). The lower proliferation against the high concentration of Pyr-OVA (1000 µg/ml) compared to the high levels of IL-4 might be explained by an over-stimulation of the cells shortening the cell viability, because IL-4 was measured after 72 h of culture, whereas

proliferation was measured after 96 h of culture. IL-4 production against AGE-OVA was also enhanced by MLN CD4$^+$ T-cells from mice sensitized with AGE-OVA. These results suggest that Pyr-OVA and AGE-OVA could have a higher T-cell immunogenicity *in vivo*, where polyclonal T-cells exist and react to allergens.

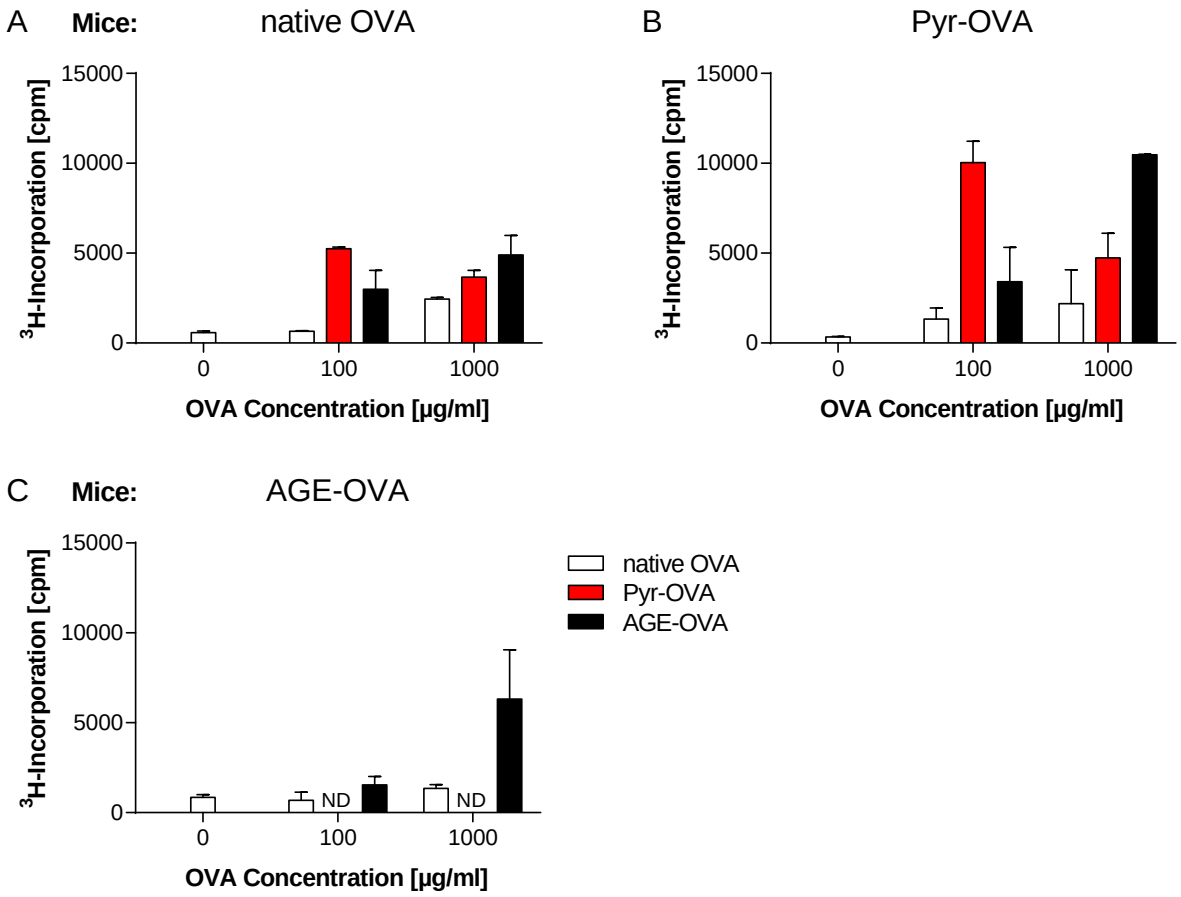


**Figure 42: Proliferation of MLN-derived CD4$^+$ T-cells from allergic mice sensitized with OVA samples and fed EW-diet.** BALB/c mice were sensitized with (A) native OVA, (B) Pyr-OVA or (C) AGE-OVA together with ALUM twice and fed EW-diet for seven days. CD4$^+$ T-cells were then isolated from the MLN of the mice and co-cultured with mitomycin-treated syngeneic splenocytes in the presence of either form of OVA for 96 h. Proliferation of CD4$^+$ T-cells was assessed by incorporation of [methyl-$^3$H]-thymidine during the last 20 h of culture. (ND: not determined; Pyr-OVA was not included for stimulation in panel C due to the limited amount of this material).

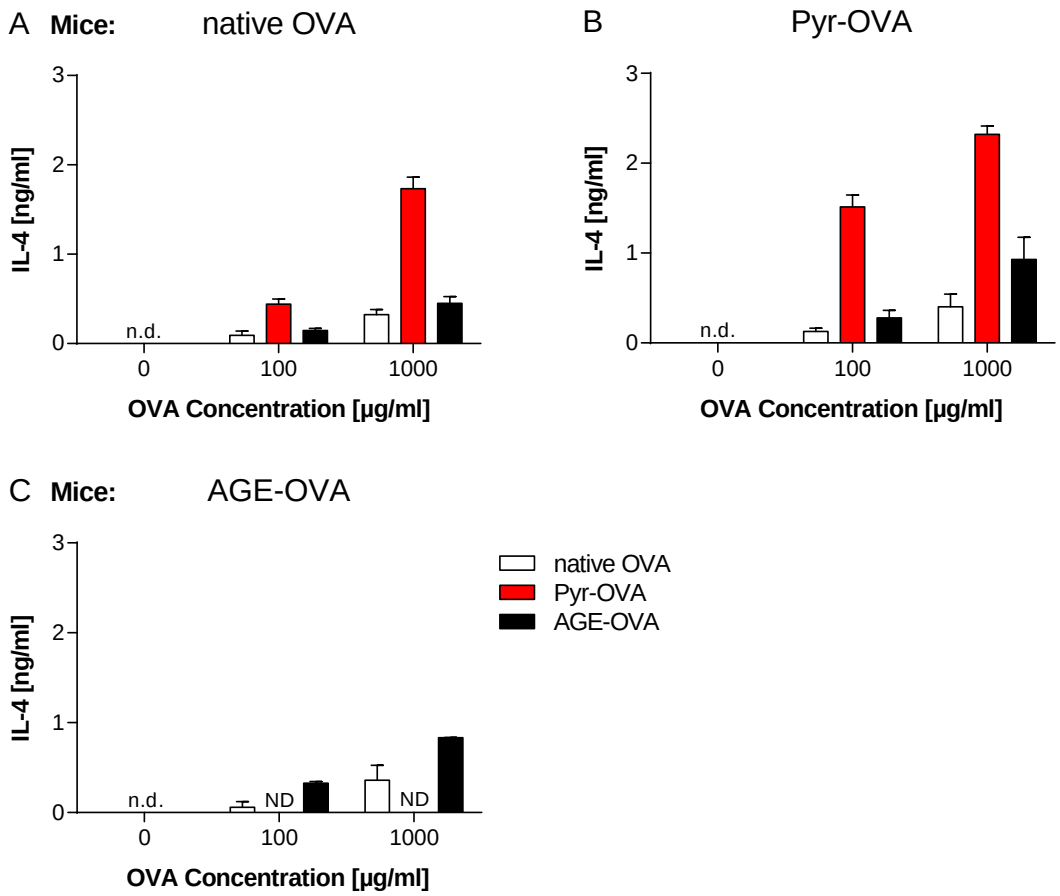


**Figure 43: IL-4 production of MLN-derived CD4$^+$ T-cells from mice sensitized with OVA samples and fed EW-diet.** BALB/c mice were sensitized with (A) native OVA, (B) Pyr-OVA or (C) AGE-OVA together with ALUM twice and fed EW-diet for seven days. CD4$^+$ T-cells were then isolated from the MLN of the mice and co-cultured with mitomycin-treated syngeneic splenocytes in the presence of either form of OVA for 72 h. The concentration of IL-4 in the cell culture supernatants was determined by ELISA. (n.d.: not detectable, below detection limit of 0.01 pg/ml; ND: not determined; Pyr-OVA was not included for stimulation in panel C due to the limited amount of this material).

To summarize, re-stimulation of MLN-derived CD4$^+$ T-cells from allergic mice with Pyr-OVA or AGE-OVA resulted in enhanced proliferation and IL-4 production compared to cells incubated with native OVA. Using *in vivo* $T_H2$-polarized CD4$^+$ T-cells these data confirm the enhanced T-cell immunogenicity of Pyr-OVA and AGE-OVA.

### 4.1.9 Discussion

#### 4.1.9.1 Modification of OVA with pyrraline enhances its $CD4^+$ T-cell immunogenicity *in vitro*

In this study, we found that modification of OVA with pyrraline, but not with CEL, CML or arginine-derivatives like MG-H1, enhances the $CD4^+$ T-cell immunogenicity of this model food allergen. Pyr-OVA also enhanced $T_H1$ and $T_H17$ cytokine production by OT-II cells and $T_H2$ cytokine production by DO11.10 cells. These results indicate that pyrraline modification of OVA does not induce a bias in T-cell polarization, but does enhance overall T-cell activation, since OT-II cells tend to induce $T_H1$- or $T_H17$-type responses, whereas DO11.10 cells tend to induce a $T_H2$-related phenotype.

Although $CD8^+$ T-cells are not the main effector cells to trigger allergic responses, the influence of glycation on the $CD8^+$ T-cell immunogenicity of OVA was of interest, because this provide some insight into the delivery pathway of glycated allergens for antigen presentation in DCs. We found that $CD8^+$ T-cell immunogenicity of OVA is not influenced by glycation. The OVAs modified with glycation structure, AGE-OVA and native OVA induced similar levels of IL-2 and IFN-γ production by OT-I-derived $CD8^+$ T-cells. These results suggest that Pyr-OVA and AGE-OVA are more efficiently delivered to the MHC class II loading pathway, not to the MHC class I loading pathway, in DCs and this subsequently enhances the activation of OVA-specific $CD4^+$ T-cells.

#### 4.1.9.2 BMDC maturation is not influenced by modification of OVA with Maillard reaction products

The maturation status of the BMDCs, which influences T-cell activation, was not affected by the OVAs modified with glycation structures. Expression of the co-stimulatory molecules CD40, CD80 and CD86, as well as of MHC class II molecules on the cell surface was not upregulated by incubation of DCs with any of the OVA samples. Incubation of the cells with either OVA sample did not induce detectable levels of IL-6 production by DCs. Thus, the enhanced $CD4^+$ T-cell immunogenicity of Pyr-OVA and AGE-OVA is not due to induction of the DC maturation process by the OVA samples. In contrast, Buttari et al. showed that AGEs of plasma $\beta_2$-glycoprotein I ($\beta_2$GPI) induce maturation of human monocyte-derived DCs.(*104*) In their study, DC maturation was induced via interaction of AGEs with RAGE followed by activation of the nuclear factor-κB signalling pathway.(*104*) In addition, AGE-modification resulted in a switch of the T-cell stimulatory capacity of $\beta_2$GPI towards $T_H2$ polarization.(*104*) In our study, Pyr-OVA and AGE-OVA enhance $T_H1$-, $T_H2$- and $T_H17$-cytokine

production by OT-II cells and DO11.10 cells, indicating that T-cell polarization is not induced by the glycated samples. The discrepancy might be explained by a different profile of glycation structures present in AGE-OVA and AGE-$\beta_2$GPI, because AGE-OVA was prepared by wet incubation of OVA with glucose at 50 °C, whereas dry incubation of $\beta_2$GPI with glucose at 37 °C was chosen for AGE-$\beta_2$GPI. Another explanation might be a varying surface receptor expression by the DCs. Hence, Ilchmann et al. showed that RAGE expression was not detected on the surface of BMDCs, whereas a high level of RAGE has been observed on human monocyte-derived DCs.(*71, 104*)

Taken together, the enhanced $CD4^+$ T-cell immunogenicity of Pyr-OVA and AGE-OVA is not caused by a promotion of the DC maturation process due to the modification of OVA with Maillard reaction products.

#### 4.1.9.3 Pyr-OVA and AGE-OVA are highly taken up by BMDCs

Besides maturation, the levels of antigen uptake by APCs have a large impact on subsequent T-cell activation. We found that Pyr-OVA and AGE-OVA were taken up by BMDCs to a stronger extent than native OVA. No enhanced uptake of CE-OVA, CM-OVA or MGO-OVA by BMDCs was observed. These results suggest that the enhanced uptake of Pyr-OVA and AGE-OVA by DCs lead to the enhanced T-cell activation by Pyr-OVA and AGE-OVA.

Recently, Rupa et al. showed that glycation of OVA with mannose (OVAMan) reduced the allergen uptake by DCs, whereas glycation with glucose (OVAGlu) did not alter the uptake level by DCs.(*109*) As a consequence, OVAMan induced less IL-2 production by naive $CD4^+$ T-cells compared to native OVA or OVAGlu.(*109*) The findings were explained by a reduced α-helical configuration of OVAMan, but not of OVAGlu, compared to native OVA.(*109*) The partial denaturation might have destroyed receptor binding sites important for antigen uptake, since it has been shown that minor changes in the secondary structure of OVA influences protein function.(*32, 109*) In our measurements of the CD-spectra, the glycated OVAs retained a similar secondary structure as does native OVA. The discrepancy between our and their observations might be explained by differences in the levels and the profiles of glycation. AGE-OVA was prepared in phosphate buffer with glucose at 50 °C, whereas dry incubation at 100 °C for a shorter period was selected in the study of Rupa et al.(*109*) Around 69.8 % of lysine residues are modified in AGE-OVA in our study, in comparison to 95.4 % in OVAMan and 93.5 % in OVAGlu, respectively.(*109*) The different incubation conditions could generate different types of glycation structures. However, taken together both studies show that the uptake levels of glycated allergens by APCs influence the overall immunogenicity of the protein.

#### 4.1.9.3.1 SR-AI/II mediates the enhanced uptake of Pyr-OVA and AGE-OVA by DCs

The identification of the receptors involved in the enhanced antigen uptake of Pyr-OVA and AGE-OVA was of particular interest, since SR-AI/II, CD36, SR-BI and galectin-3 are known AGE-binding receptors. We found that uptake of Pyr-OVA or AGE-OVA by SR-$A^{-/-}$ DCs was reduced compared to wt DCs showing that SR-AI/II mediates the uptake of Pyr-OVA and AGE-OVA. In contrast, the receptor deficiency did not impair the uptake of native OVA, CE-OVA, CM-OVA or MGO-OVA by DCs. The results suggest that SR-AI/II binds to pyrraline, but not to CEL, CML or MG-H1.

SR-AI/II is a trimer comprised of a transmembrane domain, a spacer region, a helical coiled-coil domain, a collagenous domain and a C-terminal cysteine-rich domain.(*48*) A variety of ligands, such as oxLDL or acLDL and chemically modified proteins including AGEs, bind to the collagenous domain of SR-AI/II.(*48, 55*) Previously, Nagai et al. showed that MGO-derived AGEs conjugated to BSA were not taken up by RAW264.7 cells, a murine macrophage-derived cell line expressing SR-AI/II.(*84*) Furthermore, no endocytosis of glyoxal-modified BSA, which contained high amounts of CML, by RAW264.7 cells was observed.(*84*) The results support the hypothesis that SR-AI/II does not bind the glycation structures CML and MG-H1.

SR-AI/II has been suggested to transfer its ligands to the MHC class II loading pathway for efficient T-cell activation.(*110, 111*) Consistent with this SR-AI/II function pyrraline modification enhances the $CD4^+$ T-cell immunogenicity, but not the $CD8^+$ T-cell immunogenicity of OVA. We could show that SR-AI/II is an important mediator of the enhanced $CD4^+$ T-cell immunogenicity of Pyr-OVA and AGE-OVA. This result suggests that the association of SR-AI/II with glycated food allergens might have an influence on the sensitization phase of allergy, because $T_H2$-cells, a subset of $CD4^+$ T-cells, are crucial for an efficient IgE production by B-cells.

#### 4.1.9.3.2 The mannose receptor plays a role in the uptake of Pyr-OVA and AGE-OVA by DCs

It is well known that the MR binds to natural mannose residues in OVA. Blocking of the MR with mannan resulted in a reduced uptake of native OVA, Pyr-OVA and AGE-OVA by SR-$A^{-/-}$ DCs. At first, it was thought that the reduced DC uptake of the OVA samples by mannan treatment was only due to inhibition of the binding to the natural mannose residues. However, we found that the uptake of AGE-BSA by BMDCs was also reduced after blockage of the MR with mannan, although native BSA does not possess natural ligands of the MR. These results suggest that the MR might be an AGE-binding receptor and contributes to the uptake of Pyr-OVA and AGE-OVA by recognition of the

glycation structures. However, a previous study by Burgdorf et al. showed that the MR delivers its ligands to the MHC class I loading pathway for $CD8^+$ T-cell activation.(*59*) Notably, only the $CD4^+$ T-cell immunogenicity, but not the $CD8^+$ T-cell immunogenicity, of OVA was enhanced by modification of OVA with pyrraline or AGEs. Moreover, the enhanced OVA-specific $CD4^+$ T-cell activation by Pyr-OVA and AGE-OVA was significantly attenuated in co-culture with SR-$A^{-/-}$ BMDCs. These results suggest that SR-AI/II plays a crucial role in the uptake of Pyr-OVA and AGE-OVA by wt BMDCs, which lead to an efficient delivery to the MHC class II loading pathway for antigen presentation and therefore, this enhances OVA-specific $CD4^+$ T-cell activation.

We also observed that mannan-treated SR-$A^{-/-}$ DCs took up Pyr-OVA, AGE-OVA and AGE-BSA to a small extent. The results suggest that another receptor could be involved in the endocytosis of the glycated samples by DCs, although it could only play a minor role in the uptake of Pyr-OVA and AGE-OVA. The receptors galectin-3, SR-BI or CD36, do not play a role, because their inhibition using specific inhibitors or blocking antibodies did not reduce the uptake of the OVA samples by SR-$A^{-/-}$ cells.

In summary, the strong uptake of Pyr-OVA and AGE-OVA is mediated by SR-AI/II and the MR, and another yet unknown receptor could be partially involved in the endocytosis of Pyr-OVA and AGE-OVA.

#### 4.1.9.4 Enhanced allergenic potency of Pyr-OVA and AGE-OVA

IgE antibodies, key molecules to induce type I allergic reactions, are produced by B-cells in assistance with $T_H2$-cells, a subset of $CD4^+$ T-cells. Since Pyr-OVA and AGE-OVA displayed a higher $CD4^+$ T-cell immunogenicity than native OVA, we then assessed the sensitization ability of these OVA samples. Pyr-OVA and AGE-OVA induced higher levels of OVA-specific IgE antibodies than native OVA in BALB/c mice when i.p. sensitized together with ALUM. Moreover, a strong loss of body weight and drop in body core temperature was observed in mice sensitized with Pyr-OVA or AGE-OVA compared to native OVA-sensitized mice when they were fed with EW-diet containing high amounts of OVA. These results suggest that AGE-OVA and Pyr-OVA possess a higher allergenic potency than native OVA.

Among the $CD4^+$ T-cell subsets, $T_H2$-cells play a crucial role in the induction of IgE production by B-cells. Thus, the question was raised whether or not the enhanced allergenic potency is due to a predominant induction of $T_H2$-cells by the glycation structures. However, it is very unlikely, because *in vitro* co-culture assay of BMDCs with OT-II or DO11.10 cells suggests that AGE-OVA and Pyr-OVA enhance both $T_H1$ and $T_H2$ cytokine immune responses. Previously, Bhatia et al. reported

that a chemically modified antigen bound by SR-AI/II induced dominant $T_H1$ immune responses.(*112*) However, the levels of OVA-specific IgG2a antibodies, which are a $T_H1$-type of the IgG subclasses, were only at marginal levels in all groups of mice. Moreover, the strong $T_H2$ immune response of the mice from all groups was supported by a strong production of IL-4 by $CD4^+$ T-cells and a strong proliferation of MLN-derived $CD4^+$ T-cells isolated from the allergic mice after *in vitro* re-stimulation with OVA. By assessing the cell-based immune response of the allergic mice, we found that modification of OVA with pyrraline or AGEs enhances the activation of polyclonal $CD4^+$ T-cells compared to native OVA suggesting a higher *in vivo* $CD4^+$ T-cell immunogenicity of Pyr-OVA and AGE-OVA. These results indicate that the enhanced $CD4^+$ T-cell immunogenicity of Pyr-OVA and AGE-OVA could subsequently induce the enhanced IgE production and clinical symptoms in the mice sensitized with Pyr-OVA or AGE-OVA, respectively.

In summary, a putative molecular mechanism of the enhanced $CD4^+$ T-cell immunogenicity and allergenic potency of Pyr-OVA and AGE-OVA can be proposed (figure 44). Briefly, the strong SR-AI/II-mediated uptake of Pyr-OVA and AGE-OVA compared to native OVA leads to a more efficient delivery to the MHC class II loading pathway for antigen presentation. In turn, Pyr-OVA and AGE-OVA induce stronger activation and cytokine production by allergen-specific $CD4^+$ T-cells. In the allergic status, a $T_H2$-type cytokine milieu dominates in the immune system. Thus, the activation of $T_H2$-cells, a subset of $CD4^+$ T-cells, by Pyr-OVA and AGE-OVA subsequently induces a strong B-cell activation and class switch in B-cells to produce allergen-specific IgE antibodies. The higher levels of IgE antibodies induced by Pyr-OVA and AGE-OVA compared to the unmodified allergen finally cause stronger clinical symptoms.

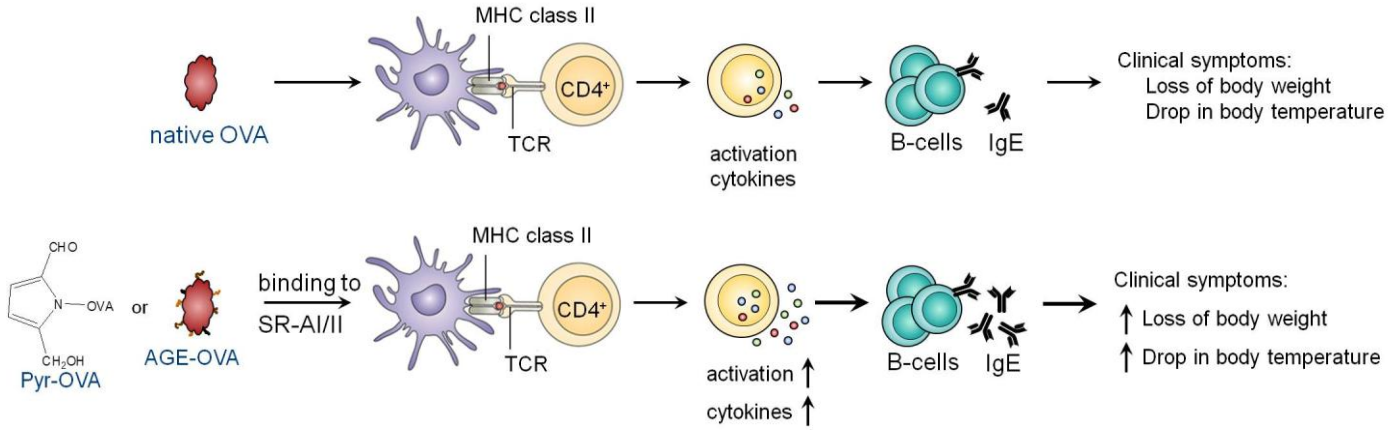


**Figure 44: Molecular mechanism of the enhanced $CD4^+$ T-cell immunogenicity and allergenic potency of Pyr-OVA and AGE-OVA.**

In conclusion, AGE- and pyrraline-modification by the Maillard reaction could be capable of enhancing the $CD4^+$ T-cell immunogenicity and subsequently the potential allergenicity of food allergens. High levels of pyrraline have been detected in commercially available roasted peanuts, a clinically relevant allergenic food.(*70*) The high contents of pyrraline in roasted peanuts together with the enhancing effect of pyrraline on the allergenicity might pose a strong risk for peanut allergic patients. Thus, the modification of food allergens by the Maillard reaction needs to be considered for food safety and allergy diagnosis, where extracts of raw foods or unprocessed purified allergens are usually used. Supplementary, the glycation profiles of common processed allergenic foods need to be identified, because only very limited information is available so far.

## 4.2 Establishment of a human cell culture system to assess the immunogenic potency of a glycated food allergen

### 4.2.1 Introduction

In the previous chapter, we found that SR-AI/II mainly mediates the uptake of AGE-OVA by murine DCs. To verify this finding in this chapter, we aimed to establish a cell culture system of human DCs or macrophages. Recent studies have shown that both DCs and macrophages are professional APCs, which take up antigens and present the processed antigens by MHC molecules to naive T-cells and hence, both cell types need to be considered for studying the immunogenicity of glycated food allergens. In humans, two types of macrophages are present, M1 and M2 macrophages. M1 macrophages have a pro-inflammatory phenotype and are involved in $T_H1$-type immune responses, whereas M2 cells have an anti-inflammatory phenotype, but are also regarded as model APCs to assist in $T_H2$-type responses. The monocyte-derived DCs as well as M1 and M2 macrophages were characterized regarding the surface expression of AGE-binding receptors, e.g. SR-AI/II, CD36 and SR-BI. The uptake of AGE-OVA by these cells was also investigated.

### 4.2.2 Characterization of human DCs

For the *in vitro* generation of human DCs, PBMCs were isolated from buffy coat by density gradient centrifugation. Magnetic separation was then performed to separate magnetically labelled $CD14^+$ monocytes from other lymphocytes. Differentiation of the $CD14^+$ monocytes into immature DCs (iDCs) was induced by culturing the cells in the presence of IL-4 and GM-CSF. Maturation of iDCs was induced by a cocktail of IL-1β, TNF-α and $PGE_2$.

Both iDCs and mature DCs (mDCs) were characterized for the expression of the co-stimulatory molecules CD80 and CD86, and of HLA-DR as well as of the MR, SR-AI/II, CD36 and SR-BI. The expression of these receptors is of interest, first, because the MR and SR-AI/II play a pivotal role in the uptake of AGE-OVA by murine DCs and second, because CD36 and SR-BI are known to bind AGEs. Co-stimulatory molecule and receptor expression was analyzed with flow cytometry.

Figure 45 shows that the co-stimulatory molecules CD80 and CD86 were expressed on the surface of iDCs and were upregulated after induction of maturation. HLA-DR is also highly expressed by both iDCs and mDCs. The expression of the MR, CD36 and SR-BI, but not of SR-AI/II, was detected on the cell surface of iDCs (figure 46). The expression levels of the MR, CD36 and SR-BI were reduced on the cell surface of mDCs. It is known that DCs reduce the expression of receptors capturing antigens, e.g. scavenger receptors and the MR, to gain T-cell stimulatory capacity in the course of

maturation.(*75*) These results suggest that proper iDCs as well as mDCs were generated in the *in vitro* cell culture system.

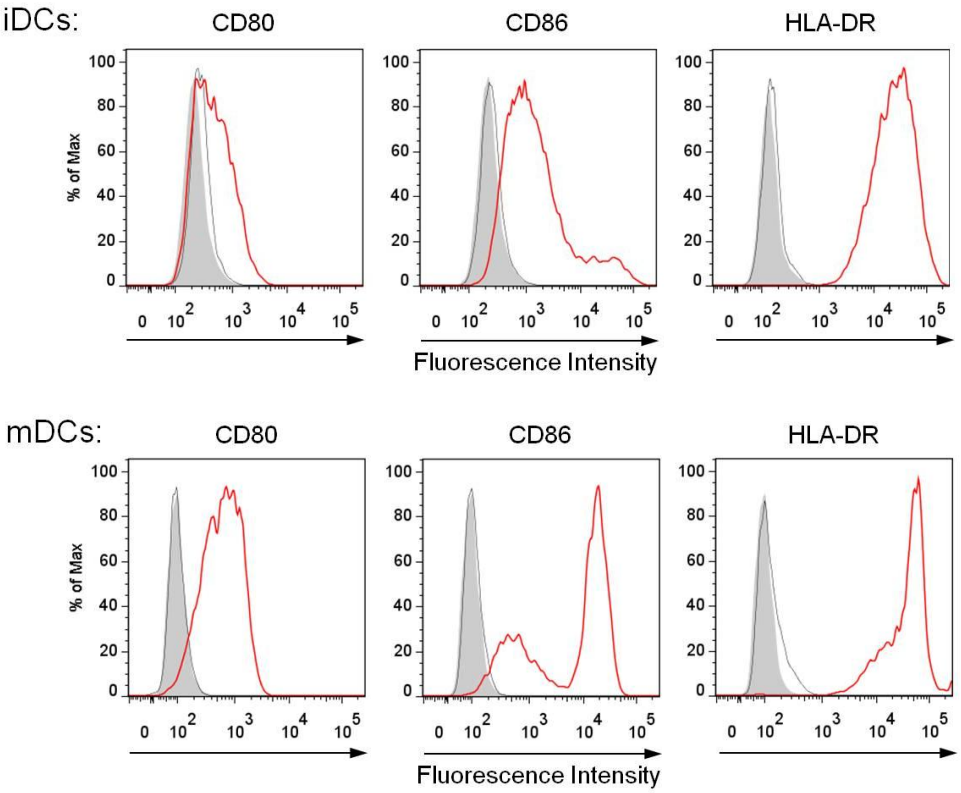


**Figure 45: Expression of co-stimulatory molecules by human dendritic cells.** Human immature DCs (iDCs) and mature DCs (mDCs) were generated from PBMCs and stained using anti-CD80, CD86 or HLA-DR mAb. The expression levels of the co-stimulatory molecules were assessed with flow cytometry. Grey areas represent unstained cells and black lines indicate cells treated with the respective isotype control antibody.

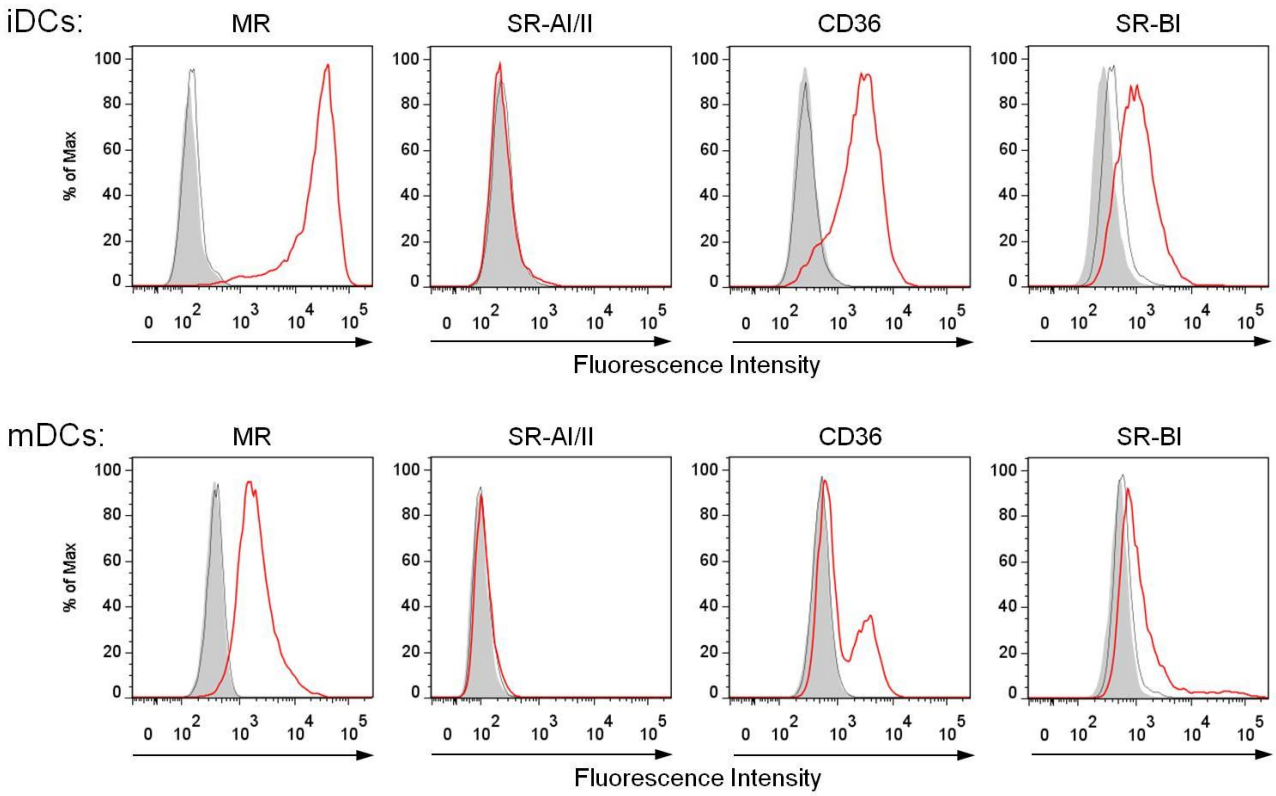


**Figure 46: Receptor expression by human dendritic cells.** Human immature DCs (iDCs) and mature DCs (mDCs) were generated from PBMCs and stained using anti-MR, SR-AI/II, CD36 or SR-BI mAb. The expression levels of the receptors were assessed with flow cytometry. Grey areas represent unstained cells and black lines indicate cells treated with the respective isotype control antibody.

### 4.2.3 Analysis of the uptake of the OVA samples by human DCs

The uptake of the glycated OVA samples by DCs has a great impact on the T-cell immunogenicity of the respective protein in the murine system. Thus, the uptake levels of glycated OVA and control OVA by human iDCs was assessed. To determine the optimal point in time for uptake measurement, human DCs were incubated for 15 min, 60 min or 240 min with FITC-labelled native OVA, inc. OVA or AGE-OVA. As a measure for the antigen uptake, the FITC intensity was determined with flow cytometry.

After 15 min of incubation (data not shown) and 60 min incubation (figure 47A) OVA samples were taken up by iDCs at similar levels. The prolongation of the incubation time to 240 min (figure 47B) enhanced the uptake of AGE-OVA by iDCs.

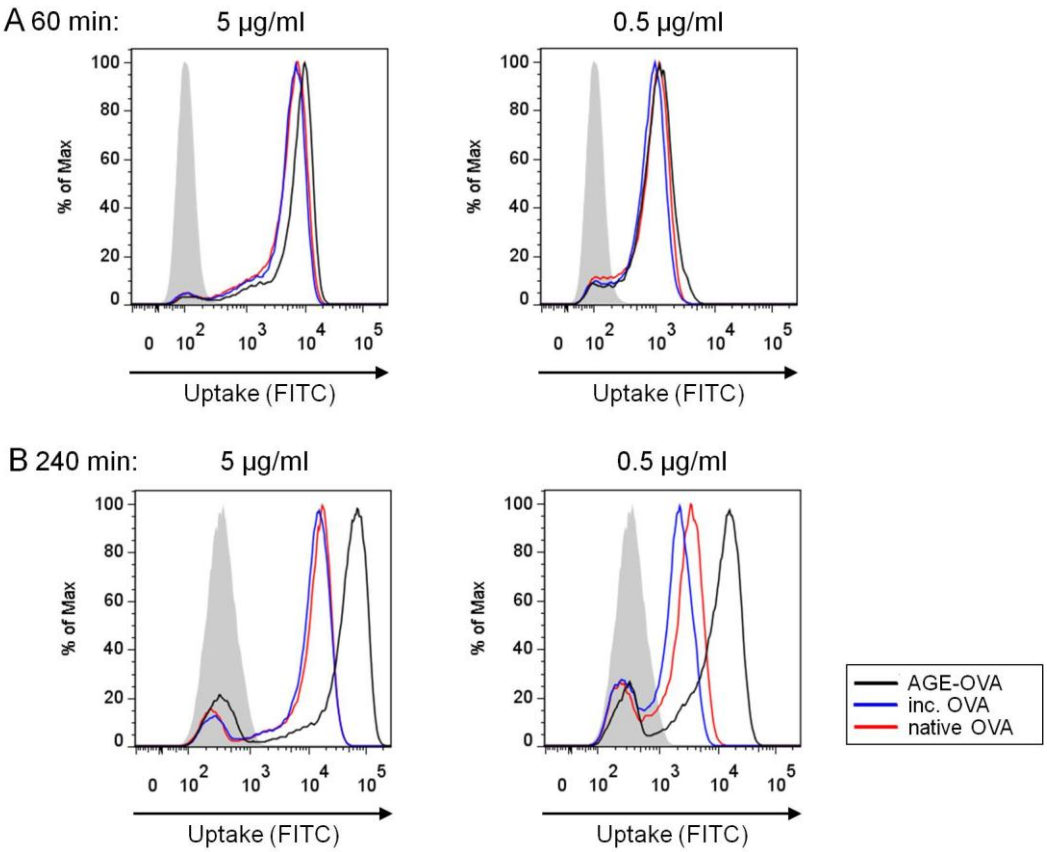


**Figure 47: Uptake of native OVA, inc. OVA and AGE-OVA by human iDCs.** PBMC-derived iDCs were incubated for (A) 60 min or (B) 240 min with FITC-labelled native OVA, inc. OVA or AGE-OVA. FITC intensity of the cells was determined with flow cytometry.

### 4.2.4 Characterization of human macrophages

Besides DCs, macrophages are prominent APCs and need to be considered for studies regarding the immunogenicity of the modified OVAs in human cells. In human macrophages, there are the two subsets M1 (pro-inflammatory) and M2 (anti-inflammatory) macrophages, which can both be generated *in vitro* by application of different cytokines.

Therefore, PBMC-derived M1 or M2 macrophages were prepared and characterized. The surface expression of the MR, SR-AI/II, CD36 and SR-BI was analyzed with flow cytometry.

All receptors of interest were detected on the cell surface of both M1 and M2 macrophages (figure 48). The MR was expressed at higher levels on the surface of M1 macrophages compared to M2 macrophages. In contrast, SR-AI/II and SR-BI were expressed at higher levels on the surface of M2 macrophages compared to the M1 phenotype. The expression levels of CD36 were comparable between M1 and M2 cells.

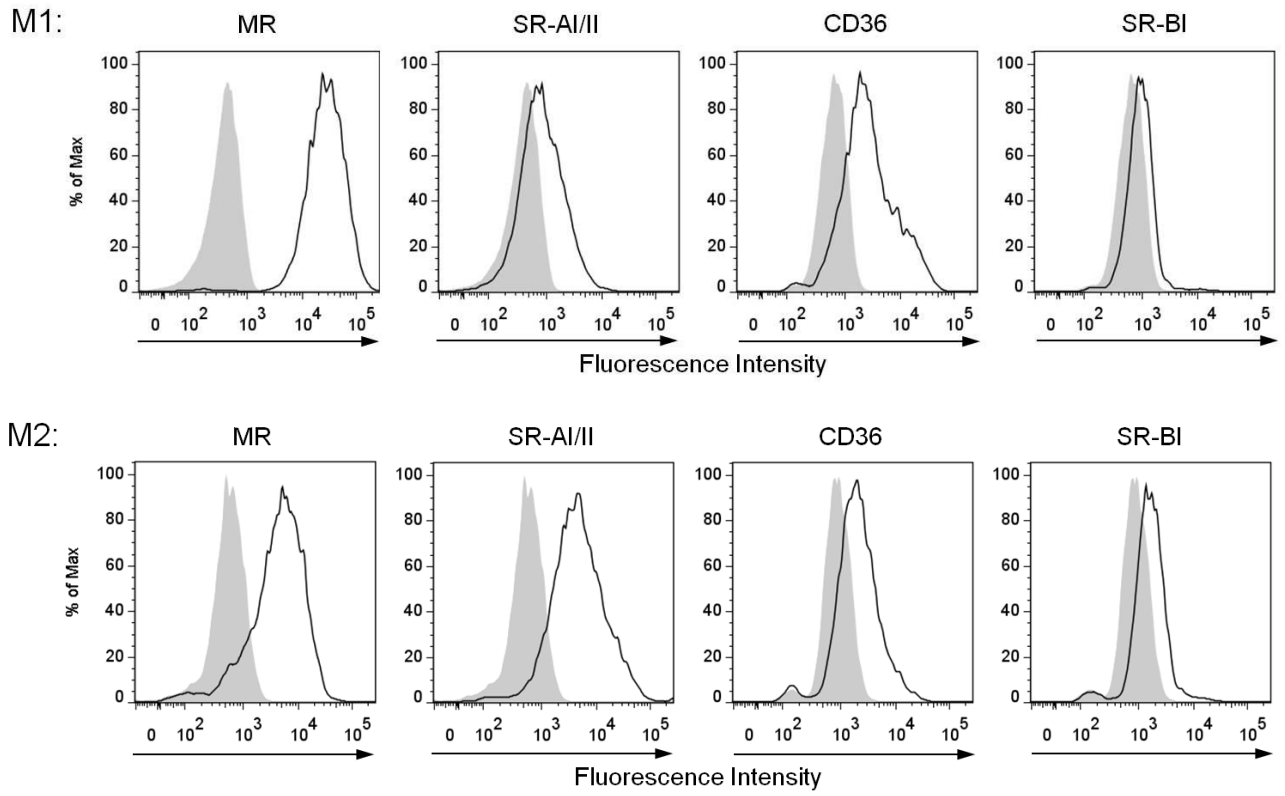


**Figure 48: Receptor expression by M1 and M2 macrophages.** Human M1 and M2 macrophages were generated from PBMCs and stained using anti-MR, SR-AI/II, CD36 or SR-BI mAb. The expression levels of the receptors were assessed with flow cytometry. Grey areas represent unstained cells.

### 4.2.5 Analysis of the uptake of the OVA samples by human macrophages

Next, the antigen uptake was assessed by incubating M1 or M2 macrophages with FITC-labelled AGE-OVA or native OVA for 15 min or 60 min.

Figure 49 shows a comparable intensity of FITC in M1 macrophages incubated with FITC-native OVA and FITC-AGE-OVA after 15 min or 60 min incubation, respectively, indicating that native OVA and AGE-OVA were taken up to a similar extent by M1 macrophages. In contrast, an enhanced uptake of AGE-OVA compared to native OVA by M2 macrophages was observed after 15 min incubation. The enhanced uptake of AGE-OVA was more pronounced after prolongation of the incubation time to 60 min.

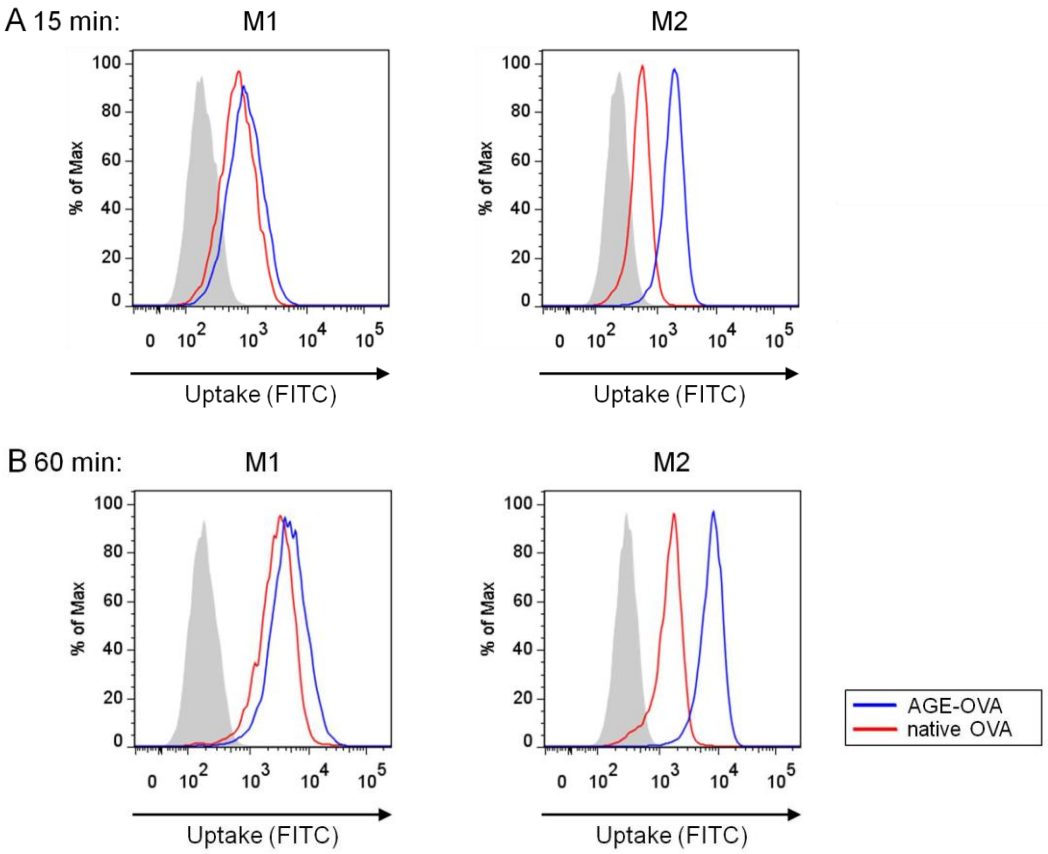


**Figure 49: Uptake of native OVA and AGE-OVA by human M1 and M2 macrophages.** PBMC-derived M1 or M2 macrophages were incubated for (A) 15 min or (B) 60 min with FITC-labelled native OVA or AGE-OVA. FITC intensity of the cells was determined with flow cytometry. Grey areas represent cells cultured without OVA.

### 4.2.6 Discussion

#### 4.2.6.1 Cultured human dendritic cells may not be a suitable model for the assessment of the immunogenicity of AGEs

To assess the immunogenicity of glycated OVA in human cells, cell culture of PBMC-derived immature and mature DCs as well as PBMC-derived M1 (pro-inflammatory) and M2 (anti-inflammatory) macrophages was established.

The maturation status of the DCs was confirmed by detecting an upregulation of the surface expression of CD80, of CD86 and of HLA-DR. Additionally, iDCs express the MR, CD36 and SR-BI, which are known to bind to AGEs. Expression of SR-AI/II was not detectable on the cell surface of both iDCs and mDCs. This was unexpected, because Jin et al. showed the expression of SR-AI/II on the surface of PBMC-derived human iDCs.(*113*) The used protocol for the isolation and generation of iDCs in both studies was very similar, except the cell culture media used for iDC differentiation, i.e. here, a serum-free synthetic medium was used, whereas Jin et al. reported the use of RPMI supplemented with FCS.(*113*) Thus, both media were compared, but in our lab no major differences in surface expression of SR-AI/II by both types of iDCs could be observed (data not shown).

By assessing the antigen uptake by human iDCs it was found that AGE-OVA is taken up to a stronger extent compared to the native allergen after 240 min incubation time. After 15 min and 60 min incubation, no differences in the uptake of AGE-OVA and native OVA could be observed.

Although AGE-OVA is taken up by iDCs, it can be concluded from these results that human iDCs might not be suitable for studying the influence of glycation on the immunogenicity of food allergens in human cells, since SR-AI/II, which plays a major role in the murine system, is not expressed by the cells.

#### 4.2.6.2 Cultured human macrophages may be a suitable model for the assessment of the immunogenicity of AGEs

In contrast to iDCs and mDCs, human macrophages express high levels of SR-AI/II. Other receptors binding to AGEs were expressed on the cell surface of M1 and M2 macrophages at different levels. M1 macrophages expressed higher levels of the MR and CD36 compared to M2 macrophages. In contrast, M2 macrophages expressed SR-AI/II and SR-BI at higher levels than M1 cells. The uptake levels of AGE-OVA and native OVA by M1 macrophages were comparable. In contrast, compared to native OVA an enhanced antigen uptake of AGE-OVA by M2 macrophages was observed. Several studies have shown that M2 macrophages serve as APCs and assist in $T_H2$ responses, like allergic

immune responses.(*76, 78, 81*) Taken together, the results suggest that M2 macrophages are suitable model APCs to assess the immunogenicity of AGEs of food allergens in human immune systems.

Future studies using M2 macrophages and peripheral T-cells derived from food allergic patients will further elucidate the T-cell immunogenicity of AGEs of food allergens in allergic individuals.

# 5 Summary

The Maillard reaction takes place between reducing sugars and compounds with free amino groups during the thermal processing of foods. In the final stage of the complex reaction cascade, the so-called Advanced Glycation Endproducts (AGEs) are formed including proteins with various glycation structures. A previous study showed that AGE-modification of ovalbumin (OVA, a major egg white allergen) prepared by thermal incubation of OVA with glucose enhances the $CD4^+$ T-cell immunogenicity of OVA.(*71*) In this study, we hypothesized that distinct glycation structure(s) contribute to the enhanced $CD4^+$ T-cell immunogenicity of crude glycated OVA (AGE-OVA). To verify this hypothesis, OVA was selectively modified with the glycation structures $N^{\varepsilon}$-carboxy-ethyllysine (CEL), $N^{\varepsilon}$-carboxymethyllysine (CML), methylglyoxal-induced hydroimidazolones (MG-H1) or pyrraline, which are representative glycation structures found in processed foods. Then, the immunogenic and allergenic properties of the modified OVAs were investigated.

First, the $CD4^+$ and the $CD8^+$ T-cell immunogenicity of the modified OVAs were assessed using a co-culture system of murine bone marrow-derived dendritic cells (BMDCs) with $CD4^+$ and $CD8^+$ T-cells isolated from transgenic mice expressing an OVA-specific T-cell receptor, respectively. OVA modified with pyrraline (Pyr-OVA), but not with CEL, CML or MG-H1, possesses a higher $CD4^+$ T-cell immunogenicity than native OVA. In contrast, the $CD8^+$ T-cell immunogenicity of all modified OVA samples was similar to that of native OVA. BMDC uptake assay using fluorescently-labelled OVA samples showed that Pyr-OVA as well as AGE-OVA, but not the other modified OVAs, were highly taken up by BMDCs compared to native OVA. The results suggest that the enhanced uptake of Pyr-OVA by BMDCs leads to its enhanced $CD4^+$ T-cell immunogenicity.

Next, the uptake mechanism of Pyr-OVA by BMDCs was investigated using inhibitors of putative cell-surface receptors for AGEs as well as BMDCs deficient for these receptors. The macrophage scavenger receptor class A (SR-AI/II) and the mannose receptor (MR) mainly mediate the uptake of Pyr-OVA and AGE-OVA by BMDCs. The uptake of Pyr-OVA and AGE-OVA was not reduced in cells treated with inhibitors of scavenger receptor class B (SR-BI), galectin-3 or blocking antibodies against CD36 suggesting that these receptors are not involved in the uptake of Pyr-OVA. In contrast, the uptake of Pyr-OVA and AGE-OVA, but not other modified OVAs was remarkably reduced in BMDCs deficient for SR-AI/II. Moreover, treatment of $SR\text{-}A^{-/-}$ BMDCs with an inhibitor of the MR further reduced the uptake of Pyr-OVA and AGE-OVA. The enhanced OVA-specific $CD4^+$ T-cell activation by Pyr-OVA and AGE-OVA was significantly attenuated in co-culture with $SR\text{-}A^{-/-}$ BMDCs. The results suggest that especially the uptake of Pyr-OVA and AGE-OVA by SR-AI/II leads

to an efficient delivery to the MHC class II loading pathway for antigen presentation and therefore, to the enhanced activation of OVA-specific $CD4^+$ T-cells.

Next, the allergenic properties of Pyr-OVA and AGE-OVA were assessed using a mouse model of intestinal allergy. BALB/c mice were i.p. sensitized with native OVA, Pyr-OVA or AGE-OVA together with ALUM, an adjuvant, twice in a two week interval. Two weeks after the last sensitization, mice were fed a diet containing egg white (EW-diet) for one week. After sensitization, enhanced levels of OVA-specific IgE antibodies were detected in mice sensitized with Pyr-OVA or AGE-OVA compared to native OVA. Feeding of the mice with EW-diet induced stronger clinical symptoms, e.g. a more severe loss of body weight and drop in body core temperature, in mice sensitized with Pyr-OVA or AGE-OVA compared to native OVA-sensitized mice. The results suggest that Pyr-OVA or AGE-OVA could possess a higher allergenic potency than native OVA. IgE antibodies, key molecules to induce type I allergic reactions, are produced by B-cells in assistance with $T_H2$-cells, a subset of $CD4^+$ T-cells. Taken together, Pyr-OVA and AGE-OVA are highly taken up by DCs via association with SR-AI/II and this subsequently enhances the $CD4^+$ T-cell activation and the IgE production.

In this study, a human cell culture system for assessment of the immunogenicity of glycated allergens was also established. We found that human macrophages, but not DCs, are a suitable model. In human DCs, SR-AI/II was not expressed on the cell surface. In contrast, human macrophages expressed high levels of SR-AI/II and other putative AGE-binding receptors on the cell surface. In particular, M1 macrophages express higher levels of the MR, whereas M2 macrophages express higher levels of SR-AI/II and SR-BI on the cell surface. Additionally, an enhanced uptake of AGE-OVA by M2 macrophages, but not by M1 macrophages, compared to native OVA was detected. M1 macrophages have a pro-inflammatory phenotype and are involved in $T_H1$-type immune responses, whereas M2 cells have an anti-inflammatory phenotype, but are also regarded as model APCs to assist in $T_H2$-type responses. The results indicate that M2 macrophages are an especially suitable model for investigating the immunogenicity of glycated food allergens.

In conclusion, this study demonstrates for the first time that pyrraline is capable of enhancing the allergenic properties of a food allergen. High amounts of pyrraline are present in roasted peanuts, a clinically relevant allergenic food. The findings suggest that the Maillard reaction could enhance the allergenic properties of some food allergens. Moreover, the influence of the Maillard reaction on the allergenicity of food allergens needs to be considered in the diagnosis of food allergy, which is usually performed using extracts of raw foods or unprocessed purified allergens. Finally, this study would contribute to elucidate the molecular mechanisms of food allergies.

# 6 Deutsche Zusammenfassung

Die Allergie ist eine Überempfindlichkeitsreaktion des Immunsystems gegen ansonsten harmlose Proteine.(*10*) Die Prävalenz von Allergien einschließlich der Nahrungsmittelallergien hat in den letzten Jahren stark zugenommen.(*1*) Epidemiologische Studien zeigen, dass ca. 1 % bis 10,8 % der Bevölkerung an einer Nahrungsmittelallergie leiden.(*1*) Die meisten allergischen Reaktionen gegen Nahrungsmittel bei Kindern werden von Milch, Hühnereiweiß, Erdnüssen und Schalentieren ausgelöst.(*1, 2*) Bei Erwachsenen jedoch wird selten eine Allergie gegen Milch oder Hühnereiweiß nachgewiesen.(*3, 4*) Neben den Pollen-assoziierten Nahrungsmittelallergien gegen Obst und Gemüse leiden erwachsene Patienten häufig an Allergien gegen Schalentiere, Nüsse, Getreide und Erdnüsse.(*3-5*) Die von den Nahrungsmitteln ausgelösten Symptome betreffen den Gastro-intestinaltrakt, die Haut sowie die Atemwege.(*6*) Zudem treten in seltenen Fällen schwere systemische anaphylaktische Schocks auf, welche lebensbedrohlich sein können.(*6*) In den meisten Fällen werden die Symptome durch eine Immunglobulin E (IgE)-vermittelte Typ-I-Hypersensitivität ausgelöst.(*7, 10*) Dabei wird das Allergen, d. h. das allergieauslösende Protein, von einer antigenpräsentierenden Zelle (APC), z. B. einer dendritischen Zelle oder einem Makrophagen, aufgenommen.(*7, 10*) Nachdem das Allergen im Zellinneren prozessiert wurde, werden antigene Peptide auf der Zelloberfläche von Molekülen des Haupthistokompatibilitätskomplex (MHC) der Klasse II präsentiert.(*7, 10*) Diese Peptide binden an einen komplementären T-Zellrezeptor (TCR) einer $CD4^+$-T-Zelle, welches zur Aktivierung und Differenzierung der T-Zelle führt.(*7, 10*) $CD4^+$-T-Zellen können in drei unterschiedliche Arten von T-Helferzellen, $T_H1$-, $T_H2$-, $T_H17$-Zellen, oder in regulatorische T-Zellen differenzieren.(*7, 10*) $T_H2$-Zellen werden durch Stimulation von naiven T-Zellen mit den Zytokinen Interleukin-4 (IL-4) und IL-13 gebildet und induzieren anschließend die Produktion von allergen-spezifischen IgE-Antikörpern durch B-Zellen.(*7, 10*) Die Antikörper binden an den $F_c\varepsilon RI$-Rezeptor auf der Oberfläche von Mastzellen und ein erneuter Kontakt mit dem Allergen führt zu Mastzellaktivierung durch Vernetzung der IgE-Antikörper.(*7, 10*) Die aktivierten Mastzellen sekretieren Histamin und andere physiologisch aktive Mediatoren, welche die allergischen Symptome auslösen.(*7, 10*) Zur Vermeidung von allergischen Symptomen wird den Patienten geraten, das entsprechende Nahrungsmittel zu meiden, da nur eine symptomatische und keine heilende Behandlung der Nahrungsmittelallergie möglich ist.(*2, 6*)

Viele Nahrungsmittel werden nicht roh, sondern in prozessierter Form, d. h. gekocht, gebraten oder geröstet, gegessen.(*23, 25*) Dabei verändern sich die Eigenschaften der Allergene durch chemische Reaktionen mit vielen Komponenten in der Matrix.(*25, 26*) Die häufigste Reaktion zwischen Proteinen und Kohlenhydraten während der thermischen Prozessierung von Nahrungsmitteln ist die Maillard

Reaktion.(*25, 26*) Bei der Maillard Reaktion reagieren freie Aminogruppen der Proteine mit der Carboxylgruppe eines reduzierenden Zuckers zu einer Vielzahl an Verbindungen, wie z. B. $N^{\varepsilon}$-Carboxyethyllysin (CEL), $N^{\varepsilon}$-Carboxymethyllysin (CML), Pentosidin, Pyrralin oder Melanoidinen.(*39*) Die Gruppe der Maillard-Produkte wird unter dem Begriff „Advanced Glycation Endproducts“ (AGEs) zusammengefasst und besteht aus mehreren hundert verschiedenen Verbindungen.(*39, 40*) In einer vorherigen Studie konnte gezeigt werden, dass AGE-modifiziertes Ovalbumin (OVA, ein Eiweißallergen), welches durch thermische Inkubation von OVA mit Glucose erzeugt wurde, eine erhöhte $CD4^+$-T-Zellimmunogenität aufweist im Vergleich zu nativem OVA.(*71*) Daraus wurde folgende Hypothese für diese Arbeit abgeleitet: Die erhöhte $CD4^+$-T-Zell-Immunogenität von AGE-OVA ist auf einzelne Maillard-Verbindungen zurückzuführen. Für die Überprüfung dieser Hypothese wurde OVA selektiv mit den Maillard-Verbindungen CEL, CML, Pyrralin und Methylglyoxal-induzierten Hydroimidazolonen (MG-H1) modifiziert. Diese Maillard-Verbindungen wurden ausgewählt, da sie teils in sehr hohen Mengen in prozessierten Nahrungsmitteln nachgewiesen wurden. Anschließend wurden die immunogenen und allergenen Eigenschaften der modifizierten OVA-Proben untersucht.

Zuerst wurden die $CD4^+$- und die $CD8^+$-T-Zell-Immunogenität der modifizierten OVA-Proben bestimmt. Dazu wurden murine dendritische Zellen (DCs) *in vitro* aus Knochenmarkszellen generiert. Außerdem wurden OVA-spezifische T-Zellen aus den Milzen von transgenen Mäusen, welche Zellen mit einem OVA-spezifischen T-Zellrezeptor besitzen, isoliert. Die DCs wurden zusammen mit den T-Zellen und den modifizierten OVA-Proben inkubiert und die Aktivierung der T-Zellen durch Bestimmung der Konzentration des Zytokins IL-2 in den Zellkulturüberständen oder durch Analyse der T-Zellproliferation untersucht. Nur für mit Pyrralin modifiziertes OVA (Pyr-OVA) konnte eine erhöhte Aktivierung von OVA-spezifischen $CD4^+$-T-Zellen und somit eine erhöhte $CD4^+$ T-Zell-Immunogenität nachgewiesen werden. Hingegen wurde die $CD8^+$-T-Zellimmunogenität von OVA durch keine der Maillard-Verbindungen beeinflusst, da nur eine geringe Aktivierung der OVA-spezifischen $CD8^+$-T-Zellen für alle Proben, einschließlich unmodifiziertem OVA, beobachtet wurde. Diese Ergebnisse legen nahe, dass Pyr-OVA und AGE-OVA im MHC-Klasse-II-Weg der dendritischen Zellen effizienter transportiert und prozessiert werden als natives OVA, wohingegen die Prozessierung im MHC-Klasse-I-Weg durch die Modifizierung nicht beeinflusst wird. Die effizientere Prozessierung und anschließende Antigenpräsentation führt zu der verstärkten Aktivierung von OVA-spezifischen $CD4^+$-T-Zellen und trägt somit wesentlich zu der $CD4^+$-T-Zell-Immunogenität der modifizierten OVA-Proben bei. Der Maturierungsstatus der DCs, welcher ebenfalls maßgeblich zu einer effizienten T-Zellaktivierung beiträgt, wurde durch die Modifikation von OVA mit Maillard-Verbindungen nicht beeinflusst. Ein wichtiger Schritt für eine effiziente Antigenpräsentation

und somit auch für die T-Zellaktivierung ist die Aufnahme des Antigens durch die APC. Für die Untersuchungen zur Aufnahme der modifizierten OVA-Proben durch DCs wurden die OVA-Proben fluoreszenzmarkiert. Die einzelnen OVA-Proben konnten aufgrund eines ähnlichen Farbstoff/Protein-Quotienten miteinander verglichen werden. Es wurde gezeigt, dass Pyr-OVA und AGE-OVA besser von den DCs aufgenommen wurden im Vergleich zu nativem OVA. Mit CEL, CML oder MG-H1 modifiziertes OVA wurde ähnlich gut wie natives OVA von den DCs aufgenommen. Aus diesen Ergebnissen wurde gefolgert, dass die verstärkte $CD4^+$ T-Zellimmunogenität von Pyr-OVA eine Folge der verstärkten Aufnahme von Pyr-OVA durch die DCs ist.

Im Folgenden wurde der Mechanismus der Aufnahme von Pyr-OVA und AGE-OVA durch die DCs untersucht. Mögliche AGE-bindende Rezeptoren, welche auf der Oberfläche von DCs exprimiert werden, sind die Scavenger-Rezeptoren Klasse A Typ I und Typ II (SR-AI/II), die Scavenger-Rezeptoren der Klasse B, SR-BI und CD36, sowie Galectin-3. Um die Bindung der modifizierten OVA-Proben an diese Rezeptoren zu untersuchen wurden entweder spezifische Inhibitoren oder Rezeptor-defiziente DCs verwendet. Die Verwendung von SR-AI/II-defizienten Zellen ergab eine reduzierte Aufnahme von Pyr-OVA und AGE-OVA, wohingegen bei Inhibition der Rezeptoren SR-BI, CD36 und Galectin-3 eine vergleichbare Aufnahme zu unbehandelten Zellen beobachtet wurde. Weiterhin wurde gezeigt, dass der Mannose-Rezeptor (MR) ebenfalls zu der verstärkten Aufnahme von Pyr-OVA und AGE-OVA beiträgt, da er nicht nur die intrinsische Glykosylierung von OVA erkennt sondern auch AGEs bindet. Jedoch scheint die MR-vermittelte Aufnahme der AGEs eine untergeordnete Rolle für die $CD4^+$-T-Zellimmunogenität von Pyr-OVA und AGE-OVA zu spielen, da die Verwendung von SR-AI/II-defizienten DCs in der Ko-Kultur mit OVA-spezifischen $CD4^+$ T-Zellen im Vergleich zu Wildtyp-DCs zu einer deutlich reduzierten $CD4^+$-T-Zellaktivierung durch Pyr-OVA und AGE-OVA führte. Aus diesem Ergebnis lässt sich folgern, dass die verstärkte $CD4^+$-T-Zellimmunogenität hauptsächlich durch die starke SR-AI/II-vermittelte Aufnahme von Pyr-OVA und AGE-OVA durch DCs, welche zu einem effizienteren Transport in den MHC-Klasse-II-Weg führt, ausgelöst wird.

Anschließend wurden die allergenen Eigenschaften von Pyr-OVA und AGE-OVA in einem Mausmodell der intestinalen Allergie untersucht. BALB/c-Mäuse wurden intraperitoneal mit nativem OVA, Pyr-OVA oder AGE-OVA in Kombination mit dem Adjuvans Aluminiumhydroxid zweimal in einem zweiwöchigen Intervall sensibilisiert. Zwei Wochen nach der letzten Sensibilisierung wurden die Mäuse für eine Woche mit einem Futter, welches hohe Mengen an Hühnereiweiß enthielt, gefüttert. Die Sensibilisierung der Mäuse mit Pyr-OVA oder AGE-OVA induzierte eine stärkere Produktion an OVA-spezifischen IgE im Vergleich zu der Sensibilisierung mit nativem OVA. Zusätzlich zeigten die Pyr-OVA- und AGE-OVA-sensibilisierten Mäuse stärkere klinische Symptome,

d. h. einen höheren Gewichtsverlust sowie Senkung der Körpertemperatur, während der Fütterung mit Hühnereiweiß-haltigem Futter als Mäuse, welche mit nativem OVA sensibilisiert wurden. Diese Ergebnisse deuten daraufhin, dass die allergene Wirkung von OVA durch die Modifizierung mit Pyrralin oder AGEs verstärkt wird. Der Zusammenhang zwischen der erhöhten $CD4^+$-T-Zellimmunogenität von Pyr-OVA und AGE-OVA und der erhöhten allergenen Wirkung ergibt sich daraus, dass die Stärke der IgE-Produktion durch B-Zellen über den Grad der Aktivierung der $CD4^+$-T-Zellen geregelt wird.

Im letzten Teil dieser Arbeit wurde eine Zellkultur-Methode mit primären humanen Zellen für die Analyse der Immunogenität von Maillard-modifizierten Allergenen etabliert. Es zeigte sich, dass humane dendritische Zellen nicht für diesen Zweck geeignet sind, da sie den SR-AI/II nicht auf der Zelloberfläche exprimieren. Humane Makrophagen hingegen weisen eine starke Oberflächen-expression von SR-AI/II und anderen AGE-bindenden Rezeptoren auf. Der MR ist verstärkt auf der Oberfläche von M1-Makrophagen zu finden, wohingegen M2-Zellen mehr Kopien der Rezeptoren SR-AI/II und SR-BI auf der Zelloberfläche tragen. Desweiteren konnte gezeigt werden, dass M2-Makrophagen, jedoch nicht M1-Zellen, AGE-OVA besser aufnehmen als natives OVA. M1-Makrophagen haben einen pro-inflammatorischen Phänotyp und wirken bei Immunreaktionen des $T_H1$-Typs mit. M2-Makrophagen besitzen einen anti-inflammatorischen Phänotyp und fungieren als APCs in Immunantworten des $T_H2$-Typs. Zusammenfassend lässt sich sagen, dass M2-Makrophagen ein sehr gutes Modellsystem für die Analyse der Immunogenität von Maillard-modifizierten Proteinen darstellen.

Diese Arbeit zeigt erstmalig, dass die Modifizierung eines Nahrungsmittelallergens mit Pyrralin, einem Produkt der Maillard-Reaktion, zu einer Verstärkung der allergenen Wirkung führt. Große Mengen an Pyrralin wurden in gerösteten Erdnüssen, welche häufig sehr starke klinische Symptome auslösen, nachgewiesen. Diese Resultate deuten daraufhin, dass die Maillard-Reaktion eine verstärkende Wirkung auf die allergenen Eigenschaften einiger Nahrungsmittelallergene hat. Deswegen sollte der Einfluss der Maillard-Reaktion auf die Allergenität von Nahrungsmittelallergenen in der Allergiediagnostik berücksichtigt werden, welche normalerweise mit Extrakten aus rohen Nahrungsmitteln oder unprozessierten aufgereinigten Allergenen durchgeführt wird. Abschließend lässt sich sagen, dass diese Arbeit zu der Aufklärung der molekularen Mechanismen der Nahrungsmittelallergie beiträgt.

# 7 References


1. Rona, R. J.; Keil, T.; Summers, C.; Gislason, D.; Zuidmeer, L.; Sodergren, E.; Sigurdardottir, S. T.; Lindner, T.; Goldhahn, K.; Dahlstrom, J.; McBride, D.; Madsen, C., The prevalence of food allergy: A meta-analysis. *J. Allergy Clin. Immunol.* **2007,** *120*, 638-646.
2. Sicherer, S. H.; Sampson, H. A., Food allergy. *J. Allergy Clin. Immunol.* **2010,** *125*, S116-S125.
3. Moneret-Vautrin, D.; Morisset, M., Adult food allergy. *Curr. Allergy Asthma Rep.* **2005,** *5*, 80-85.
4. Chaudhry, R.; Oppenheimer, J., Update on Food Allergy in Adults. *Curr. Allergy Asthma Rep.* **2012,** *12*, 311-320.
5. Yun, J.; Katelaris, C. H., Food allergy in adolescents and adults. *Intern. Med. J.* **2009,** *39*, 475-478.
6. Lee, L. A.; Burks, A. W., Food Allergies: Prevalence, Molecular Characterization, and Treatment/Prevention Strategies. *Annu. Rev. Nutr.* **2006,** *26*, 539-565.
7. Larché, M.; Akdis, C. A.; Valenta, R., Immunological mechanisms of allergen-specific immunotherapy. *Nat. Rev. Immunol.* **2006,** *6*, 761–771.
8. Kostadinova, A. I.; Willemsen, L. E. M.; Knippels, L. M. J.; Garssen, J., Immunotherapy – risk/benefit in food allergy. *Pediatr. Allergy Immunol.* **2013,** *24*, 633-644.
9. Jones, S. M.; Burks, A. W.; Dupont, C., State of the art on food allergen immunotherapy: Oral, sublingual, and epicutaneous. *J. Allergy Clin. Immunol.* **2014,** *133*, 318-323.
10. Murphy, K. T., P.; Walport, M., *Janeway's Immunobiology*. 7th edition ed.; Garland Sciences: New York and London, 2007.
11. Zhu, J.; Paul, W. E., CD4 T cells: fates, functions, and faults. *Blood* **2008,** *112*, 1557-1569.
12. Hasan, S. A.; Wells, R. D.; Davis, C. M., Egg hypersensitivity in review. *Allergy Asthma Proc.* **2013,** *34*, 26-32.
13. Benhamou, A. H.; Caubet, J. C.; Eigenmann, P. A.; Nowak-Węgrzyn, A.; Marcos, C. P.; Reche, M.; Urisu, A., State of the art and new horizons in the diagnosis and management of egg allergy. *Allergy* **2010,** *65*, 283-289.
14. Sicherer, S. H.; Wood, R. A.; Vickery, B. P.; Jones, S. M.; Liu, A. H.; Fleischer, D. M.; Dawson, P.; Mayer, L.; Burks, A. W.; Grishin, A.; Stablein, D.; Sampson, H. A., The natural history of egg allergy in an observational cohort. *J. Allergy Clin. Immunol.* **2014,** *133*, 492-499.e8.
15. Savage, J. H.; Matsui, E. C.; Skripak, J. M.; Wood, R. A., The natural history of egg allergy. *J. Allergy Clin. Immunol.* **2007,** *120*, 1413–1417.
16. Mine, Y.; Yang, M., Recent advances in the understanding of egg allergens: basic, industrial, and clinical perspectives. *J. Agric. Food Chem.* **2008,** *56*, 4874–4900.
17. Huntington, J. A.; Stein, P. E., Structure and properties of ovalbumin. *J. Chromatogr. B Biomed. Sci. Appl.* **2001,** *756*, 189–198.
18. Stein, P. E.; Leslie, A. G. W.; Finch, J. T.; Carrell, R. W., Crystal structure of uncleaved ovalbumin at 1·95 Å resolution. *J. Mol. Biol.* **1991,** *221*, 941-959.
19. Yamashita, K.; Tachibana, Y.; Kobata, A., The structures of the galactose-containing sugar chains of ovalbumin. *J. Biol. Chem.* **1978,** *253*, 3862-3869.
20. Thaysen-Andersen, M.; Mysling, S.; Højrup, P., Site-Specific Glycoprofiling of N-Linked Glycopeptides Using MALDI-TOF MS: Strong Correlation between Signal Strength and Glycoform Quantities. *Anal. Chem.* **2009,** *81*, 3933-3943.

21. Mine, Y.; Rupa, P., Fine mapping and structural analysis of immunodominant IgE allergenic epitopes in chicken egg ovalbumin. *Protein Eng.* **2003,** *16*, 747-752.

22. Mine, Y.; Yang, M., Epitope characterization of ovalbumin in BALB/c mice using different entry routes. *Biochim. Biophys. Acta* **2007,** *1774*, 200-212.

23. Sathe, S. K.; Sharma, G. M., Effects of food processing on food allergens. *Mol. Nutr. Food Res.* **2009,** *53*, 970–978.

24. Astwood, J. D.; Leach, J. N.; Fuchs, R. L., Stability of food allergens to digestion in vitro. *Nat. Biotechnol.* **1996,** *14*, 1269–1273.

25. Lepski, S.; Brockmeyer, J., Impact of dietary factors and food processing on food allergy. *Mol. Nutr. Food Res.* **2013,** *57*, 145-152.

26. Mills, E. N.; Sancho, A. I.; Rigby, N. M.; Jenkins, J. A.; Mackie, A. R., Impact of food processing on the structural and allergenic properties of food allergens. *Mol. Nutr. Food Res.* **2009,** *53*, 963–969.

27. Gruber, P.; Vieths, S.; Wangorsch, A.; Nerkamp, J.; Hofmann, T., Maillard reaction and enzymatic browning affect the allergenicity of Pru av 1, the major allergen from cherry (Prunus avium). *J. Agric. Food Chem.* **2004,** *52*, 4002–4007.

28. Bohle, B.; Zwolfer, B.; Heratizadeh, A.; Jahn-Schmid, B.; Antonia, Y. D.; Alter, M.; Keller, W.; Zuidmeer, L.; van, R. R.; Werfel, T.; Ebner, C., Cooking birch pollen-related food: divergent consequences for IgE- and T cell-mediated reactivity in vitro and in vivo. *J. Allergy Clin. Immunol.* **2006,** *118*, 242–249.

29. Ballmer-Weber, B. K.; Hoffmann, A.; Wüthrich, B.; Lüttkopf, D.; Pompei, C.; Wangorsch, A.; Kästner, M.; Vieths, S., Influence of food processing on the allergenicity of celery: DBPCFC with celery spice and cooked celery in patients with celery allergy. *Allergy* **2002,** *57*, 228-235.

30. Jimenez-Saiz, R.; Belloque, J.; Molina, E.; Lopez-Fandino, R., Human immunoglobulin E (IgE) binding to heated and glycated ovalbumin and ovomucoid before and after in vitro digestion. *J. Agric. Food Chem.* **2011,** *59*, 10044–10051.

31. Martos, G.; Lopez-Exposito, I.; Bencharitiwong, R.; Berin, M. C.; Nowak-Wegrzyn, A., Mechanisms underlying differential food allergy response to heated egg. *J. Allergy Clin. Immunol.* **2011,** *127*, 990–997.

32. Golias, J.; Schwarzer, M.; Wallner, M.; Kverka, M.; Kozakova, H.; Srutkova, D.; Klimesova, K.; Sotkovsky, P.; Palova-Jelinkova, L.; Ferreira, F.; Tuckova, L., Heat-Induced Structural Changes Affect OVA-Antigen Processing and Reduce Allergic Response in Mouse Model of Food Allergy. *PLoS. One* **2012,** *7*, e37156.

33. Rosen, J. P.; Selcow, J. E.; Mendelson, L. M.; Grodofsky, M. P.; Factor, J. M.; Sampson, H. A., Skin testing with natural foods in patients suspected of having food allergies: Is it a necessity? *J. Allergy Clin. Immunol.* **1994,** *93*, 1068-1070.

34. Nakamura, A.; Watanabe, K.; Ojima, T.; Ahn, D.-H.; Saeki, H., Effect of Maillard Reaction on Allergenicity of Scallop Tropomyosin. *J. Agric. Food Chem.* **2005,** *53*, 7559-7564.

35. Malanin, K.; Lundberg, M.; Johansson, S. G. O., Anaphylactic reaction caused by neoallergens in heated pecan nut. *Allergy* **1995,** *50*, 988-991.

36. Beyer, K.; Morrow, E.; Li, X. M.; Bardina, L.; Bannon, G. A.; Burks, A. W.; Sampson, H. A., Effects of cooking methods on peanut allergenicity. *J. Allergy Clin. Immunol.* **2001,** *107*, 1077–1081.

37. Maleki, S. J.; Chung, S. Y.; Champagne, E. T.; Raufman, J. P., The effects of roasting on the allergenic properties of peanut proteins. *J. Allergy Clin. Immunol.* **2000,** *106*, 763–768.

38. Maillard, L. C., Action des acides aminés dur les sucres; formation des mélanoidines par voie méthodique. *Comptes rendus hebdomadaires des séances de l'Académie des sciences* **1912,** *154*, 66 - 68.

39. Henle, T., Protein-bound advanced glycation endproducts (AGEs) as bioactive amino acid derivatives in foods. *Amino Acids* **2005,** *29*, 313–322.

40. Ledl, F.; Schleicher, E., Die Maillard-Reaktion in Lebensmitteln und im menschlichen Körper – neue Ergebnisse zu Chemie, Biochemie und Medizin. *Angew. Chem.* **1990,** *102*, 597-626.

41. Toda, M.; Heilmann, M.; Ilchmann, A.; Vieths, S., The Maillard reaction and food allergies: is there a link? *Clin. Chem. Lab. Med.* **2014,** *52*, 1-7.

42. van Boekel, M. A. J. S., Formation of flavour compounds in the Maillard reaction. *Biotechnol. Adv.* **2006,** *24*, 230-233.

43. Parker, J. K., The kinetics of thermal generation of flavour. *J. Sci. Food Agric.* **2013,** *93*, 197-208.

44. Goldin, A.; Beckman, J. A.; Schmidt, A. M.; Creager, M. A., Advanced glycation end products: sparking the development of diabetic vascular injury. *Circulation* **2006,** *114*, 597–605.

45. Schmidt, A. M.; Vianna, M.; Gerlach, M.; Brett, J.; Ryan, J.; Kao, J.; Esposito, C.; Hegarty, H.; Hurley, W.; Clauss, M., Isolation and characterization of two binding proteins for advanced glycosylation end products from bovine lung which are present on the endothelial cell surface. *J. Biol. Chem.* **1992,** *267*, 14987-14997.

46. Neeper, M.; Schmidt, A. M.; Brett, J.; Yan, S. D.; Wang, F.; Pan, Y. C.; Elliston, K.; Stern, D.; Shaw, A., Cloning and expression of a cell surface receptor for advanced glycosylation end products of proteins. *J. Biol. Chem.* **1992,** *267*, 14998–15004.

47. Vlassara, H.; Li, Y. M.; Imani, F.; Wojciechowicz, D.; Yang, Z.; Liu, F. T.; Cerami, A., Identification of galectin-3 as a high-affinity binding protein for advanced glycation end products (AGE): a new member of the AGE-receptor complex. *Mol. Med.* **1995,** *1*, 634–646.

48. Plüddemann, A.; Neyen, C.; Gordon, S., Macrophage scavenger receptors and host-derived ligands. *Methods* **2007,** *43*, 207–217.

49. Horiuchi, S.; Sakamoto, Y.; Sakai, M., Scavenger receptors for oxidized and glycated proteins. *Amino Acids* **2003,** *25*, 283–292.

50. Araki, N.; Higashi, T.; Mori, T.; Shibayama, R.; Kawabe, Y.; Kodama, T.; Takahashi, K.; Shichiri, M.; Horiuchi, S., Macrophage scavenger receptor mediates the endocytic uptake and degradation of advanced glycation end products of the Maillard reaction. *Eur. J. Biochem.* **1995,** *230*, 408–415.

51. Ohgami, N.; Nagai, R.; Ikemoto, M.; Arai, H.; Kuniyasu, A.; Horiuchi, S.; Nakayama, H., Cd36, a member of the class b scavenger receptor family, as a receptor for advanced glycation end products. *J. Biol. Chem.* **2001,** *276*, 3195–3202.

52. Ohgami, N.; Nagai, R.; Miyazaki, A.; Ikemoto, M.; Arai, H.; Horiuchi, S.; Nakayama, H., Scavenger receptor class B type I-mediated reverse cholesterol transport is inhibited by advanced glycation end products. *J. Biol. Chem.* **2001,** *276*, 13348–13355.

53. Areschoug, T.; Gordon, S., Scavenger receptors: role in innate immunity and microbial pathogenesis. *Cellular Microbiology* **2009,** *11*, 1160-1169.

54. Mukhopadhyay, S.; Pluddemann, A.; Gordon, S., Macrophage pattern recognition receptors in immunity, homeostasis and self tolerance. *Adv. Exp. Med. Biol.* **2009,** *653*, 1–14.

55. Doi, T.; Higashino, K.; Kurihara, Y.; Wada, Y.; Miyazaki, T.; Nakamura, H.; Uesugi, S.; Imanishi, T.; Kawabe, Y.; Itakura, H., Charged collagen structure mediates the recognition of negatively charged macromolecules by macrophage scavenger receptors. *J. Biol. Chem.* **1993,** *268*, 2126–2133.

56. Dumic, J.; Dabelic, S.; Flögel, M., Galectin-3: An open-ended story. *Biochim. Biophys. Acta* **2006,** *1760*, 616-635.

57. Liu, F.-T.; Patterson, R. J.; Wang, J. L., Intracellular functions of galectins. *Biochim. Biophys. Acta* **2002,** *1572*, 263-273.

58. Zhu, W.; Sano, H.; Nagai, R.; Fukuhara, K.; Miyazaki, A.; Horiuchi, S., The Role of Galectin-3 in Endocytosis of Advanced Glycation End Products and Modified Low Density Lipoproteins. *Biochem. Biophys. Res. Commun.* **2001,** *280*, 1183-1188.

59. Burgdorf, S.; Lukacs-Kornek, V.; Kurts, C., The mannose receptor mediates uptake of soluble but not of cell-associated antigen for cross-presentation. *J. Immunol.* **2006,** *176*, 6770–6776.

60. Geijtenbeek, T. B.; Gringhuis, S. I., Signalling through C-type lectin receptors: shaping immune responses. *Nat. Rev. Immunol.* **2009,** *9*, 465–479.

61. Wills-Karp, M., Allergen-specific pattern recognition receptor pathways. *Curr. Opin. Immunol.* **2010,** *22*, 777–782.

62. East, L.; Isacke, C. M., The mannose receptor family. *Biochim. Biophys. Acta* **2002,** *1572*, 364–386.

63. Gazi, U.; Martinez-Pomares, L., Influence of the mannose receptor in host immune responses. *Immunobiology* **2009,** *214*, 554-561.

64. Joffre, O. P.; Segura, E.; Savina, A.; Amigorena, S., Cross-presentation by dendritic cells. *Nat. Rev. Immunol.* **2012,** *12*, 557-569.

65. Chung, S. Y.; Champagne, E. T., Association of end-product adducts with increased IgE binding of roasted peanuts. *J. Agric. Food Chem.* **2001,** *49*, 3911–3916.

66. Vissers, Y. M.; Blanc, F.; Skov, P. S.; Johnson, P. E.; Rigby, N. M.; Przybylski-Nicaise, L.; Bernard, H.; Wal, J. M.; Ballmer-Weber, B.; Zuidmeer-Jongejan, L.; Szepfalusi, Z.; Ruinemans-Koerts, J.; Jansen, A. P.; Savelkoul, H. F.; Wichers, H. J.; Mackie, A. R.; Mills, C. E.; Adel-Patient, K., Effect of Heating and Glycation on the Allergenicity of 2S Albumins (Ara h 2/6) from Peanut. *PLoS One* **2011,** *6*, e23998.

67. Vissers, Y. M.; Iwan, M.; Adel-Patient, K.; Stahl, S. P.; Rigby, N. M.; Johnson, P. E.; Mandrup, M. P.; Przybylski-Nicaise, L.; Schaap, M.; Ruinemans-Koerts, J.; Jansen, A. P.; Mills, E. N.; Savelkoul, H. F.; Wichers, H. J., Effect of roasting on the allergenicity of major peanut allergens Ara h 1 and Ara h 2/6: the necessity of degranulation assays. *Clin. Exp. Allergy* **2011,** *41*, 1631–1642.

68. Taheri-Kafrani, A.; Gaudin, J. C.; Rabesona, H.; Nioi, C.; Agarwal, D.; Drouet, M.; Chobert, J. M.; Bordbar, A. K.; Haertle, T., Effects of heating and glycation of beta-lactoglobulin on its recognition by IgE of sera from cow milk allergy patients. *J. Agric. Food Chem.* **2009,** *57*, 4974–4982.

69. Nakamura, A.; Sasaki, F.; Watanabe, K.; Ojima, T.; Ahn, D.-H.; Saeki, H., Changes in Allergenicity and Digestibility of Squid Tropomyosin during the Maillard Reaction with Ribose. *J. Agric. Food Chem.* **2006,** *54*, 9529-9534.

70. Prausnitz, C. K., H., Studien über die Überempfindlichkeit. *Zentralbl. Bakteriol.* **1921,** *86*, 160-169.

71. Ilchmann, A.; Burgdorf, S.; Scheurer, S.; Waibler, Z.; Nagai, R.; Wellner, A.; Yamamoto, Y.; Yamamoto, H.; Henle, T.; Kurts, C.; Kalinke, U.; Vieths, S.; Toda, M., Glycation of a food allergen by the Maillard reaction enhances its T-cell immunogenicity: role of macrophage scavenger receptor class A type I and II. *J. Allergy Clin. Immunol.* **2010,** *125*, 175–183.

72. Banchereau, J.; Paczesny, S.; Blanco, P.; Bennett, L.; Pascual, V.; Fay, J.; Palucka, A. K., Dendritic Cells. *Ann. N. Y. Acad. Sci.* **2003,** *987*, 180-187.

73. Steinman, R. M.; Banchereau, J., Taking dendritic cells into medicine. *Nature* **2007,** *449*, 419-426.

74. Joffre, O.; Nolte, M. A.; Spörri, R.; Sousa, C. R. e., Inflammatory signals in dendritic cell activation and the induction of adaptive immunity. *Immunol. Rev.* **2009,** *227*, 234-247.

75. Banchereau, J.; Briere, F.; Caux, C.; Davoust, J.; Lebecque, S.; Liu, Y.-J.; Pulendran, B.; Palucka, K., Immunobiology of Dendritic Cells. *Annu. Rev. Immunol.* **2000,** *18*, 767-811.

76. Lawrence, T.; Natoli, G., Transcriptional regulation of macrophage polarization: enabling diversity with identity. *Nat. Rev. Immunol.* **2011,** *11*, 750-761.

77. Martinez, F. O.; Gordon, S.; Locati, M.; Mantovani, A., Transcriptional Profiling of the Human Monocyte-to-Macrophage Differentiation and Polarization: New Molecules and Patterns of Gene Expression. *J. Immunol.* **2006,** *177*, 7303-7311.

78. Biswas, S. K.; Mantovani, A., Macrophage plasticity and interaction with lymphocyte subsets: cancer as a paradigm. *Nat. Immunol.* **2010,** *11*, 889-896.

79. Gordon, S., Alternative activation of macrophages. *Nat. Rev. Immunol.* **2003,** *3*, 23-35.

80. Hume, D. A., Macrophages as APC and the Dendritic Cell Myth. *J. Immunol.* **2008,** *181*, 5829-5835.

81. Kumar, S.; Dwivedi, P. D.; Das, M.; Tripathi, A., Macrophages in food allergy: An enigma. *Mol. Immunol.* **2013,** *56*, 612-618.

82. Stöhr, R.; Federici, M., Insulin resistance and atherosclerosis: convergence between metabolic pathways and inflammatory nodes. *Biochem. J.* **2013,** *454*, 1-11.

83. Maddur, M. S.; Miossec, P.; Kaveri, S. V.; Bayry, J., Th17 Cells: Biology, Pathogenesis of Autoimmune and Inflammatory Diseases, and Therapeutic Strategies. *Am. J. Pathol.* **2012,** *181*, 8-18.

84. Nagai, R.; Matsumoto, K.; Ling, X.; Suzuki, H.; Araki, T.; Horiuchi, S., Glycolaldehyde, a reactive intermediate for advanced glycation end products, plays an important role in the generation of an active ligand for the macrophage scavenger receptor. *Diabetes* **2000,** *49*, 1714–1723.

85. Nakajou, K.; Horiuchi, S.; Sakai, M.; Hirata, K.; Tanaka, M.; Takeya, M.; Kai, T.; Otagiri, M., CD36 Is Not Involved in Scavenger Receptor–Mediated Endocytic Uptake of Glycolaldehyde- and Methylglyoxal-Modified Proteins by Liver Endothelial Cells. *J. Biochem.* **2005,** *137*, 607-616.

86. Murphy, K. M.; Heimberger, A. B.; Loh, D. Y., Induction by antigen of intrathymic apoptosis of CD4+CD8+TCRlo thymocytes in vivo. *Science* **1990,** *250*, 1720-3.

87. Hogquist, K. A.; Jameson, S. C.; Heath, W. R.; Howard, J. L.; Bevan, M. J.; Carbone, F. R., Pillars Article: T Cell Receptor Antagonist Peptides Induce Positive Selection. Cell. 1994. 76: 17–27. *J. Immunol.* **2012,** *188*, 2046-2056.

88. Barnden, M. J.; Allison, J.; Heath, W. R.; Carbone, F. R., Defective TCR expression in transgenic mice constructed using cDNA-based [agr]- and [bgr]-chain genes under the control of heterologous regulatory elements. *Immunol. Cell Biol.* **1998,** *76*, 34-40.

89. Suzuki, H.; Kurihara, Y.; Takeya, M.; Kamada, N.; Kataoka, M.; Jishage, K.; Ueda, O.; Sakaguchi, H.; Higashi, T.; Suzuki, T.; Takashima, Y.; Kawabe, Y.; Cynshi, O.; Wada, Y.; Honda, M.; Kurihara, H.; Aburatani, H.; Doi, T.; Matsumoto, A.; Azuma, S.; Noda, T.; Toyoda, Y.; Itakura, H.; Yazaki, Y.; Kodama, T., A role for macrophage scavenger receptors in atherosclerosis and susceptibility to infection. *Nature* **1997,** *386*, 292–296.

90. Gasic-Milenkovic, J.; Dukic-Stefanovic, S.; Deuther-Conrad, W.; Gartner, U.; Munch, G., Beta-amyloid peptide potentiates inflammatory responses induced by lipopolysaccharide, interferon - gamma and 'advanced glycation endproducts' in a murine microglia cell line. *Eur. J. Neurosci.* **2003,** *17*, 813–821.

91. Glorieux, G.; Helling, R.; Henle, T.; Brunet, P.; Deppisch, R.; Lameire, N.; Vanholder, R., In vitro evidence for immune activating effect of specific AGE structures retained in uremia. *Kidney Int.* **2004,** *66*, 1873–1880.

92. Henle, T.; Bachmann, A., Synthesis of pyrraline reference material. *Z. Lebensm. Unters. Forsch.* **1996,** *202*, 72–74.

93. Henle, T.; Walter, A.; Haeßner, R.; Klostermeyer, H., Detection and identification of a protein-bound imidazolone resulting from the reaction of arginine residues and methylglyoxal. *Z. Lebensm. Unters. Forsch.* **1994,** *199*, 55–58.

94. Henle, T.; Walter, H.; Krause, I.; Klostermeyer, H., Efficient determination of individual maillard compounds in heat-treated milk products by amino acid analysis. *Int. Dairy J.* **1991,** *1*, 125-135.

95. Wellner, A.; Huettl, C.; Henle, T., Formation of Maillard reaction products during heat treatment of carrots. *J. Agric. Food Chem.* **2011,** *59*, 7992–7998.

96. Förster, A.; Kuhne, Y.; Henle, T., Studies on absorption and elimination of dietary maillard reaction products. *Ann. N. Y. Acad. Sci.* **2005,** *1043*, 474–481.

97. Lottspeich, F.; Engels, J. W., *Bioanalytik*. 2nd ed.; Spektrum Akademischer Verlag: Heidelberg, 2006.

98. Laemmli, U. K., Cleavage of Structural Proteins during the Assembly of the Head of Bacteriophage T4. *Nature* **1970,** *227*, 680-685.

99. Luttmann, W.; Bratke, K.; Küpper, M.; Myrtek, D., *Der Experimentator: Immunologie*. 3rd ed.; Spektrum Akademischer Verlag: Heidelberg, 2009.

100. Hilmenyuk, T.; Bellinghausen, I.; Heydenreich, B.; Ilchman, A.; Toda, M.; Grabbe, S.; Saloga, J., Effects of glycation of the model food allergen ovalbumin on antigen uptake and presentation by human dendritic cells. *Immunology* **2009**.

101. Burggraf, M.; Nakajima-Adachi, H.; Hachimura, S.; Ilchmann, A.; Pemberton, A. D.; Kiyono, H.; Vieths, S.; Toda, M., Oral tolerance induction does not resolve gastrointestinal inflammation in a mouse model of food allergy. *Mol. Nutr. Food Res.* **2011,** *55*, 1475-1483.

102. Robertson, J. M.; Jensen, P. E.; Evavold, B. D., DO11.10 and OT-II T Cells Recognize a C-Terminal Ovalbumin 323–339 Epitope. *J. Immunol.* **2000,** *164*, 4706-4712.

103. Burgdorf, S.; Scholz, C.; Kautz, A.; Tampe, R.; Kurts, C., Spatial and mechanistic separation of cross-presentation and endogenous antigen presentation. *Nat. Immunol.* **2008,** *9*, 558–566.

104. Buttari, B.; Profumo, E.; Capozzi, A.; Facchiano, F.; Saso, L.; Sorice, M.; Riganò, R., Advanced glycation end products of human β2 glycoprotein I modulate the maturation and function of DCs. *Blood* **2011,** *117*, 6152-6161.

105. Price, C. L.; Sharp, P. S.; North, M. E.; Rainbow, S. J.; Knight, S. C., Advanced Glycation End Products Modulate the Maturation and Function of Peripheral Blood Dendritic Cells. *Diabetes* **2004,** *53*, 1452-1458.

106. Cherayil, B. J.; Weiner, S. J.; Pillai, S., The Mac-2 antigen is a galactose-specific lectin that binds IgE. *J. Exp. Med.* **1989,** *170*, 1959-1972.

107. Nieland, T. J. F.; Shaw, J. T.; Jaipuri, F. A.; Duffner, J. L.; Koehler, A. N.; Banakos, S.; Zannis, V. I.; Kirchhausen, T.; Krieger, M., Identification of the Molecular Target of Small Molecule Inhibitors of HDL Receptor SR-BI Activity. *Biochemistry* **2008,** *47*, 460-472.

108. He, H.; MacKinnon, K. M.; Genovese, K. J.; Nerren, J. R.; Swaggerty, C. L.; Nisbet, D. J.; Kogut, M. H., Chicken scavenger receptors and their ligand-induced cellular immune responses. *Mol. Immunol.* **2009,** *46*, 2218–2225.

109. Rupa, P.; Nakamura, S.; Katayama, S.; Mine, Y., Effects of ovalbumin glycoconjugates on alleviation of orally induced egg allergy in mice via dendritic-cell maturation and T-cell activation. *Mol. Nutr. Food Res.* **2014,** *58*, 405-417.

110. Burgdorf, S.; Kautz, A.; Böhnert, V.; Knolle, P. A.; Kurts, C., Distinct Pathways of Antigen Uptake and Intracellular Routing in CD4 and CD8 T Cell Activation. *Science* **2007,** *136*, 612–616.

111. Nicoletti, A.; Caligiuri, G.; Törnberg, I.; Kodama, T.; Stemme, S.; Hansson, G. K., The macrophage scavenger receptor type A directs modified proteins to antigen presentation. *Eur. J. Immunol.* **1999,** *29*, 512-521.

112. Bhatia, S.; Mukhopadhyay, S.; Jarman, E.; Hall, G.; George, A.; Basu, S. K.; Rath, S.; Lamb, J. R.; Bal, V., Scavenger receptor-specific allergen delivery elicits IFN-γ-dominated immunity and directs established TH2-dominated responses to a nonallergic phenotype. *J. Allergy Clin. Immunol.* **2002,** *109*, 321-328.

113. Jin, J. O.; Park, H. Y.; Xu, Q.; Park, J. I.; Zvyagintseva, T.; Stonik, V. A.; Kwak, J. Y., Ligand of scavenger receptor class A indirectly induces maturation of human blood dendritic cells via production of tumor necrosis factor-alpha. *Blood* **2009,** *113*, 5839–5847.

# 8 Attachments

## Curriculum Vitae

### Personal Information

| | |
|---|---|
| First / family name | **Monika Hofmann née Heilmann**<br>Dipl.-Ing. chemistry |
| Date and place of birth | 25 March 1985 in 65812 Bad Soden, Taunus / Germany |
| Family status | married, no children |
| Nationality | German |

### Academic Education

| | |
|---|---|
| since 04 / 2010 | **PhD thesis** at the Paul-Ehrlich-Institut in Langen in the group of Dr. Masako Toda in cooperation with Prof. Dr. Harald Kolmar as PhD supervisor at the Technische Universität Darmstadt<br>title: "*The influence of the Maillard reaction on allergenicity of food allergens*"<br>techniques: protein analysis, ELISA, cell culture and cellular assays, flow cytometry |
| 08 / 2009 – 02 / 2010 | **Diploma thesis** at the Paul-Ehrlich-Institut in Langen in the group of PD Dr. Johannes Dodt in cooperation with Prof. Dr. Harald Kolmar as diploma supervisor at the Technische Universität Darmstadt<br>title: "*Regulation of coagulation factor V by the Hyaluronan-binding protease HABP*", grade 1.0<br>tasks: anion exchange and size exclusion chromatography, Western Blotting, factor V activity tests |
| 10 / 2004 – 02 / 2010 | **Diploma studies** in chemistry at the Technische Universität Darmstadt with focus on biochemistry and organic chemistry as well as basics in chemical technology,<br>graduate engineer in chemistry (Dipl.-Ing.), grade 1.2 |

### School Education

| | |
|---|---|
| 08 / 2001 – 07 / 2004 | **High school** (Berufliches Gymnasium) in Oberursel (Feldbergschule Oberursel), general higher education entrance qualification (Abitur), with focus on mathematics and economics,<br>grade 1.3 |
| 08 / 1995 – 07 / 2001 | **High school** (Gymnasium), in Oberursel (Gymnasium Oberursel) |

## Internships

| | |
|---|---|
| 03 / 2010 – 03 / 2010 | Paul-Ehrlich-Institut, Langen,<br>internship in a biochemical laboratory applying phage display for identifying a binding antibody for a coagulation factor |
| 10 / 2001 – 10 / 2001 | Sanofi-Aventis Deutschland GmbH, Frankfurt am Main,<br>internship in an analytical chemical laboratory performing qualitative as well as quantitative analysis |

## Further Education (Courses)

Certificate in toxicology and handling of hazardous substances

Introductory course for working with laboratory animals (according to FELASA B) by DKFZ Heidelberg

## Language Skills

| | |
|---|---|
| German | (native) |
| English | (very good, PhD studies in an English-speaking group) |
| French | (basic knowledge) |

## DP Knowledge

Enhanced knowledge in Microsoft Office, Windows, ChemBioOffice, GraphPad Prism, as well as basic knowledge in Aspen Plus®

Darmstadt, September 2014

## Project-related list of publications

**Journal article:**

**Heilmann M.**, Wellner A., Gadermaier G., Ilchmann A., Briza P., Krause M., Nagai R., Burgdorf S., Scheurer S., Vieths S., Henle T., Toda M., Ovalbumin modified with pyrraline, a Maillard reaction product, shows enhanced T cell immunogenicity, *J. Biol. Chem.*, **2014**; *289*, 7919 - 7928. doi: 10.10174/ jbc.M113. 52362

**Contributions to international or national congresses:**

**Oral presentations:**

**Heilmann M.**, Wellner A., Henle T., Vieths S., Toda M., Scavenger receptor class A mediates enhanced T-cell immunogenicity of ovalbumin modified with pyrraline, a glycation structure; 25. Mainzer Allergie-Workshop, 7 - 8 March **2013**, Mainz/Germany.

**Heilmann M.**, Wellner A., Vieths S., Henle T., Toda M., Pyrraline modification enhances T-cell immunogenicity of ovalbumin, a food allergen; 11th International Symposium on the Maillard Reaction, 16 - 20 September **2012**, Nancy/France.

**Heilmann M.**, Wellner A., Vieths S., Henle T., Toda M., Influence of the Maillard reaction on immunogenicity and allergenicity of food allergens; 24. Mainzer Allergie-Workshop, 22 - 23 March **2012**, Mainz/Germany

**Poster presentations:**

**Heilmann M.**, Wellner A., Vieths S., Henle T., Toda M., Scavenger receptor class A mediates enhanced T-cell immunogenicity of ovalbumin modified with pyrraline, a glycation structure; EAACI 11$^{th}$ Immunology WinterSchool, 27 - 30 January **2013**, Pichl/Austria.

**Heilmann M.**, Wellner A., Vieths S., Henle T., Toda M., Pyrraline modification enhances T-cell immunogenicity of ovalbumin, a food allergen; 11$^{th}$ International Symposium on the Maillard Reaction, 16 - 20 September **2012**, Nancy/France.

**Heilmann M.**, Wellner A., Henle T., Vieths S., Toda M., Influence of the Maillard reaction on immunogenicity and allergenicity of food allergens; EAACI-GA$^2$LEN 10$^{th}$ Immunology WinterSchool, 12 - 15 February **2012**, Åre/Sweden.

Monika Hofmann

Eberstädter Marktstraße 10
64297 Darmstadt

# Erklärung

Ich erkläre hiermit, dass ich meine Dissertation selbständig und nur mit den angegebenen Hilfsmitteln angefertigt habe.

Darmstadt, den 01. September 2014

_____

Monika Hofmann

Monika Hofmann
Eberstädter Marktstraße 10
64297 Darmstadt

## Erklärung

Ich erkläre hiermit, noch keinen Promotionsversuch unternommen zu haben.

Darmstadt, den 01. September 2014

Monika Hofmann